NONLINEAR FREE SURFACE EFFECTS: EXPERIMENTS AND THEORY

by

Martin Greenhow
and
Woei-Min Lin

REPORT NO. 83-10

MASSACHUSETTS INSTITUTE OF TECHNOLOGY
DEPARTMENT OF OCEAN ENGINEERING
CAMBRIDGE, MASS. 02139

NONLINEAR FREE SURFACE EFFECTS: EXPERIMENTS AND THEORY

by

Martin Greenhow
and
Woei-Min Lin

REPORT NO. 83-19

September 1983

This research was carried out under

Office of Naval Research
Contract N00014-82-K-0198, MIT/OSP 91783

and

National Science Foundation,
Contract 8210649-MEA, MIT/OSP 93348

avoided in the real fluid by the formation of jets, which at the scale of the experiments, quickly break up into spray under the action of surface tension. Nevertheless it is known that potential theory is adequate to describe the formation of jets and therefore some local model, valid around the intersection point and based on potential theory, is being sought for later matching to appropriate far field conditions. Such far field or outer solutions may be calculated with existing programs, and it is hoped that when complemented by an inner solution, they will provide a reasonably complete description of many extreme wave or extreme motion problems e.g., ship capsize and slamming.

For the most part the experiments have been performed at high speed: this means that it is approximately correct to ignore gravity in the local region and this effects a considerable simplification to the theory. Indeed the known theories of jets all ignore the influence of gravity by letting the origin be in free fall. This appears to be justified in the present context also.

The experiments are compared with the results of existing theories and earlier work as far as possible. However, the water exit problem of a cylinder (relevant to cross members in the splash zone) appears to be largely unstudied, possibly because of the extremely complex nature of the breaking as the cylinder leaves the free surface, where cortices shed by the cylinder as it moves through the fluid may influence the free surface as the cylinder leaves the fluid. For the other problems studied (the impulsive start of a wavemaker, cylinder entry and wedge entry) vorticity is not thought to be important and the resulting breaking appears to be closely similar to the breaking of waves. Support for this conjecture is being sought.

SECURITY CLASSIFICATION OF THIS PAGE (When Data Entered)

REPORT DOCUMENTATION PAGE

READ INSTRUCTIONS BEFORE COMPLETING FORM

1. REPORT NUMBER: 83-19	2. GOVT ACCESSION NO.: AD-A161 979
3. RECIPIENT'S CATALOG NUMBER:	
4. TITLE (and Subtitle): NON-LINEAR FREE SURFACE EFFECTS: EXPERIMENTS AND THEORY	5. TYPE OF REPORT & PERIOD COVERED: TECHNICAL REPORT
	6. PERFORMING ORG. REPORT NUMBER:
7. AUTHOR(s): MARTIN GREENHOW; WOEI-MIN LIN	8. CONTRACT OR GRANT NUMBER(s): N00014-82-K-0198
9. PERFORMING ORGANIZATION NAME AND ADDRESS: DEPARTMENT OF OCEAN ENGINEERING, MASSACHUSETTS INSTITUTE OF TECHNOLOGY, 77 MASSACHUSETTS AVE., CAMBRIDGE, MA 02139	10. PROGRAM ELEMENT, PROJECT, TASK AREA & WORK UNIT NUMBERS:
11. CONTROLLING OFFICE NAME AND ADDRESS: OFFICE OF NAVAL RESEARCH, DEPARTMENT OF THE NAVY, ARLINGTON, VA 22217	12. REPORT DATE: SEPTEMBER 1983
	13. NUMBER OF PAGES: 95
14. MONITORING AGENCY NAME & ADDRESS (if different from Controlling Office):	15. SECURITY CLASS. (of this report): UNCLASSIFIED
	15a. DECLASSIFICATION/DOWNGRADING SCHEDULE:

16. DISTRIBUTION STATEMENT (of this Report)

APPROVED FOR PUBLIC RELEASE: DISTRIBUTION UNLIMITED

17. DISTRIBUTION STATEMENT (of the abstract entered in Block 20, if different from Report)

18. SUPPLEMENTARY NOTES

19. KEY WORDS (Continue on reverse side if necessary and identify by block number)

WATERWAVES
SLAMMING
UNSTEADY HYDRODYNAMICS
WAVEMAKER
NON LINEAR FREE-SURFACE FLOWS

20. ABSTRACT (Continue on reverse side if necessary and identify by block number)

The object of this report is to present the results of some simple two-dimensional experiments in which the surface of the water is displaced a good deal from its undisturbed position, and for which linear theory is likely to be in error. Particular attention is paid to the point of intersection of the free surface and a moving body, where the confluence of boundary conditions can cause singularities in the free surface displacements and velocities, as predicted by linear theory. These singularities appear to be

DD FORM 1 JAN 73 1473 EDITION OF 1 NOV 65 IS OBSOLETE
S/N 0102-014-6601

SECURITY CLASSIFICATION OF THIS PAGE (When Data Entered)

TABLE OF CONTENTS

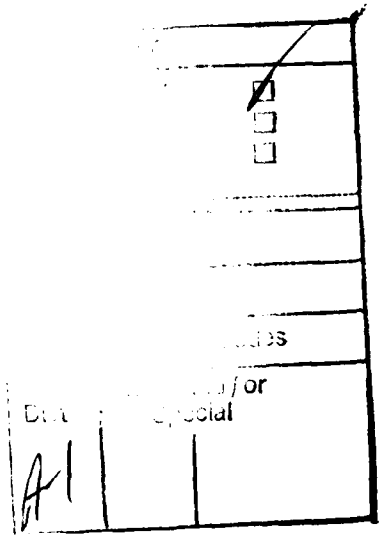

LIST OF FIGURES

ABSTRACT

The object of this report is to present the results of some simple two-dimensional experiments in which the surface of the water is displaced a good deal from its undisturbed position, and for which linear theory is likely to be in error. Particular attention is paid to the point of intersection of the free surface and a moving body, where the confluence of boundary conditions can cause singularities in the free surface displacements and velocities, as predicted by linear theory. These singularities appear to be avoided in the real fluid by the formation of jets, which at the scale of the experiments, quickly break up into spray under the action of surface tension. Nevertheless it is known that potential theory is adequate to describe the formation of jets and therefore some local model, valid around the intersection point and based on potential theory, is being sought for later matching to appropriate far field conditions. Such far field or outer solutions may be calculated with existing programs, and it is hoped that when complemented by an inner solution, they will provide a reasonably complete description of many extreme wave or extreme motion problems e.g., ship capsize and slamming.

For the most part the experiments have been performed at high speed: this means that it is approximately correct to ignore gravity in the local region and this effects a considerable simplification to the theory. Indeed the known theories of jets all ignore the influence of gravity by letting the origin be in free fall. This appears to be justified in the present context also.

The experiments are compared with the results of existing theories and earlier work as far as possible. However, the water exit problem of a cylinder (relevant to cross members in the splash zone) appears to be largely unstudied, possibly because of the extremely complex nature of the breaking as the cylinder leaves the free surface, where vortices shed by the cylinder as it moves through the fluid may influence the free surface as the cylinder leaves the fluid. For the other problems studied (the impulsive start of a wavemaker, cylinder entry and wedge entry) vorticity is not thought to be important and the resulting breaking appears to be closely similar to the breaking of waves. Support for this conjecture is being sought.

1. INTRODUCTION

As pointed out by Greenhow et al (1982) the numerical simulation of phenomena such as ship capsize depends upon correct positioning of the points of intersection of the free surface and the body surface. In that paper these two points were put in "by hand" and their positioning justified by appeal to earlier experiments. Although the results of the calculation and overturning of the body were predicted with fairly good accuracy, this is probably because any slight misplacement of the intersection points would have only a small influence on the very large overturning moment. For most other problems (e.g., radiation of waves into calm water by large body motions), non-linear theory will show only comparatively small changes from the results predicted by transient linear theory (see e.g., Maskell and Ursell (1970)). In this case it is clearly essential to place the intersection points accurately, but one then runs into a fundamental problem; namely, that at least within linear theory, the velocity potential ceases to be analytic in some cases, resulting in infinite free surface displacements, while in other cases the velocity potential remains regular and the free surface of finite displacement, as in the case of a standing wave against a wall. Indeed Stoker (1948) has shown that the solution to the linearised problem of waves against a wall can be thought of as a summation of two composite standing wave solutions: one is symmetric about the wall and is thus regular, while the other has logarithmic singularity at the wall. Consequently, if the wavefield is prescribed to be an incoming wave at infinity the solution becomes physically unacceptable at the wall, because one

is forced to include both types of solution to satisfy the condition at infinity. Stoker shows that no non-trivial solution which dies away at infinity exists, and thus there is no hope of adding further solutions to avoid this singularity at the origin. This is also proved by Lewy (1950) for the case of waves against a flat dock lying along the negative x-axis. The two types of standing wave solution for this problem, one regular and one singular are presented by Friedrichs and Lewy (1948).

In both cases (wall and dock) we have what Lewy calls a "confluence of boundary conditions". The complementary problem of waves generated by a wavemaker and consideration of possible singularities at the confluences of the boundary conditions has been presented by Kravtchenko (1954). He considers the following problem:

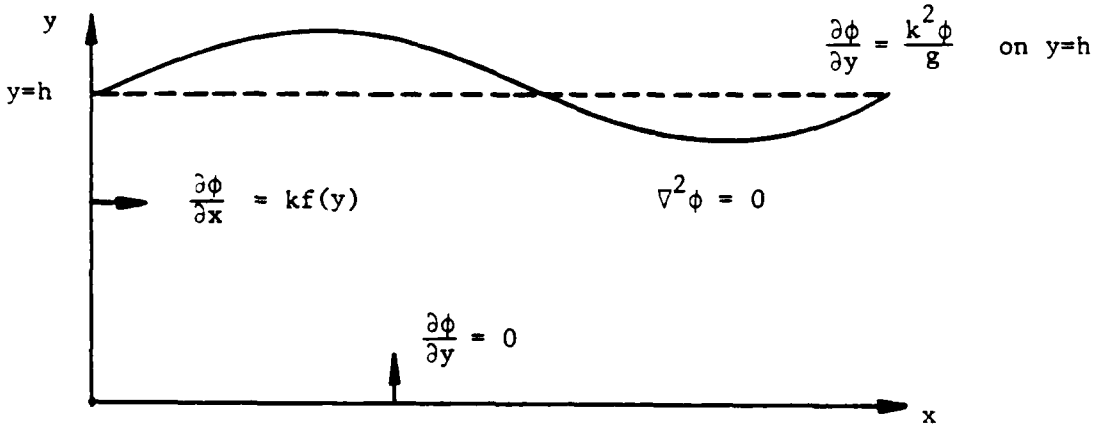

and shows:

$$\left.\frac{\partial^2 \phi}{\partial x \partial y}\right|_{\substack{x=0 \\ y=h}} = \frac{\partial}{\partial x} \frac{k^2 \phi(h)}{g} = \frac{k^3}{g} f(h)$$

while

$$\left.\frac{\partial^2\phi}{\partial y \partial x}\right|_{\substack{x=0\\y=h}} = \frac{\partial}{\partial y}\, kf(y)\,\Big|_{y=h} = kf'(h)$$

so the condition for regularity at the free surface and wavemaker intersection is $g\, f'(h) = k^2 f(h)$; in other words the wavemaker motion must itself have wave-like depth attenuation at the free surface for regularity. Otherwise, Kravtchenko shows that we have a logarithmically singular velocity potential and free surface. Similarly at the wavemaker/bottom confluence we must have $f'(0) = 0$ for regularity.

The above solutions are perhaps of limited relevance to this report because they are steady state solutions, whilst here we deal with essentially unsteady motion. Nevertheless, the conclusion that the only regular solution for the diffraction problems is one which has regular standing waves at infinity is interesting; if we prescribe any other boundary condition here we must expect the behavior at the origin to be singular, and this result may hold for unsteady motions also. This is certainly the case for the impulsive start of a wavemaker described in section 2. A singular solution is predicted which agrees well with the experiments, except around the point of intersection where a jet is formed.

2. THE IMPULSIVE START OF A WAVEMAKER

In order to study the nature of the singularity in time dependent flow we consider perhaps the simplest case possible--the impulsive start of a wavemaker initially at rest in calm water of constant depth h. The closely related problem of impulsive acceleration of a wavemaker is thought to model the initial stages of the motion of a dam under earthquake loading. The linearised theory of this problem has been studied by Chwang and Housner (1978) and also by Chwang (1978). The major concern of these papers is the hydrodynamic pressures up the dam face, and not the free surface displacement. Indeed the boundary conditions at the free surface are actually applied at the undisturbed free surface level. Nevertheless the free surface displacement at the dam can be calculated, and in particular it has elevation proportional to $\tan\theta$ at the dam face. Evidently this is a singularity when θ , the dam angle, is $\pi/2$ (i.e., the dam is vertical) and a simple analogue is given by Housner (1980) to explain its presence. Chwang (1983), on the other hand, solves to first order the initial value problem in a small time expansion. He shows the free surface to be singular at the intersection point, but does not give the simple closed form shown below in equation 2.3 for his infinite summation in the expression for the free surface elevation. Peregrine (1972) considers the wavemaker fixed and the flow at infinity to be uniform and directed towards the wavemaker. One then solves the following problem:

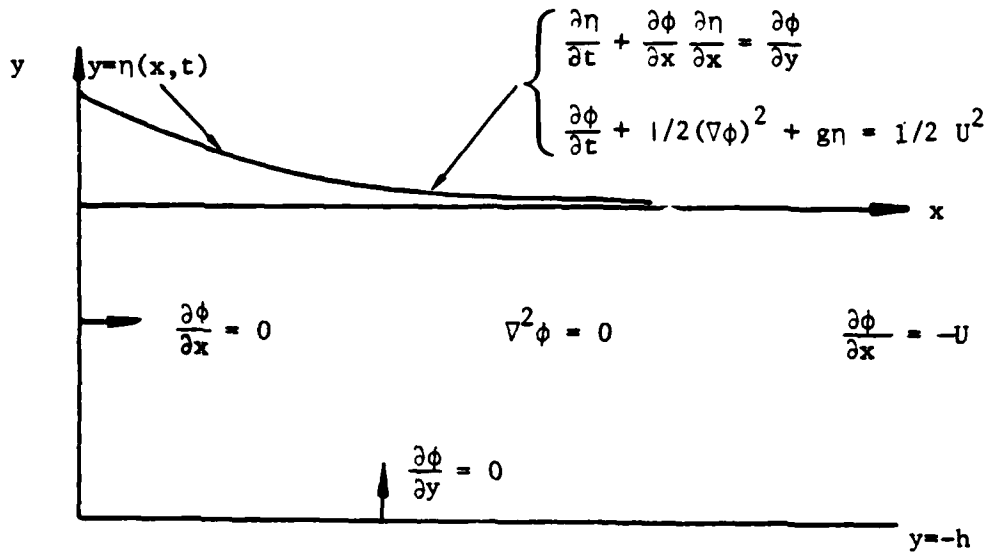

Peregrine shows that the small time expansions:

$$\begin{cases} \phi = \phi_0 + \phi_1 t + \phi_2 t^2 + \ldots \\ \eta = \eta_0 + \eta_1 t + \eta_2 t^2 + \ldots \end{cases} \qquad (2.1)$$

yield the first order solution:

$$\phi_0 = -Ux + \sum_{n=0}^{\infty} \frac{2Uh}{(n+1/2)^2\pi^2} \sin\left[(n+1/2)\frac{\pi y}{h}\right] \exp\left[-(n+1/2)\frac{\pi x}{h}\right] \qquad (2.2)$$

$$\eta_0 = 0$$

$$\eta_1 = \frac{-2U}{\pi} \ln\left[\tanh\left(\frac{\pi x}{4h}\right)\right] \qquad (2.3)$$

Notice that these solutions are still those of the linearised problem with the non-linearity arising only at higher orders of t .

It is clear that the free surface does become singular, so that further approximations become more singular. This is also the conclusion drawn by Newman (1982) who treats the infinite depth case using Lagrangian analysis. (For the related problem of dam breaking using the same type of analysis see Stoker (1957).) Lin (1983) has extended this analysis to finite depth giving the same result as equation 2.3 although he has not been able to obtain higher order solutions yet. Nevertheless we appear to be dealing with a singular perturbation scheme (see Van Dyke (1975)), which although valid throughout most of the fluid, ceases to be valid near the wavemaker. This suggests some sort of matching of inner and outer solutions and Peregrine (1972) attempts to find a suitable inner solution. Since it is not clear what solution should be it was decided to photograph the flow. This apparently had not been done before and the results are interesting and surprising.

Experimental Details

In order to photograph the impulsive flow generated by the wavemaker a small tank was built of 1/2" plexiglass sheet as shown in figure 2.1. The sledgehammer was drawn back with the wire to any prescribed stroke, and then released to fall under gravity striking a steel plate at the rear of a stiff wooden wavemaker. Contacts, one of which was at the top of the wavemaker and the other fixed, were used to trigger an electronic flash unit when the wavemaker reached

any desired position. Another circuit triggered an oscilloscope when the wavemaker started moving and a signal from the flash unit to the oscilloscope provided a very accurate method of timing the photographs (to within 0.001s). We used a conventional 35mm camera with the shutter held open before the flash in an otherwise dark room. The flash, of duration less than 0.6×10^{-6} s and 10^{8} peak candle power, was easily sufficient to provide good illumination and freeze the motion of the fluid and wavemeker.

Results and Discussion

Figure 2.2 shows the effect of water depth when the wavemaker is struck by the sledgehammer released from its full stroke position. In all cases we note that the water rises smoothly up the wavemaker and ejects a jet from the intersection point. It should be noted that these effects are extremely difficult to see without photography because the entire sequence shown only last about 0.2 seconds. Before detailed examination of the flow we make the following remarks:

i) In the cases examined the free surface always rises up the wavemaker becoming almost parallel to it before a jet is ejected at a considerable angle to the wavemaker (almost perpendicularly). The smooth free surface never approaches the wavemaker at large angles as in more moderate wavemaker behavior usually observed in wave tanks.

ii) The ejected jet quickly breaks up under the action of surface tension and possibly air currents caused by the wavemaker. This results in spray.

iii) As the wavemaker slows down the jet grows and "peels off" the wavemaker surface; see photo #1/2 in figure 2.2.

iv) On the basis of #1/17 and other photographs in figure 2.2 we conclude that the flow is very uniform across the tank and hence is a two-dimensional flow. (The ejected jet however quickly breaks up.)

v) The finite radius of the wavemaker results in the lower edge getting close to the free surface and flow under the wavemaker. This has an important effect upon the flow, shown in figure 2.3, for small water depths but does not appear to be important in deep water, at least on the "positive" side of the wavemaker.

vi) The photographs #1/23,#1/24 and #1/25 in figure 2.4 are in some ways relevant to numerical simulations of the bow and stern wave problem, where initial start-up from rest with constant velocity or acceleration would result in similar profiles. Dagan and Tulin (1972) propose a model for bow wave breaking in which a jet rises up the bow and does not return to the fluid, and this is probably a good approximation in the early stages. At later times however a quasi-steady turbulence region forms in front of the bow (see Dagan (1972)). Turbulence also appears to be important at the stern except in the special case where the wave leaves a transom stern at its lowest point horizontally.(See Coleman and Haussling (1981) who show that in this case the numerical simulations of the initial value problem approach the steady state solution of Vanden-Broeck (1980).)

vii) There is some flow around the sides of the wavemaker due to the small clearance needed (about 2mm each side). This results in some disturbance of the smooth profile on the positive side of the wavemaker and the falling water on the negative side adds to an already turbulent region close to the wavemaker; see photos #3/7, 3/8, 3/9, 3/10 and 3/11 in figure 2.5. (The light area on the right of these photos is due to rather poor reflection by a foil mirror used to illuminate the positive side of the wavemaker.)

Let us consider the flow for a depth of 10 cm in more detail on the positive side of the wavemaker. A time sequence is shown in photographs #4/1, 4/2, 4/3, 4/4, 4/6, 4/7 and 4/8 of figure 2.6, while figure 2.7 shows that over the short duration of the experiment the wavemaker velocity (taken at the undisturbed surface level) was essentially constant at 1.39 m/s. Figure 2.8 shows a comparison of the theoretical result from equation 2.3 and the experiments. Because the wavemaker rotates rather than translates it is necessary to measure the x-coordinate out from the wavemaker at the height y. Nevertheless the agreement between the theory and experiment is excellent and similarly good agreement is found for other water depths (20 cms in figure 2.9 and 30 cm in figure 2.10 where we encounter a considerable vibration in the tank). Not surprisingly the theory breaks down at the actual point of intersection and we have a jet ejected at a very large angle to the wavemaker. This jet's existence does not seem to be due to either surface tension or wavemaker roughness: as an example, photo #6/19 of figure 2.11 shows the result with a smooth plexiglass front to the wavemaker and soap solution in the water. The surface profiles are identical except for

the jet which breaks up in a slightly different fashion, presumably because of the altered surface tension.

A consequence of the theoretical result (equation 2.3) is that when the wavemaker reaches the same position, the free surface profile will be the same, regardless of the initial speed U (provided this is constant during the experiment). Photographs #2/3 and 2/18 in figure 2.12 show two runs photographed when the wavemaker reaches the same position but initially having very different velocities, as can be seen from the times (and the water falling behind the wavemaker). On the positive side of the wavemaker however the free surface profiles are virtually indistinguishable as predicted by the theory.

It therefore seems that we have an excellent description of the outer fluid region away from the wavemaker which breaks down in the inner region very close to the wavemaker. One is forced then to consider the question of whether potential theory can describe this region also, in some local model which could subsequently be matched to the outer region. It is known that jet-like solutions exist as solution to gravity free potential flow problems and Longuet-Higgins (1980) proposes that the Dirichlet-hyperbola is a suitable model for the jet in a breaking wave. Similar, perhaps non-rotating, models could be used in the present context also but we have the additional boundary condition to satisfy on the wavemaker (at least locally). An alternative, and possibly easier approach is the semi-Lagrangian approach of John (1953) which has been applied to the jet region by Longuet-Higgins (1983) and also the entire overturning region by

Greenhow (1983). It may well be possible to extend this latter model to include the wavemaker boundary condition and some preliminary work to this end will be presented in the future.

Alternatively the position of the intersection point from the experiments could be used as input to a purely numerical calculation as in Greenhow (1982).

The analogy with, and the suitability of the breaking wave jet solutions may not be apparent in the present case. The next solution describes the high speed water entry of a wedge: here similar jets are ejected and the resulting flow looks very similar indeed to a breaking wave's crest region. In any case the fluid flow for either problem is highly time dependent and will require suitable theories, like John's approach, which at present require gravity to be neglected. This is probably realistic in the local region of the jet.

3. THE HIGH SPEED ENTRY OF A WEDGE INTO CALM WATER

We now look at the problem of a wedge falling under gravity for some distance before penetrating the free surface of calm water. This problem is relevant to the slamming of ships and has received considerable attention in the past. Most recent experimental work has been concerned with measuring the pressures on the body as it enters the water, especially when the deadrise angle (angle between body and free surface) is very small. In this case experiments show a considerably smaller pressure than those predicted by theoryμ see Chuang (1967). Ogilvie (1963) seeks to explain this difference by allowing the fluid to be compressible, but later work by Verhagen (1967), Chuang (1966), Chuang (1967) and Lewison and Maclean (1968) all show that trapped air between the body and free surface is important because it causes a deflection of the free surface before the body makes contact with it. Lewison and Maclean also show that if the deadrise angle is small enough ($<2^{\circ}$ or 3°) air is forced down into the water forming effectively a single phase. This effect called πcoalescenceπ may be important in the related problem of wave impact on flat members (see Kjeldsen (1981)). In our experiments we do not encounter either of the above effects, and so we can ignore the air, and the compressibility of the water entirely.

The wedge data is shown in figure 3.1. Each wedge is ballasted with lead shot to depth b except in the photos #20 in figure 3.12,

where we increased the mass of the wedge to 1.262 Kg to ensure that the wedge did not slow down appreciably during the first stages of entry. This does not appear to make much difference to the free surface profile although the body dynamics are altered when the wedge penetration is large. For the other wedges considered the velocity was essentially constant during the early stages of entry as can be seen from the photograph times (accuracy $\pm$ 0.005s).

In all cases the deadrise angles were large and consequently the formula for the maximum keel pressure given by Wagner (see Chuang 1967) is expected to hold. However, no systematic experimental study of the free surface displacement after entry appears to be available and the current experiments attempt to fill in this gap (some experimental results are shown from figure 3.2 to 3.12) so that comparison may be made with existing theories, which fall into two basic groups:

i) Transient linear theory. Yim (1971) and Chapman (1979) have both treated the problem by linearising around the undisturbed free surface but treating the body condition exactly. Both works include gravity and Chapman gives free surface profiles which do not rise up the wedge as high as in the experiments and for which no jets are ejected (see figure 3.13). A linearised theory of water entry in the large Froude number limit (essentially ignoring gravity) has been given by Moran (1961) who regards both water entry and exit of slender bodies as equivalent problems. (This is certainly not the case for the cylinder entering (section 4) and exiting (section 5) through the free surface, although the cylinder is clearly not a

slender body.)

ii) Self-similar flows. The theories of Dobrovol'skaya (1969) and Garabedian (1953) both ignore gravity, which is probably a good approximation for the high entry speeds of the experiments, and seek solutions in terms of similarity variables x/Vt and y/Vt where V is the velocity of entry. Within this framework both solutions are fully nonlinear both in regard to the actual position of the wedge and the actual position of the free surface. Garabedian treats oblique wedge entry but his solution is not entirely physical since the free surface pressures are unequal on either side of the wedge. Nevertheless, his method is interesting being closely similar to the method of John (1953) for time-dependent free surface flows but with the additional assumption of self-similarity built in. We discuss John's method and its possible application below.

Dobrovol'skaya's solution is for symmetric wedge entry and gives much more realistic free surface profiles than those of linear theory (the free surface overturns for example). However the self-similarity assumption appears to be too restrictive, and the theory cannot predict the jets which essentially develop in a non-self-similar way (see Longuet-Higgins (1983)). A comparison is given in figure 3.13. It is seen that the lack of the jet results in incorrect profiles and in particular the water rises too far up the wedge in the self-similar solution.

It is interesting to compare the surface profiles generated by the wedge entry with the ellipse solution of New (1983). In that

paper New seeks to model the underside, or loop, of a plunging breaker by a relatively simple elliptic solution of John's (1953) free surface equation:

$$z_{tt} = ir(w,t)\, z_w \qquad (3.1)$$

New finds that his elliptic solution has much in common with the breaking wave loop having strong rotation about the ellipse, as well as the ellipse rotating as a whole, and remarkably accurate free surface comparisons over a limited part of the wave when compared with numerical calculations and experiments. The eccentricity of the ellipse, which is left undetermined by the theory, is chosen to be $\sqrt{3}$ for good fits to the breaking waves loop, although the reason for this number is unexplained. Another interesting feature of the solution is that the r-function in equation 3.1 is $r = (1 + t^2)^{-2}$, which in the large time limit is identical with the r-function of the Dirichlet-hyperbola of Longuet-Higgins (1983). Thus Greenhow (1983) was able to combine solutions of both the loop and the jet in the large time limit to give a fairly complete description of the overturning of the crest, although no attempt was made to match to the outer flow.

In the present case we might also expect solutions of equation 3.1 to be valid, with unknown constants arising in the theory being determined by satisfying the body boundary condition. Certainly comparison of the elliptic solutions of New with the loop region arising from the wedge entry (see figure 3.14) gives very strong support to this conjecture. In this case we need solutions of

equation 3.1 generated with $r = (1 + t^2)^{-2}$ instead of the large time limit as in Greenhow (1983) and Longuet-Higgins (1983). An exact parabolic flow for the jet has already been found, as well as other solutions, but as yet no attempt has been made to compare with the experiments; nor has the body boundary condition been satisfied. Nevertheless the approach is very promising and will be developed further. It is particularly interesting that $\sqrt{3}$ - ellipses fit all the wedge experiments regardless of the wedge angle: consequently one might expect them to be valid for cylinder entry also, regarding the entry angle as variable. We explore this in the next section.

4. THE HIGH SPEED ENTRY OF A CYLINDER INTO CALM WATER

We now consider the free surface profiles caused by a cylinder dropped into calm water. The problem is of considerable importance to the offshore industry where cross members may be in the splash zone of the incident waves, and therefore continually entering (exiting) the water. The comparison and in some cases equivalence of the slamming problem with the splash zone problem has recently been studied extensively by Ridley (1982). Theoretical work on the problem is somewhat limited in scope: Faltinsen et al (1977) model the problem by linear theory with gravity omitted. This simple approach, probably valid for high entry speeds, appears to be well justified by the experiments of Sollied (1976). Although Sollied has filmed the resulting flow his photographs only show elevations of the free surface and not depressions, and the fluid motion is not that clear. We present a detailed sequence of photographs (figures 4.1 and 4.3) for water entry of a half-buoyant and neutrally buoyant cylinder.

As previously mentioned it is possible to fit the $\sqrt{3}$ - ellipse of New into the loops of water caused by the cylinder entry (see figure 4.5). A new feature displayed by the cylinder is the remarkable straight lines of the cavity formed behind the cylinder. The jets thrown up eventually become unstable and the collapsing cavity behind the cylinder throws up another jet. The shape of this jet is conjectured to be very similar to a non-rotating Dirichlet hyperbola: McIver and Peregrine (1981) show that the crest of an overdriven standing wave is related to this flow, given by Longuet-Higgins (1972). Figure 4.6 compares the present experiment

with the profile given by McIver and Peregrine, with fairly good agreement around the crest. While the free surface is quite difficult to define in this case, it is interesting to speculate if such flows are common to all final stages of water entry. Some recent studies of axisymmetric, rather than 2-dimensional, jets of this type have been studied by Longuet-Higgins (1983), Milgram (1969), Laventier and Chabat (1977), and Harlow and Shannon (1967), for a variety of methods of exciting this ejected jet. Nevertheless, all the jets appear to have very similar form and closely relate to the Dirichlet-hyperbola at least around the crest.

5. THE CYLINDER EXIT PROBLEM

As mentioned previously the cylinder exit from initially calm water appears to be a very complicated and little studied problem. In the photos presented in Figure 5.1, the neutrally buoyant cylinder rests on the tank bottom and is extracted by applying a constant force equal to the cylinder weight. This results in surface elevations above the cylinder and an interesting form of breaking, which Peregrine has termed "waterfall breaking". It is likely that vortices shed by the cylinder interact with the free surface to complicate the breaking, which may be caused by a pressure inversion across the free surface. (Certainly there will be a region of very low pressure immediately behind the cylinder as it leaves the free surface.) The breaking does appear to be truly two-dimensional and not caused by wall effect (see Figure 5.2).

Despite the lack of solution for this problem there exist some related flows which may shed some light on the problem. A crude approximation might be to ignore the free surface altogether and consider it to be a marked line of particles in an infinite fluid. The resulting deformation of this line for flow caused by a sphere has been given by Lighthill (1955). As far as the body forces are concerned a good approach is probably the method of Faltinsen et al (1977) mentioned in the previous section on cylinder entry.

As far as the free surface elevation is concerned, the related flow caused by a source beneath the free surface has been analysed by Peregrine (1972) and later by Vanden-Broeck et al (1978). Peregrine

shows that there is a limiting strength to the source (also dependent upon its depth) beyond which the flow will not be steady. Vanden-Broeck et al show that Peregrine's expansion always diverges. Nevertheless Peregrine's solution for large source strengths does show a pressure inversion of the type conjectured above and this may lead to breaking.

Obviously the study of this extremely complicated problem is very incomplete at present. From the practical standpoint force measurements are clearly needed; from the theoretical point of view more photographs with different exit speeds, as well as more streamlined bodies will probably be needed to provide inspiration!

ACKNOWLEDGEMENTS

We would like to thank Mr. Paul Eberhardt for building the tank used in the experiments, Professor Edgerton for loaning the electronic flash unit and his advice and encouragement and Dr. D.H. Peregrine for his very useful comments.

REFERENCES

Chapman, R.B. 1979. Large amplitude motion of two-dimensional floating bodies. J. Ship Res. Vol. 23, no. 1.

Chuang, S.L. 1966. Experiments on flat bottom slamming. J. Ship Res. Vol. 10, no. 1.

Chuang, S.L. 1967. Experiments on slamming of wedge shaped bodies. J. Ship Res. Vol. 11, no. 3.

Chwang, A.T. and Housner, G. 1978. Hydrodynamic pressure on sloping dams during earthquakes: Part I. momentum method. J. Fluid Mech. Vol. 87, part 2.

Chwang, A.T. 1978. Hydrodynamic pressure on sloping dams during earthquakes: Part II. exact theory. J. Fluid Mech. Vol. 87, part 2.

Chwang, A.T. 1983. Nonlinear hydrodynamic pressure on an accelerating plate. Phys. Fluids. Vol. 25, no. 2.

Coleman, R. and Haussling, H. 1981. Nonlinear waves behind an accelerating transom stern. Paper II-3. Third Int. Conf. Num. Ship Hydro., Paris.

Dagan, G. 1972. Nonlinear ship wave theory. Ninth Symp. Naval Hydro. Paris.

Dagan, G. and Tulin, M.P. 1972. Two-dimensional free surface gravity flows past blunt bodies. J. Fluid Mech. Vol. 51.

Dobrovol'skaya, Z.N. 1969. On some problems of similarity flow of fluid with a free surface. J. Fluid Mech. Vol. 36, part 4.

Faltinsen, O., Kjeerland O., Nottveit, A. and Vinje, T. 1977. Water impact loads and dynamic response of horizontal circular cylinders in offshore structures. O.T.C. Houston.

Friedrichs, K. and Lewy, H. 1948. The dock problem. Commun. Pure Appl. Math. Vol. 1, no. 2.

Garabedian, P.R. 1953. Oblique water entry of a wedge. Commun. Pure Appl. Math. Vol. 6.

Greenhow, M., Vinje, T., Brevig, P. and Taylor, J. 1982. A theoretical and experimental study of capsize of Salter's Duck in extreme waves. J. Fluid Mech. Vol. 118.

Greenhow, M. 1983. Free surface flows related to breaking waves. J. Fluid Mech. Vol. 134.

Harlow, F. and Shannan, J. 1967. The splash of a liquid drop. J. Appl. Phys. Vol. 38, no. 10.

Housner, G. 1980. The momentum-balance method in earthquake engineering. Mechanics Today. Vol. 5.

John, F. 1953. Two dimensional potential flows with a free boundary. Commun. Pure Appl. Math. Vol. 6.

Kjeldsen, S.P. 1981. Shock pressures from deep water breaking waves. Proc. Int. Symp. Hydro. Ocean Eng. Trondheim, Norway.

Kravtchenko, J. 1954. Remarques sur le calcul des amplitudes de la houle lineaire engendree par un batteur. Proc. Fifth Conf. Coastal Eng., 50-61.

Laventier, M. and Chabot, B. 1977. Effects hydrodynamiques et modeles mathematiques. Editions de Moscou.

Lewison, G. and Maclean, W. 1968. On the cushioning of water impact by entrapped air. J. Ship Res. Vol. 12, no. 2.

Lewy, H. 1950. Developments at the confluence of analytic boundary conditions. Univ. of Calif. Publ. in Math. Vol. 1.

Lighthill, M.J. 1955. Drift. J. Fluid Mech. Vol. 1.

Lin, W-M. 1983. The impulsive motion of a wavemaker-finite depth case. Unpublished note. MIT.

Longuet-Higgins, M.S. 1972. A class of exact, time dependent, free surface flows. J. Fluid Mech. Vol. 55.

Longuet-Higgins, M.S. 1980. On the forming of sharp corners at a free surface. Proc. Roy. Soc. London. Series A. Vol. 371.

Longuet-Higgins, M.S. 1983. Rotating hyperbolic flow: particle trajectories and parametric representation. Q.J. Mech. Appl. Math. Vol. 36.

Longuet-Higgins, M.S. 1983. Bubbles, breaking waves and hyperbolic jets at a free surface. J. Fluid Mech. Vol. 127.

Maskell, S. and Ursell, F. 1970. The transient motion of a floating body. J. Fluid Mech. Vol. 44, part 2.

McIver, P. and Peregrine, D.H. 1981. Comparison of numerical and analytical results for waves that are starting to break. Proc. Int. Symp. Hydro. Ocean Eng. Trondheim, Norway.

Milgram, J. 1969. The motion of a fluid in a cylinder container with a free surface following vertical impact. J. Fluid Mech. Vol. 37.

Moran, J.P. 1961. The vertical water-exit and entry of slender symmetric bodies. J. Aerospace Sciences.

Newman, J.N. 1982. The impulsive motion of a wavemaker. Unpublished note.

Ogilvie, T.F. 1963. Compressibility effects in ship slamming. Schiffstechnik Bd 10. Heft 53.

Peregrine, D.H. 1972. Flow due to a vertical plate moving in a channel.

Unpublished note.

Peregrine, D.H. 1972. A line source beneath a free surface. Math. Res. Center. Univ. of Wisconsin Tech. Report 1248.

Ridley, J.A. 1982. A study of some theoretical aspects of slamming. N.M.I. R158.

Stoker, J.J. 1947. Surface waves in water of variable depth. Q.J. Appl. Math. Vol. 5, no. 1.

Stoker, J.J. 1957. Water waves. Interscience Publishers Inc.

Sollied. 1976. Beregning an krefter pa stag ved slagaktige pakjenninge. Student project. Div. Ship Hydro. N.T.H. Trondheim, Norway.

Vanden-Broeck, J.M., Schwartz, L. and Tuck, E. 1978. Divergent low-Froude number series expansions of nonlinear free surface flow problems. Proc. Roy. Soc. London. Series A. Vol. 361.

Vanden-Broeck, J.M. 1980. Nonlinear stern waves. J. Fluid Mech. Vol. 96.

VanDyke, M. 1975. Perturbation methods in fluid mechanics. The Parabolic Press.

Verhagen, J.H.G. 1967. The impact of a flat plate on a water surface. J. Ship Res. Vol. 11, no. 4.

Yim, B. 1971. Investigation of gravity and ventilation effects in water entry of thin foils in nonsteady flows of water at high speeds. Proc. I.U.T.A.M. Symp. Leningrad.

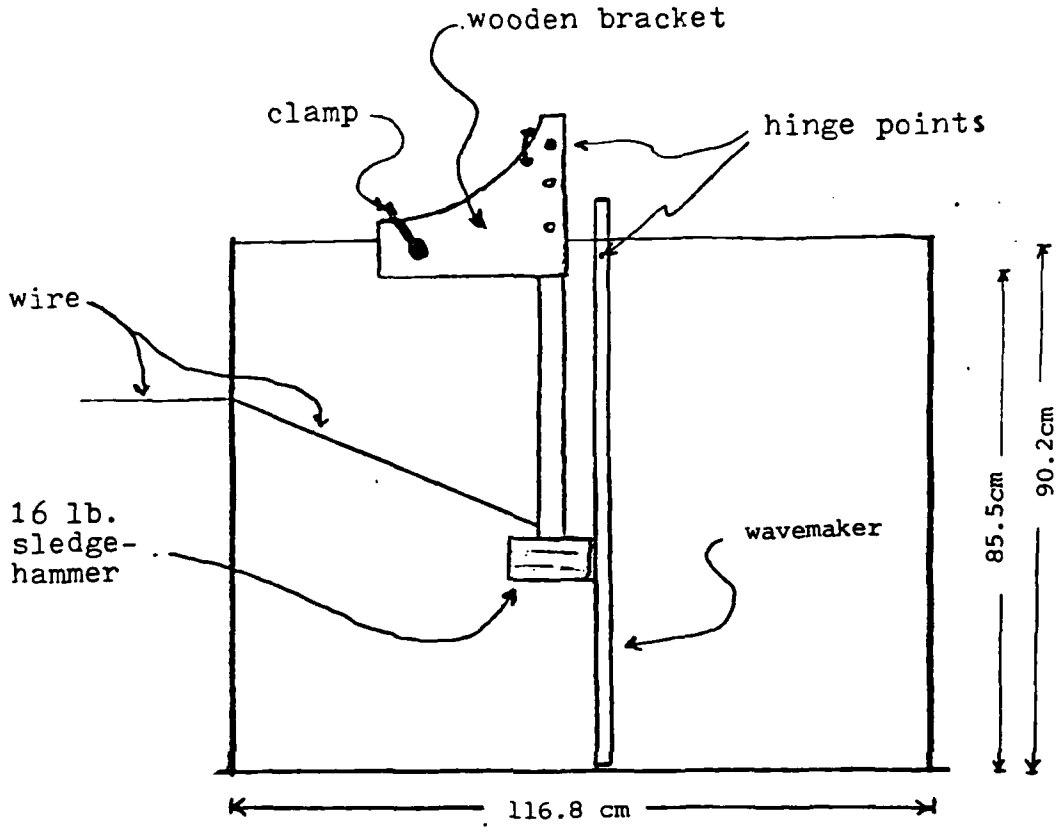

Figure 2.1 Tank configuration, dimension 90.2x10.2x116.8 cms

Depth = 5 cm

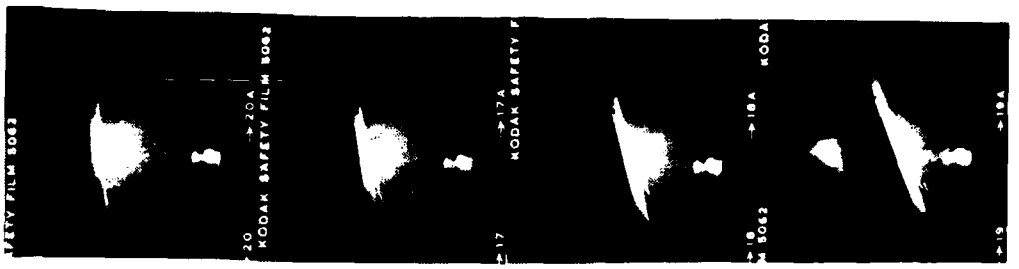

#1/21, t=0.03s #1/18, t=0.08s #1/19, t=0.15s #1/20, t=0.24s

Depth = 10 cm

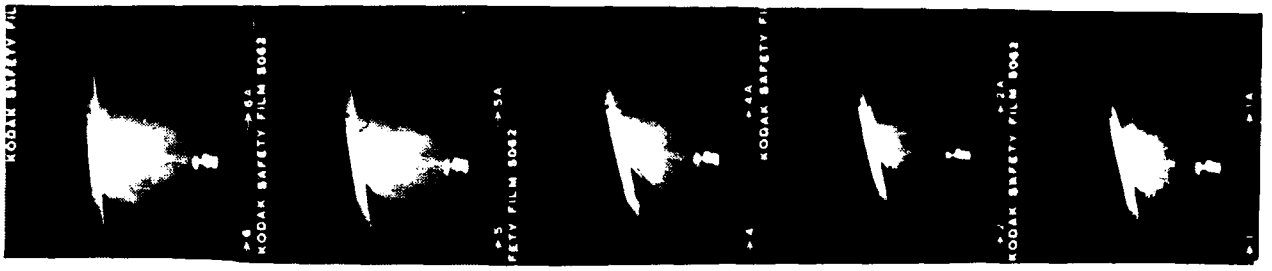

#1/7, t=0.04s #1/6, t=0.08s #1/5, t=0.155s #1/3, t=0.165s #1/2, t=0.17s

Depth = 15 cm

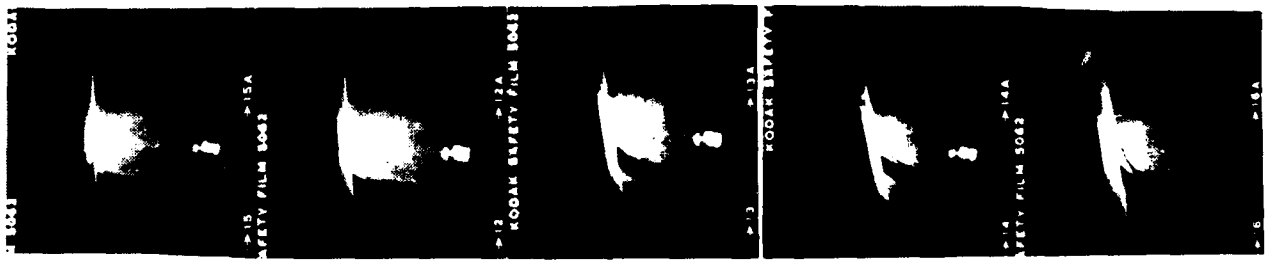

#1/16, t=0.03s #1/13, t=0.06s #1/14, t=0.13s #1/15, t=0.20s #1/17, t=0.13s (oblique view)

Depth = 20 cm

Depth = 30 cm

#1/8, t=0.06s #1/9, t=0.21s #1/10, t=0.21s #1/12, t=0.09s #1/11, t=0.10s

Figure 2.2 Effect of water depth.

Depth = 10 cm, Clearance = 5.5 cm

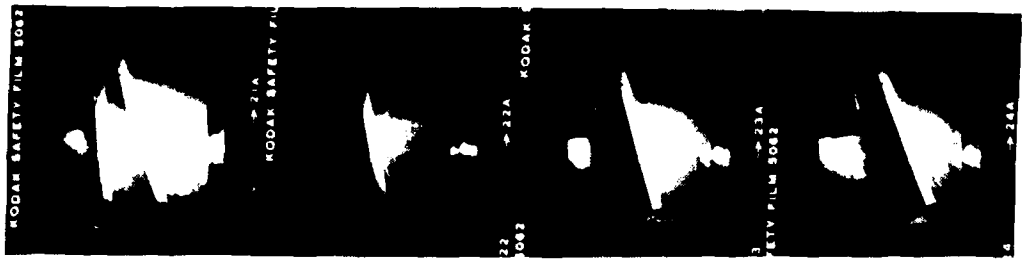

#1/22, t=0.035s #1/23, t=0.095s #1/24, t=0.16s #1/25, t=0.25s

Depth = 10 cm, Clearance = 0.0 cm

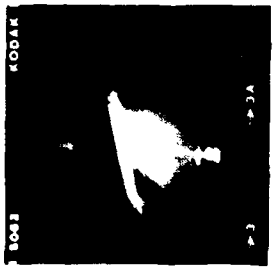

#1/4, t=0.155s

Depth = 20 cm, Clearance = 5.5 cm

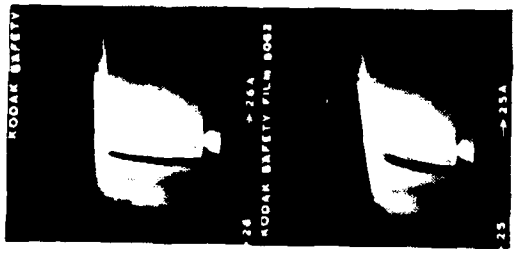

#1/27, t=0.11s #1/26, t=0.125s

Figure 2.3 Effect of bottom clearance.

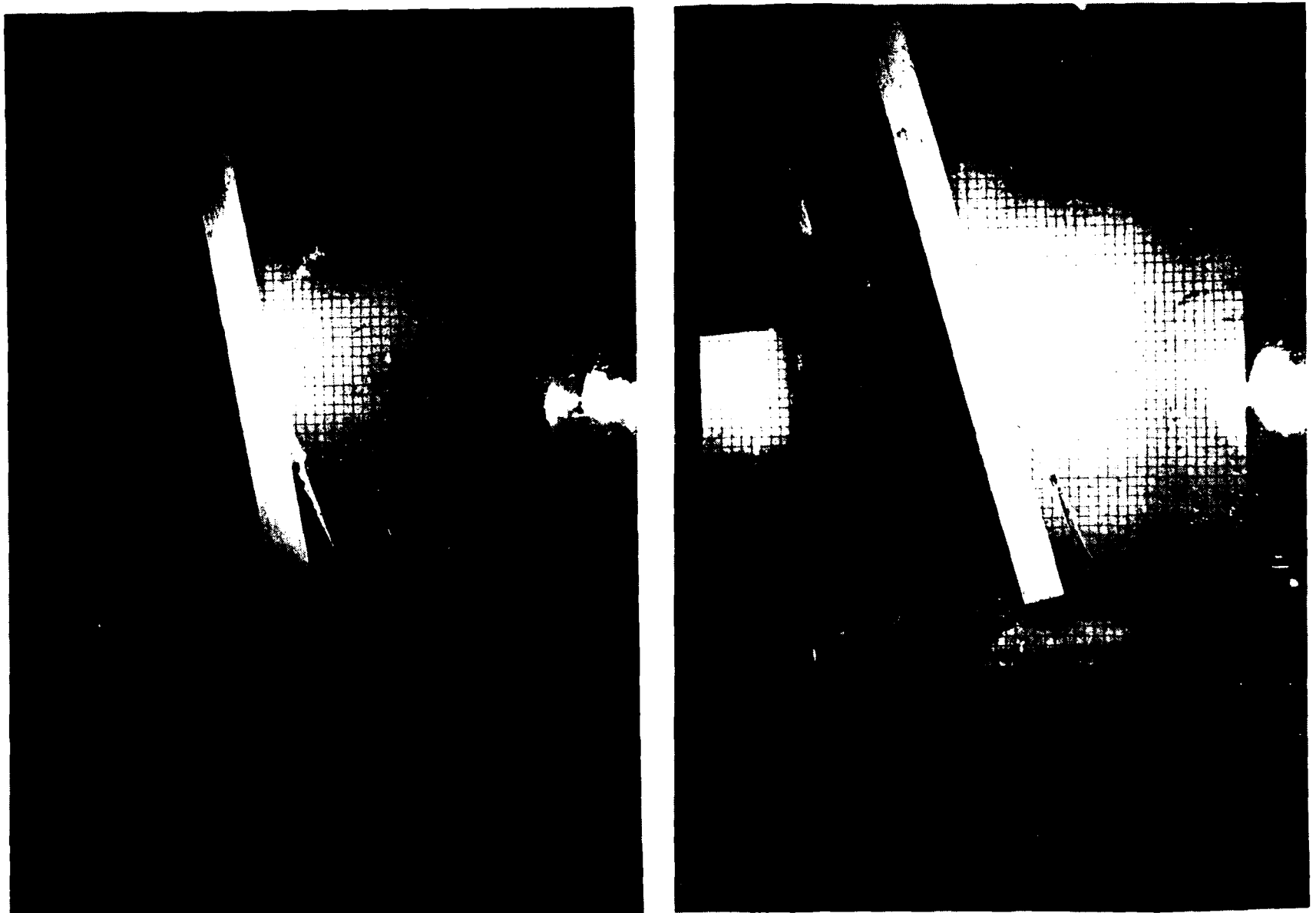

#1/23, t=0.095s

#1/24, t=0.16s

Figure 2.4 Effect of bottom clearance

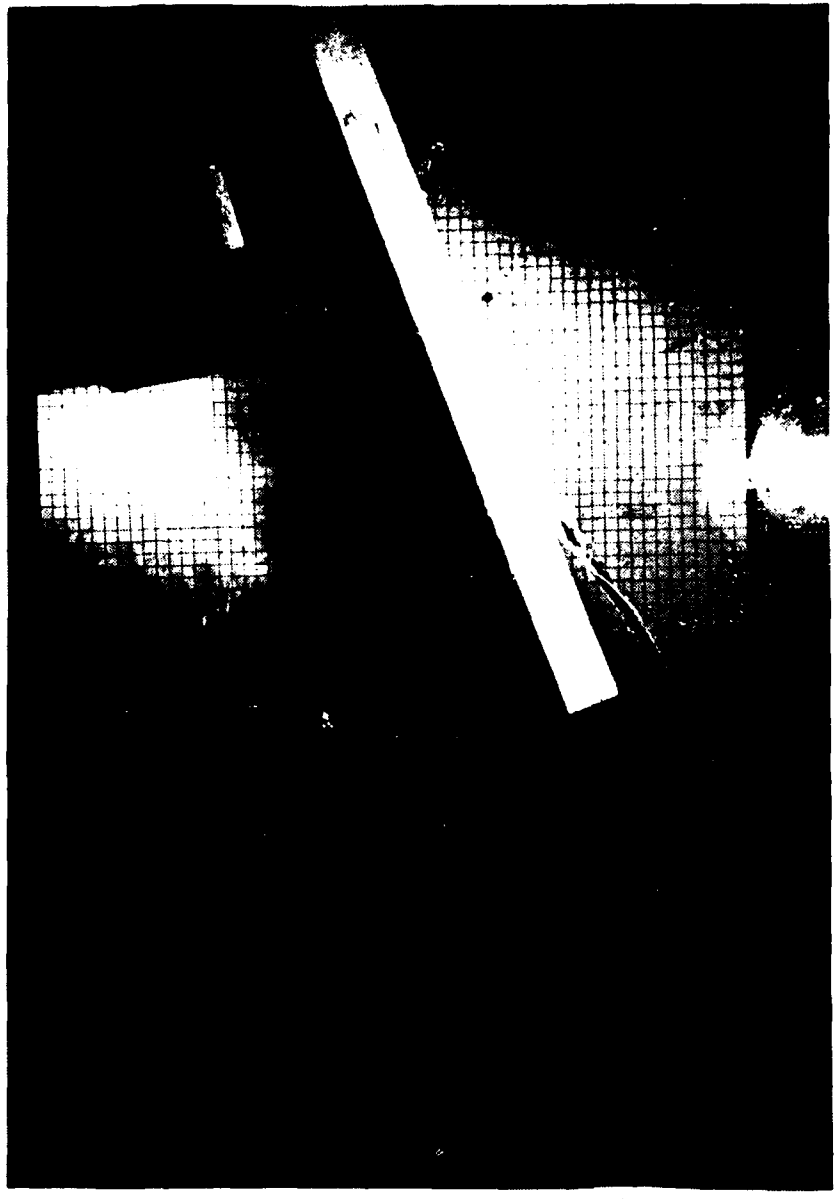

#1/25, t=0.25s

Figure 2.4 (cont'd)

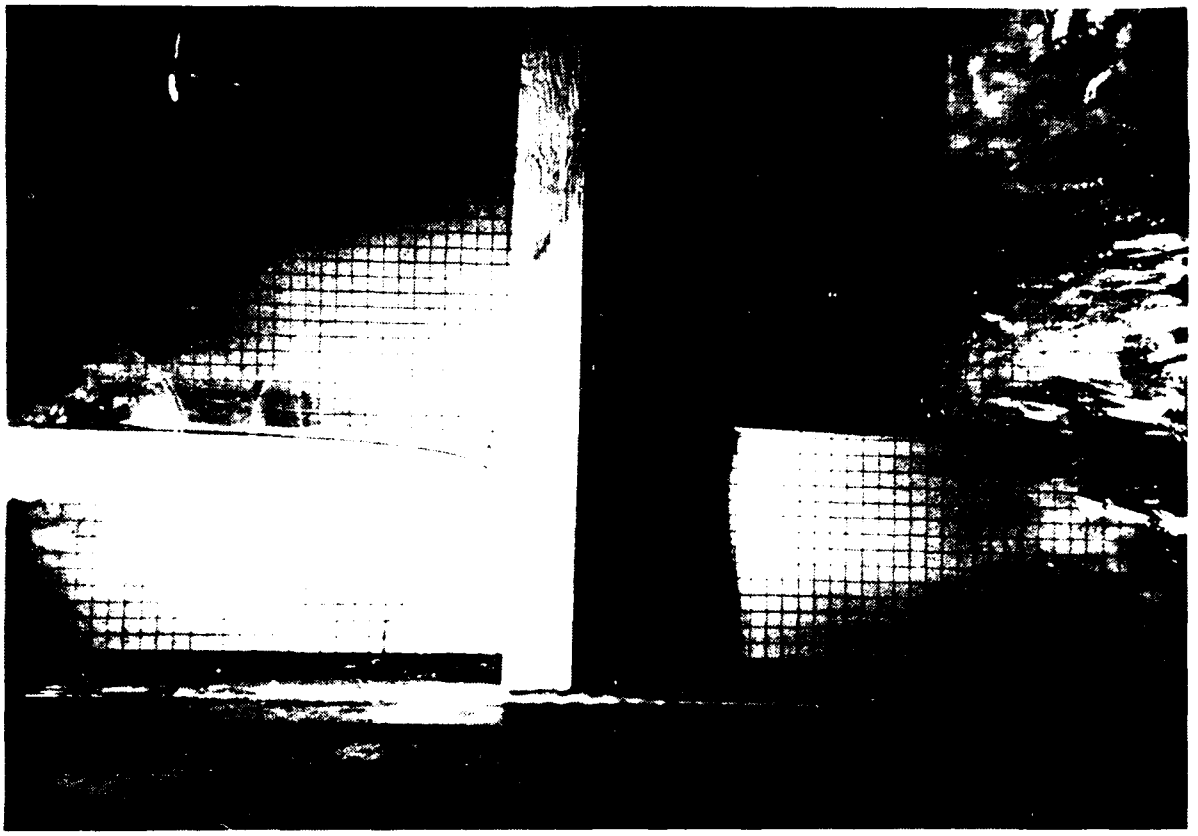

#3/7, t=0.001s

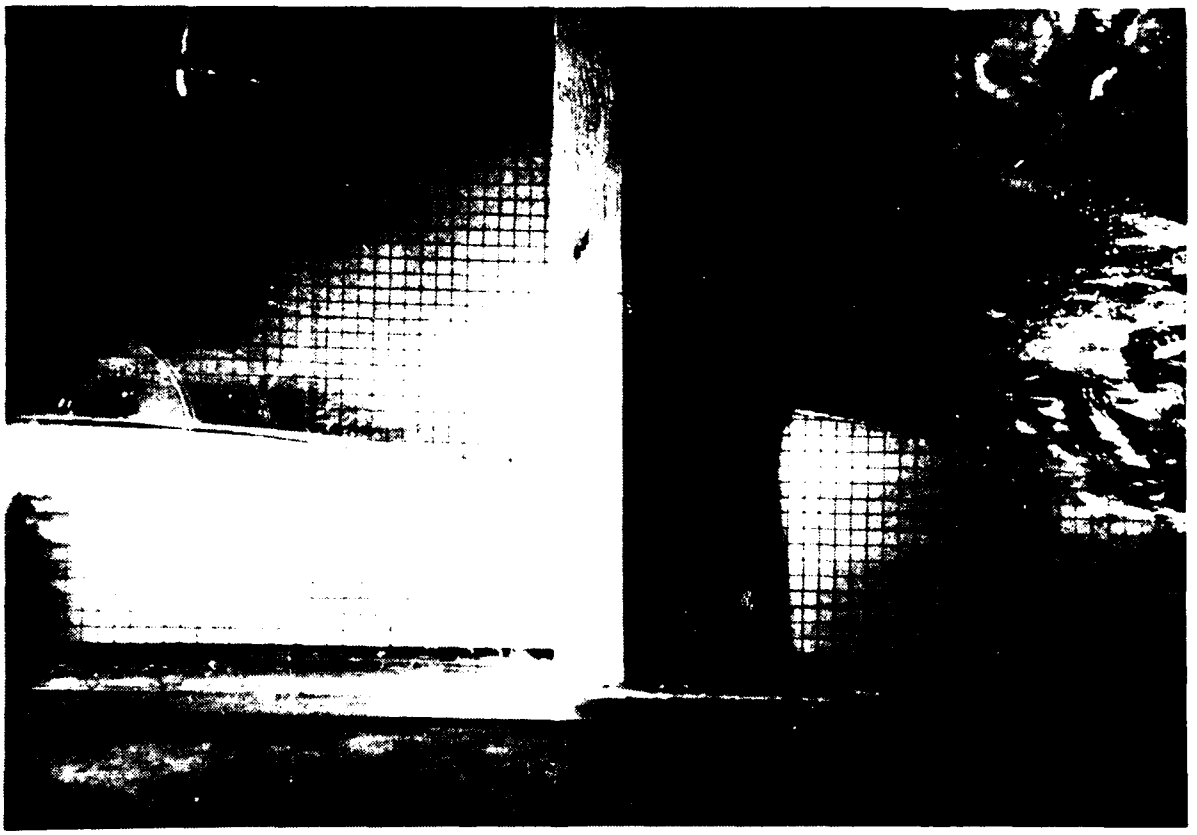

#3/8, t=0.038s

Figure 3.5 Effect of side clearence

#3/9, t=0.062s

#3/10, t=0.096s

Figure 2.5 (Cont'd)

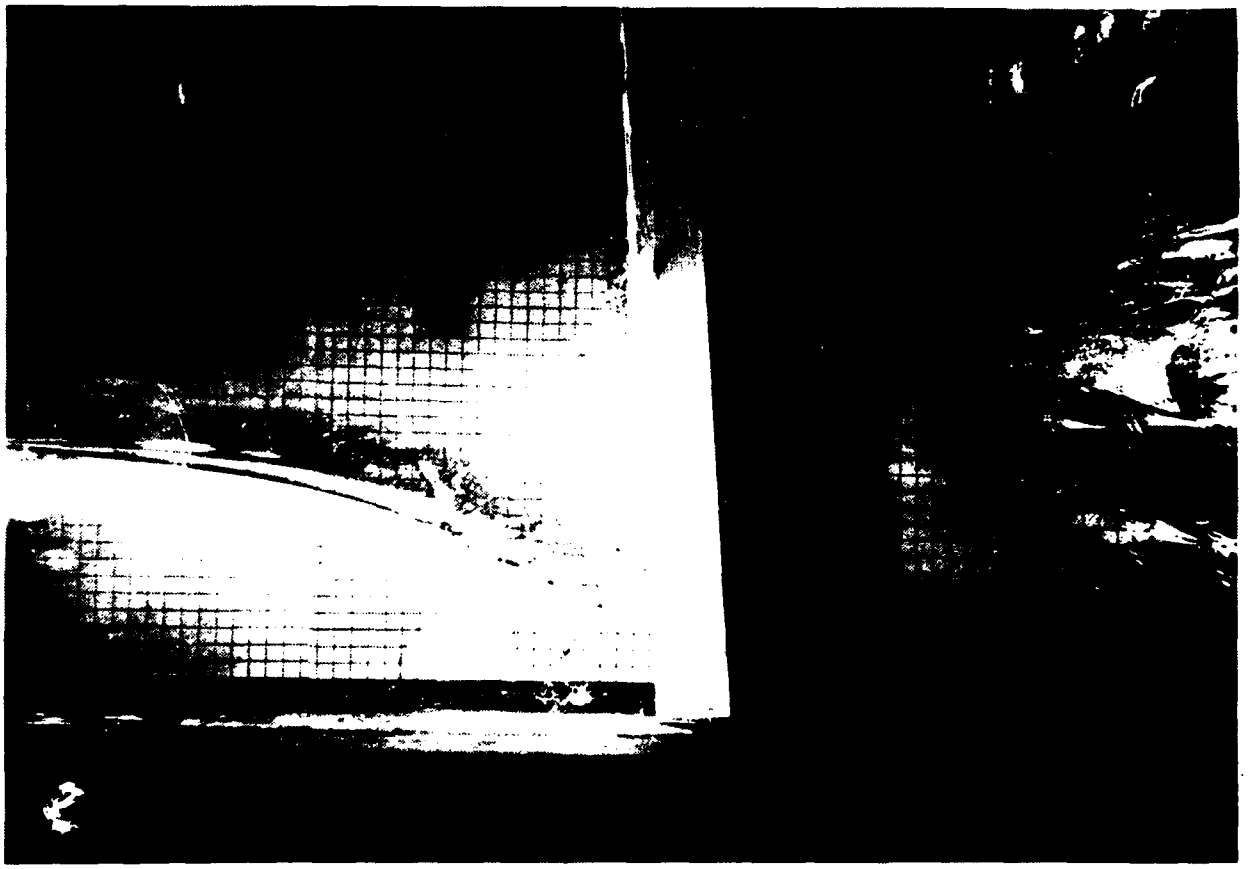

#3/11, t=0.094s

Figure 2.5 (cont'd)

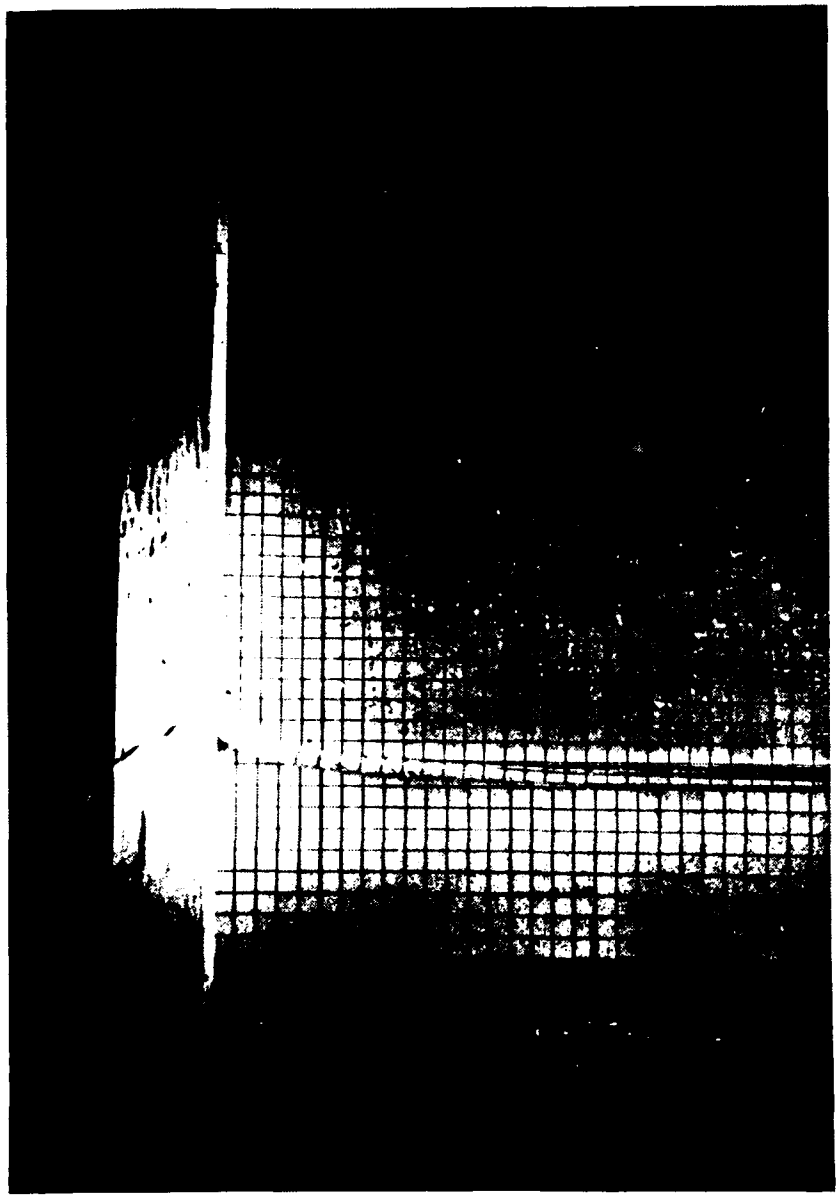

#4/1, t=0.009s

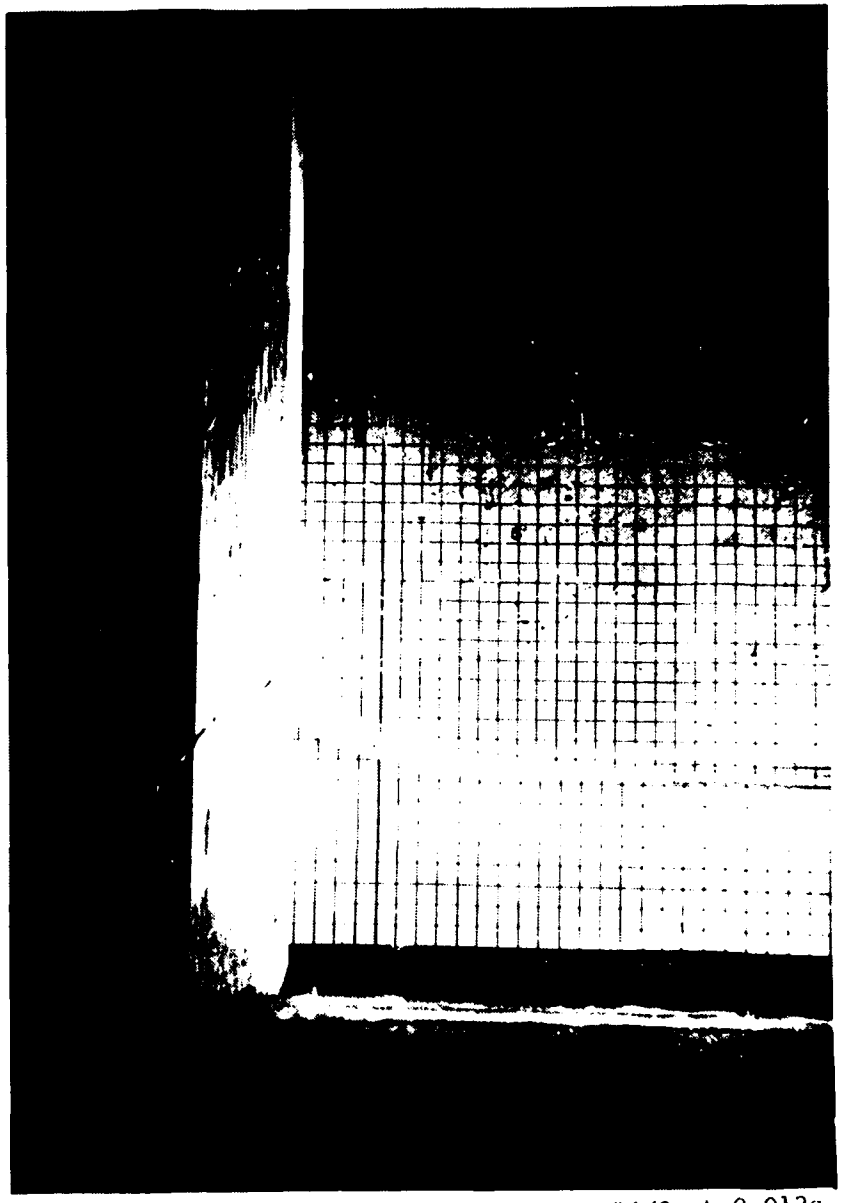

#4/2, t=0.012s

Figure 2.6 Impulsive motion of wavemaker, depth=10 cms

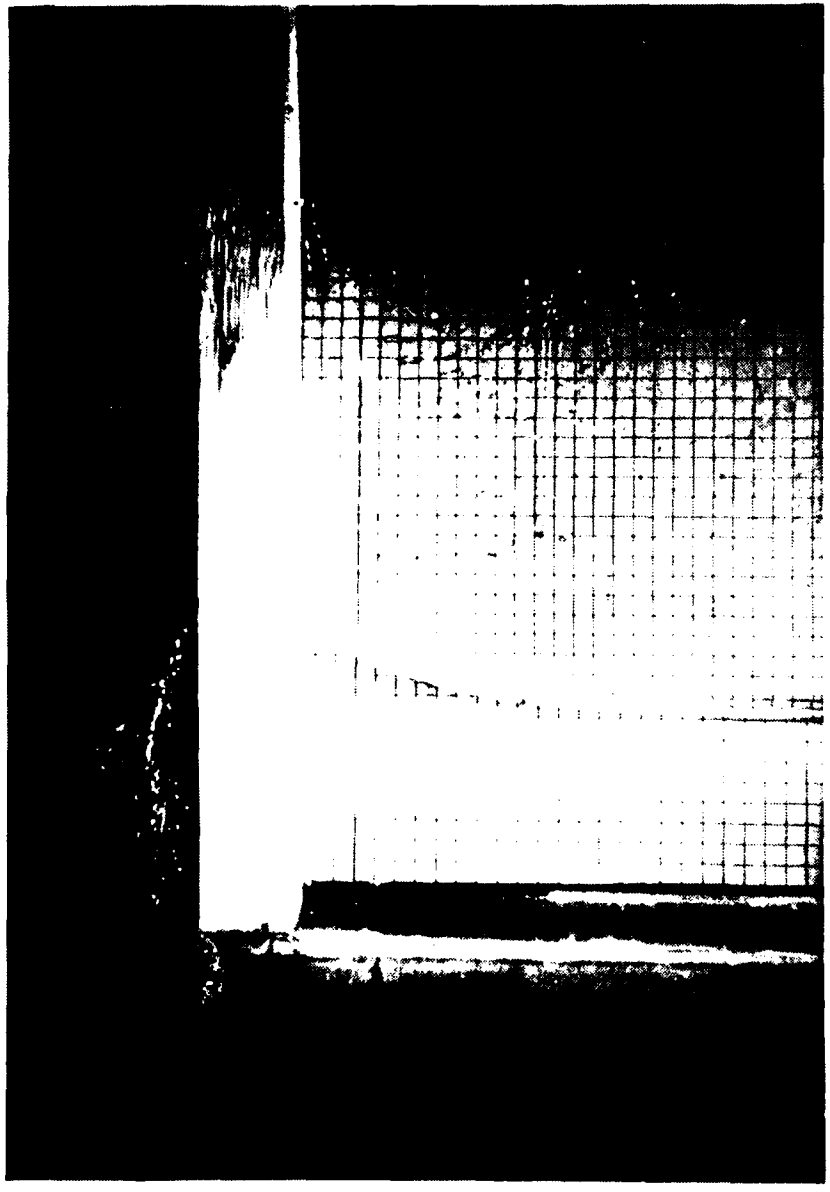

#4/3, t=0.023s

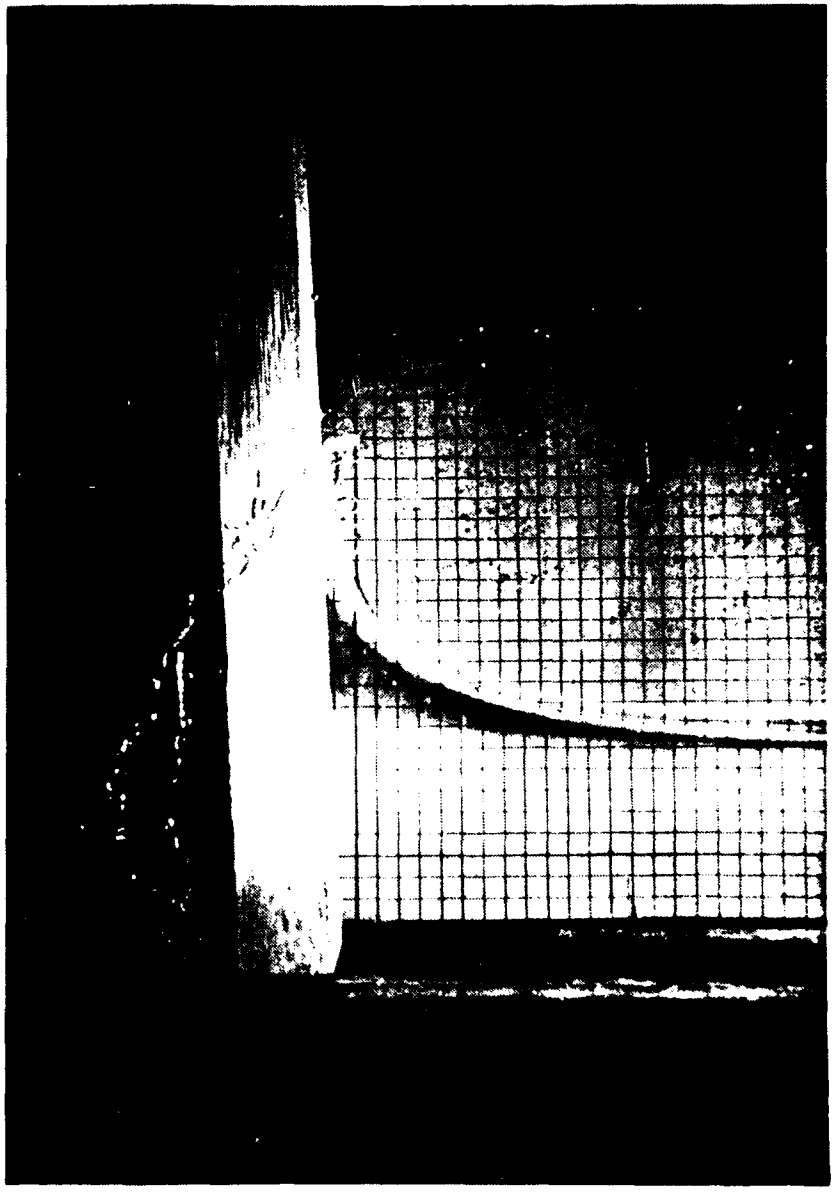

#4/4, t=0.037s

Figure 2.6 (cont'd)

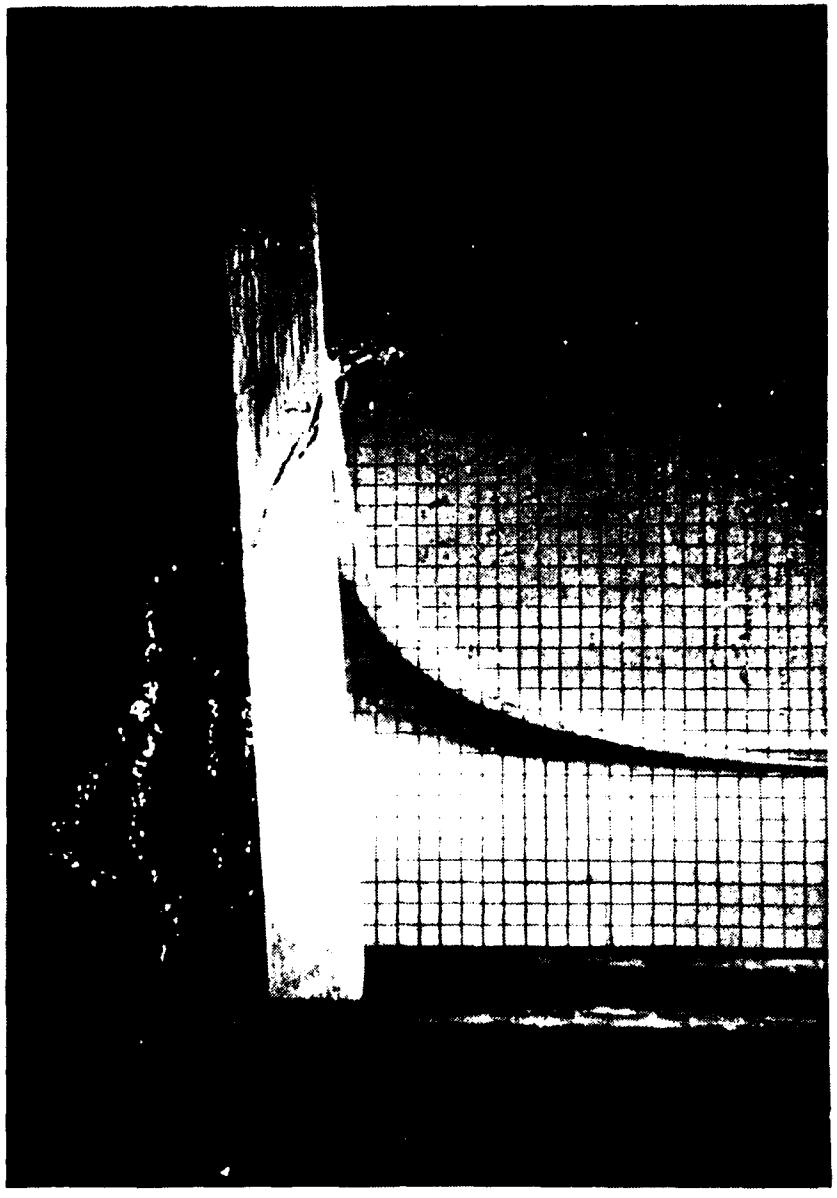

#4/6, t=0.04[illegible]s

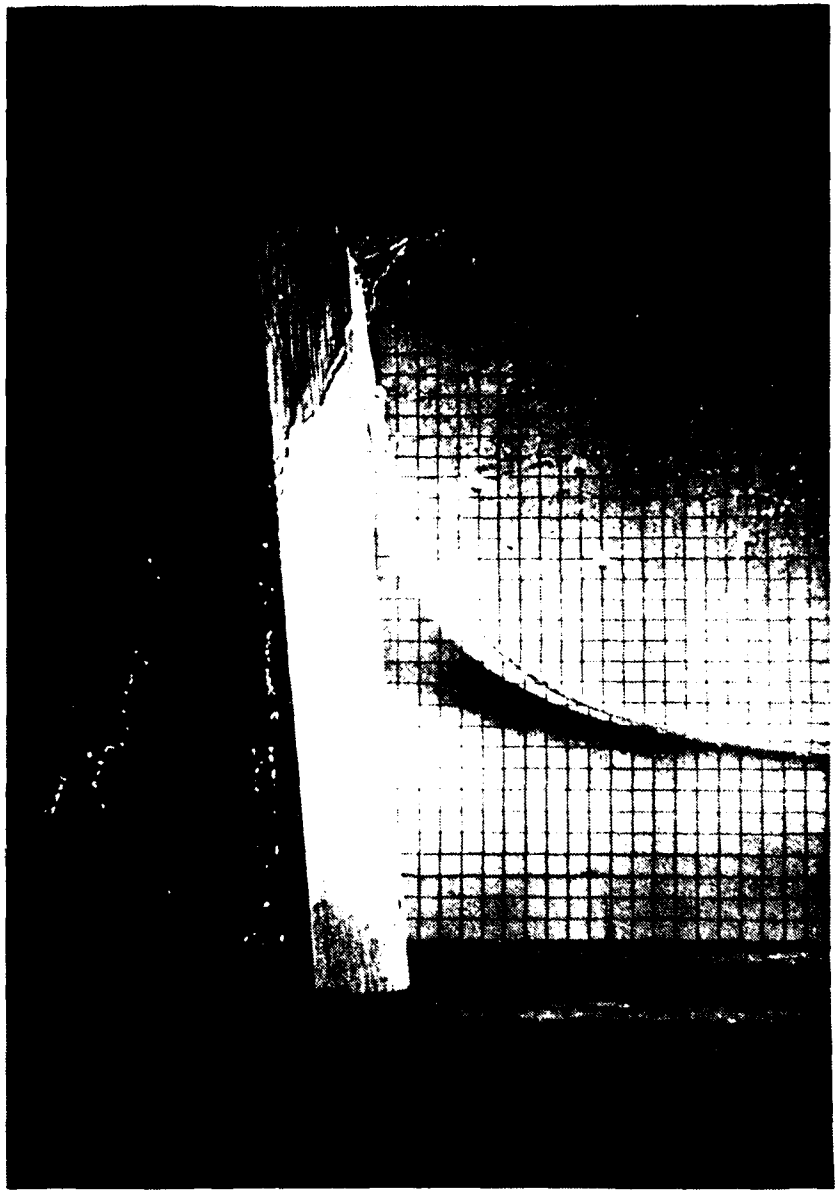

#4/7, t=0.061s

Figure [illegible]

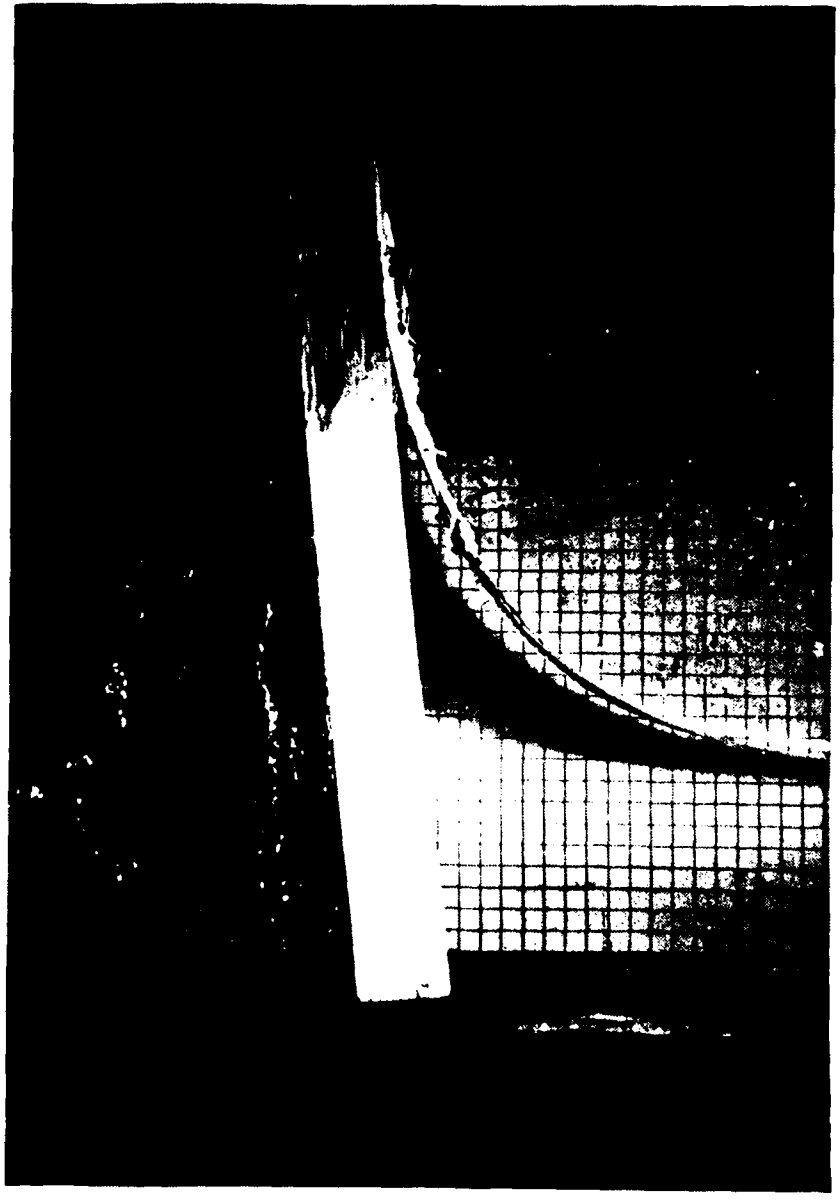

#4/8, t=0.080s

Figure 2.6 (cont'd)

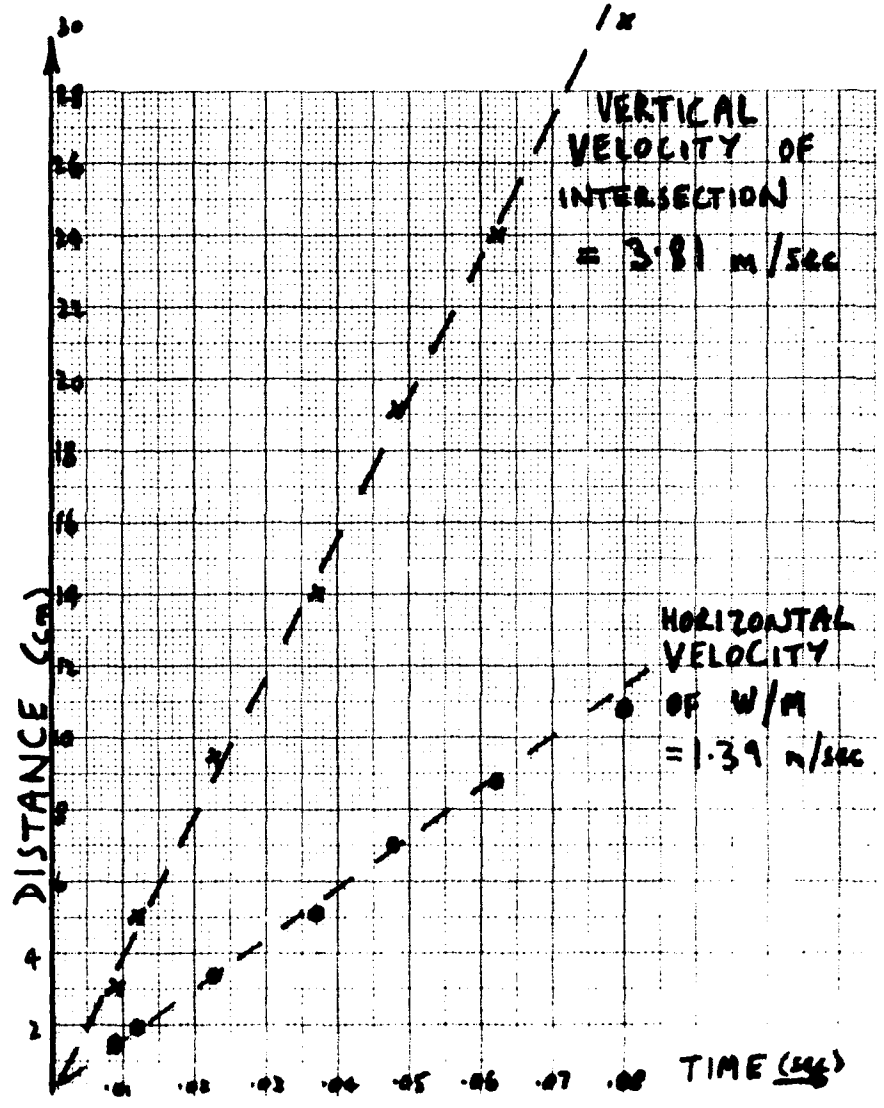

Figure 2.7 Vertical Velocities.

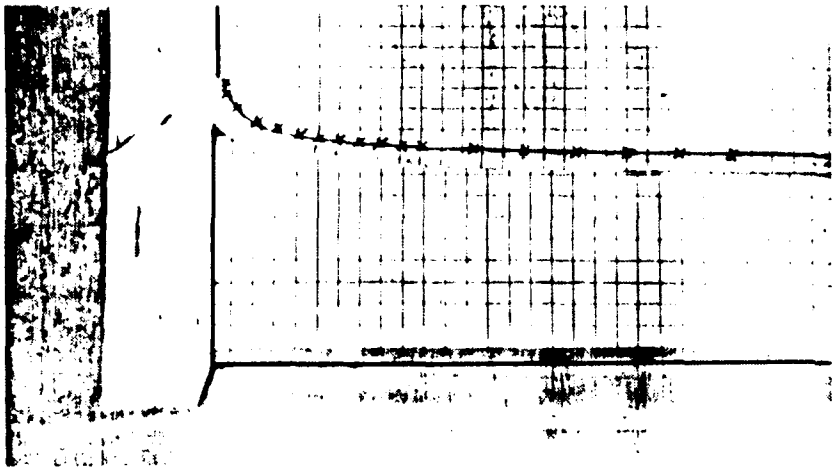

#4/1, t = 0.009s

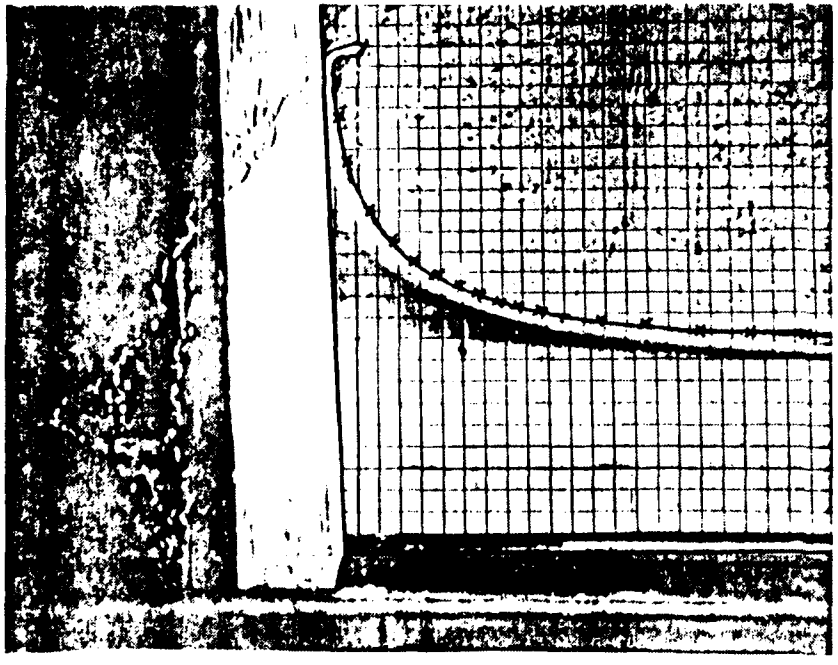

#4/4, t = 0.037s

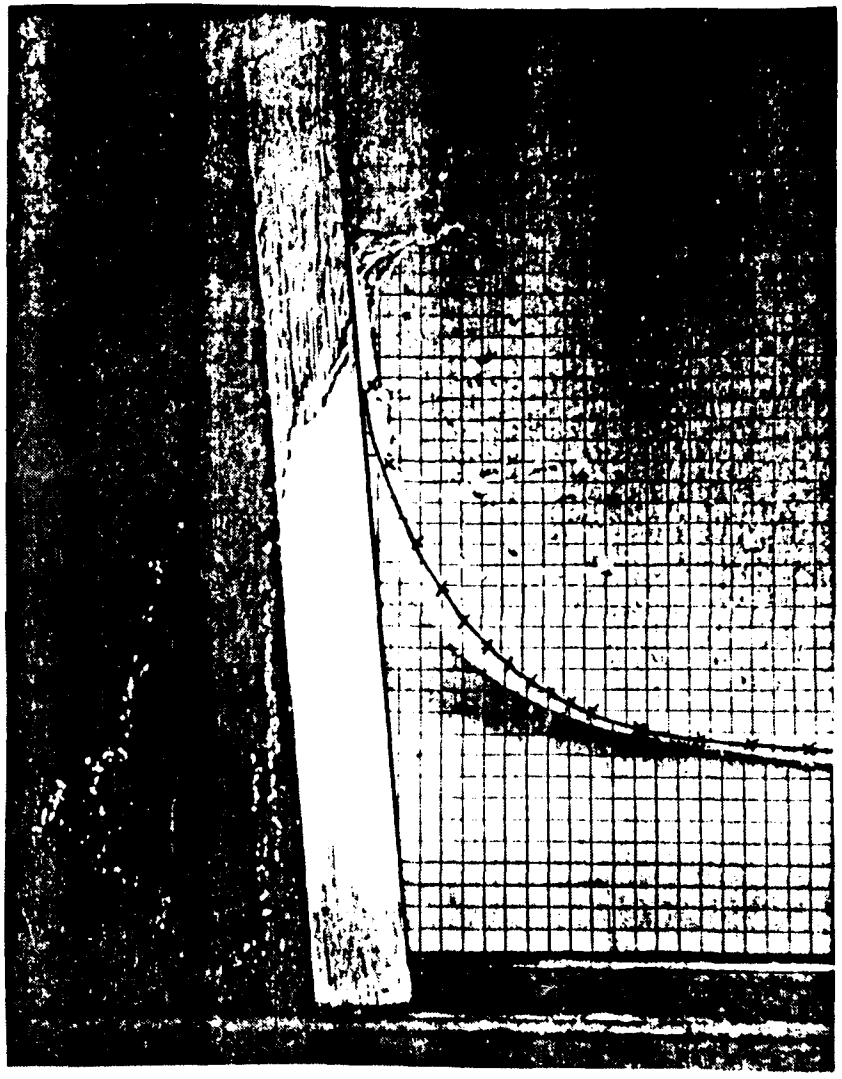

#4/7, t = 0.061s

Figure 2.8 Comparison of theory (x) and experiment (-)

#4/11, t = 0.051s

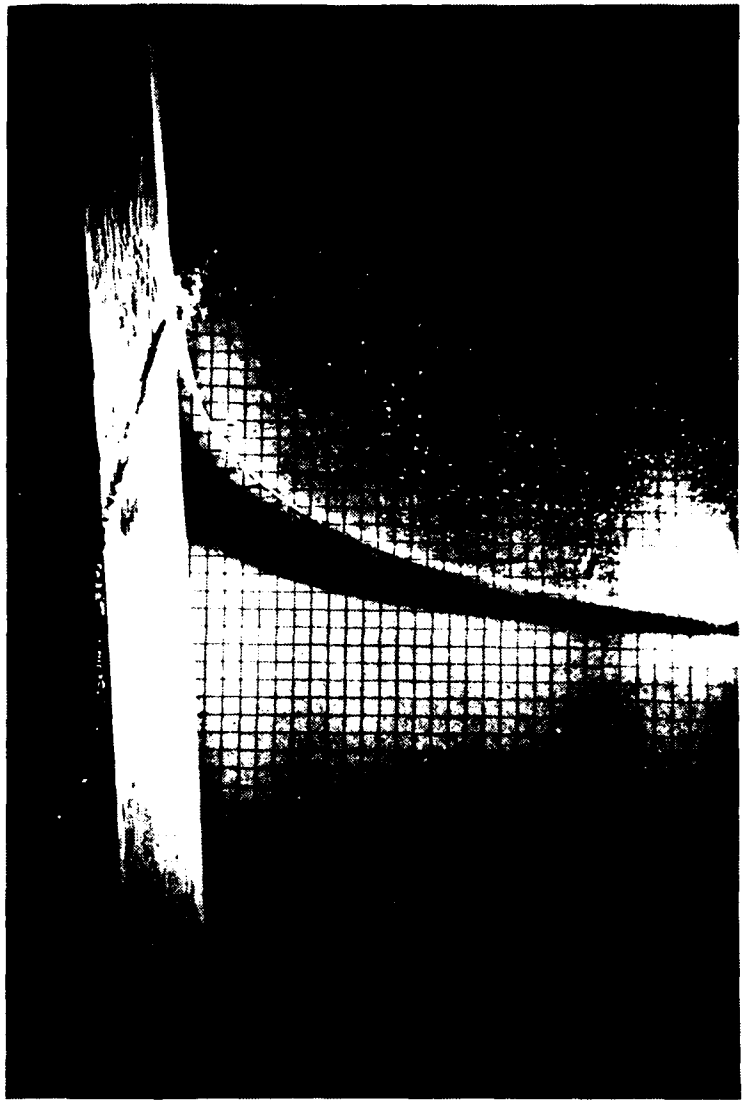

1/12, t = 0.093s

Figure 3.9 Impulsive motion of wavemaker, depth [illegible] cm.

#4/17, t = 0.106s

Figure 2.10 Impulsive motion of wavemaker, depth = 30 cm.

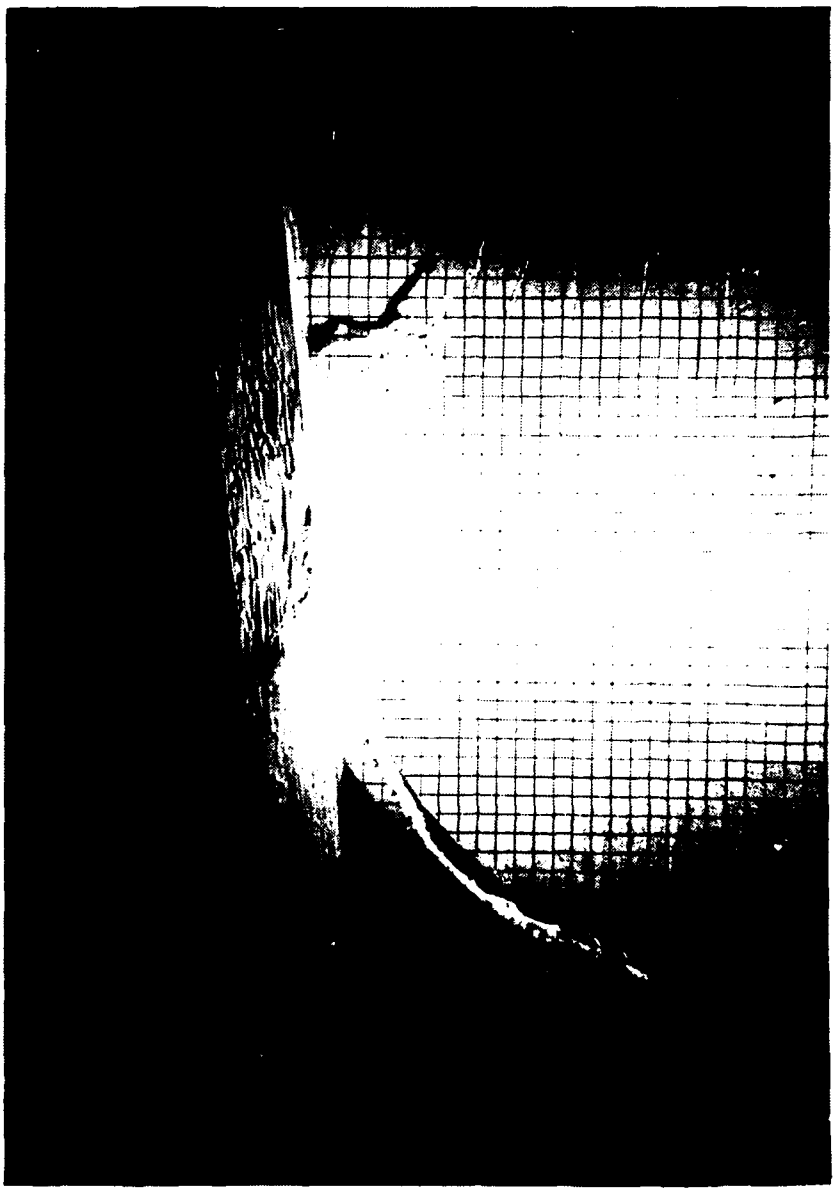

#6/19, t = 0.087s

Figure 2.11 Experiment with smooth wavemaker front and soap solution in the water.

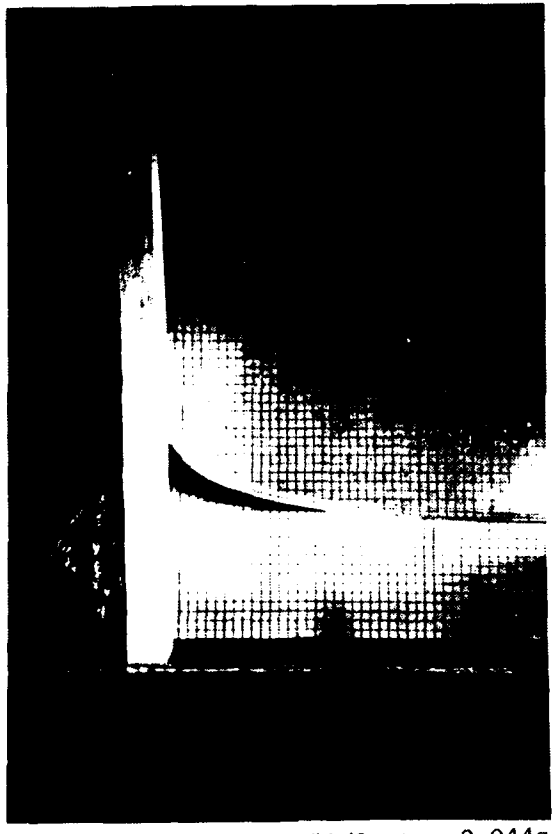

#2/3, t = 0.044s

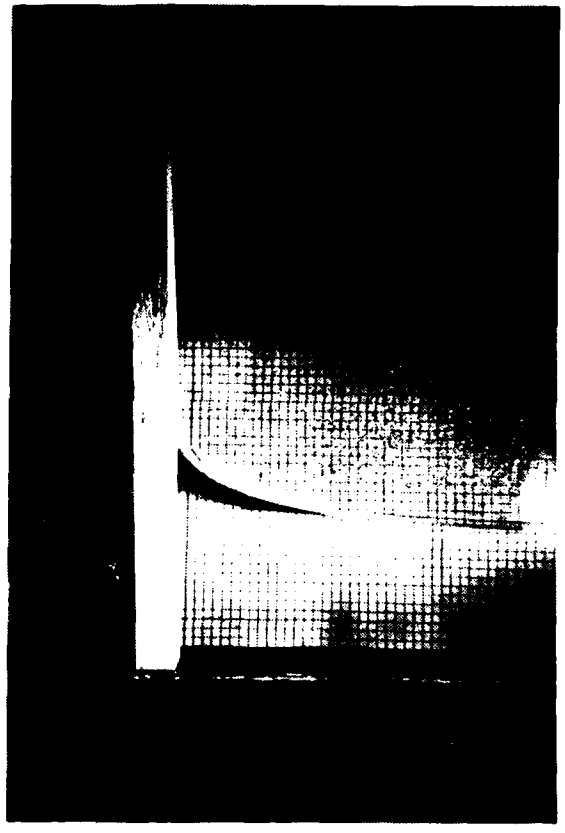

#2/18, t = 0.110s

Figure 2.12 Comparison of wave profiles with different initial wavemaker velocities, and the same wavemaker displacement.

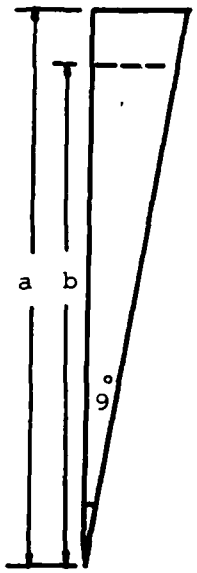

a=15.2 cm
b=13.0 cm

a=15.5 cm
b=13.0 cm

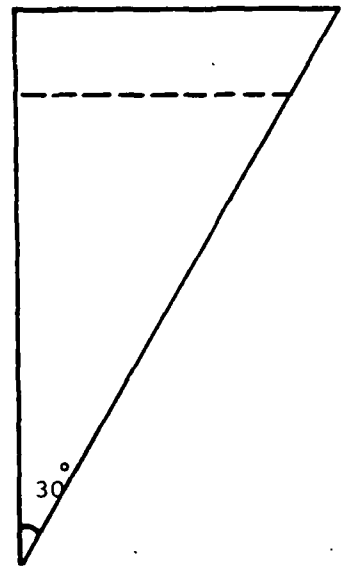

a=13.5 cm
b=11.0 cm

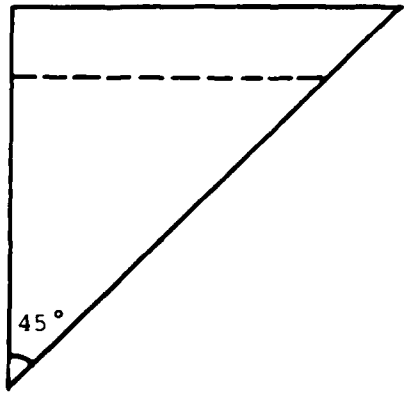

a=11.4 cm
b= 9.0 cm

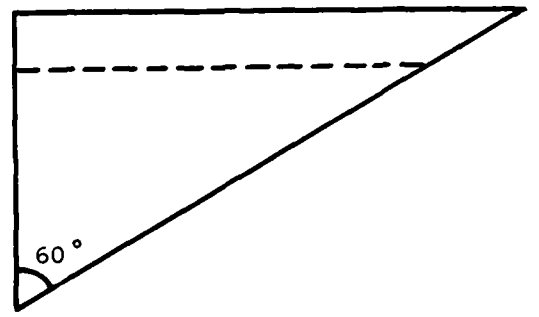

a=6.3 cm
b=5.0 cm

Figure 3.1 Wedge data (half-section)

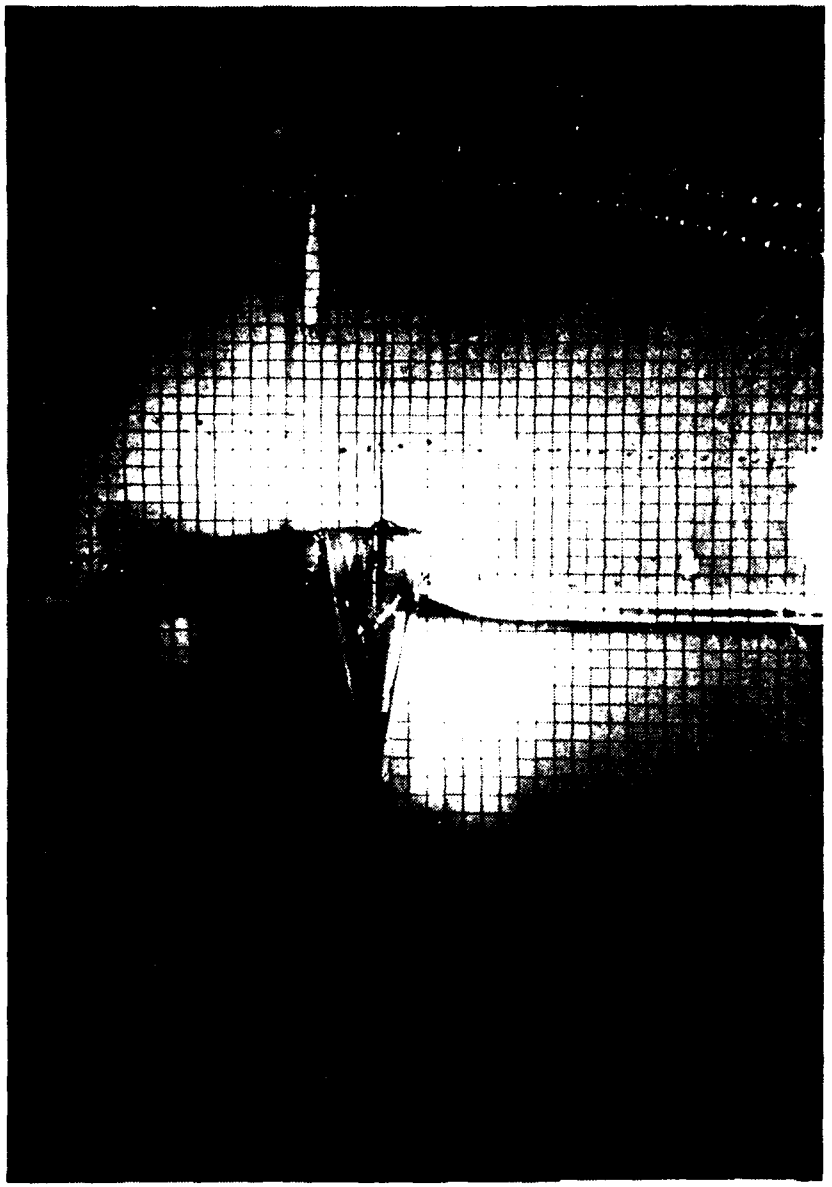

#14/15, t = 0.21s

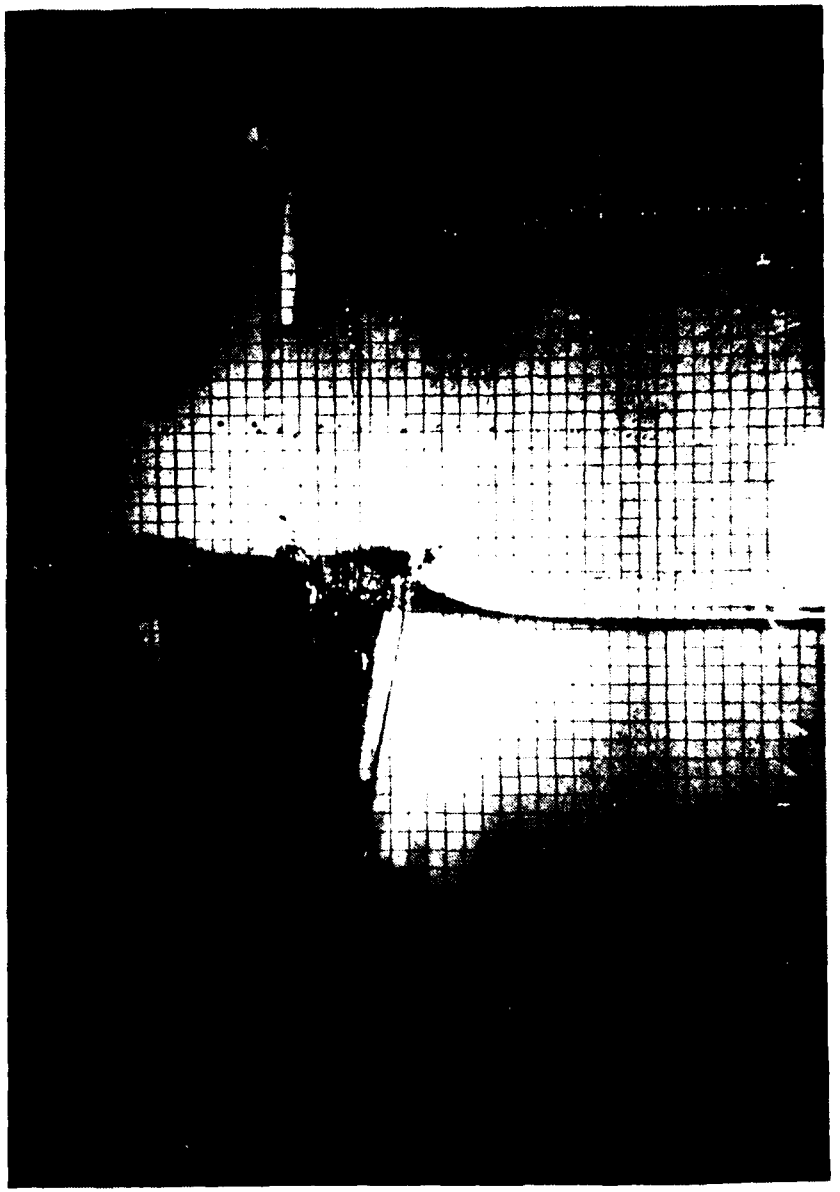

#14/16, t = 0.22s

Figure [illegible] Water entry of 9° wedge.

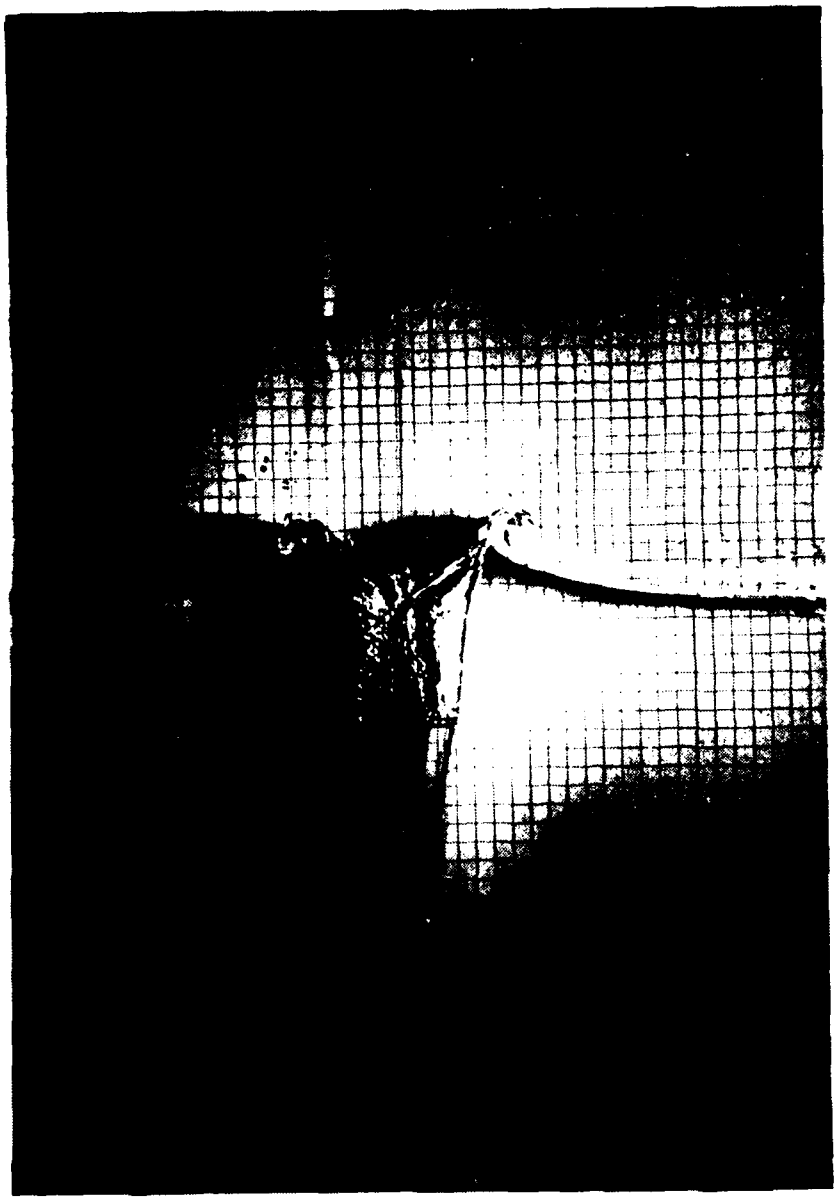

#14/18, t = 0.24s

Figure 3.2 (cont'd)

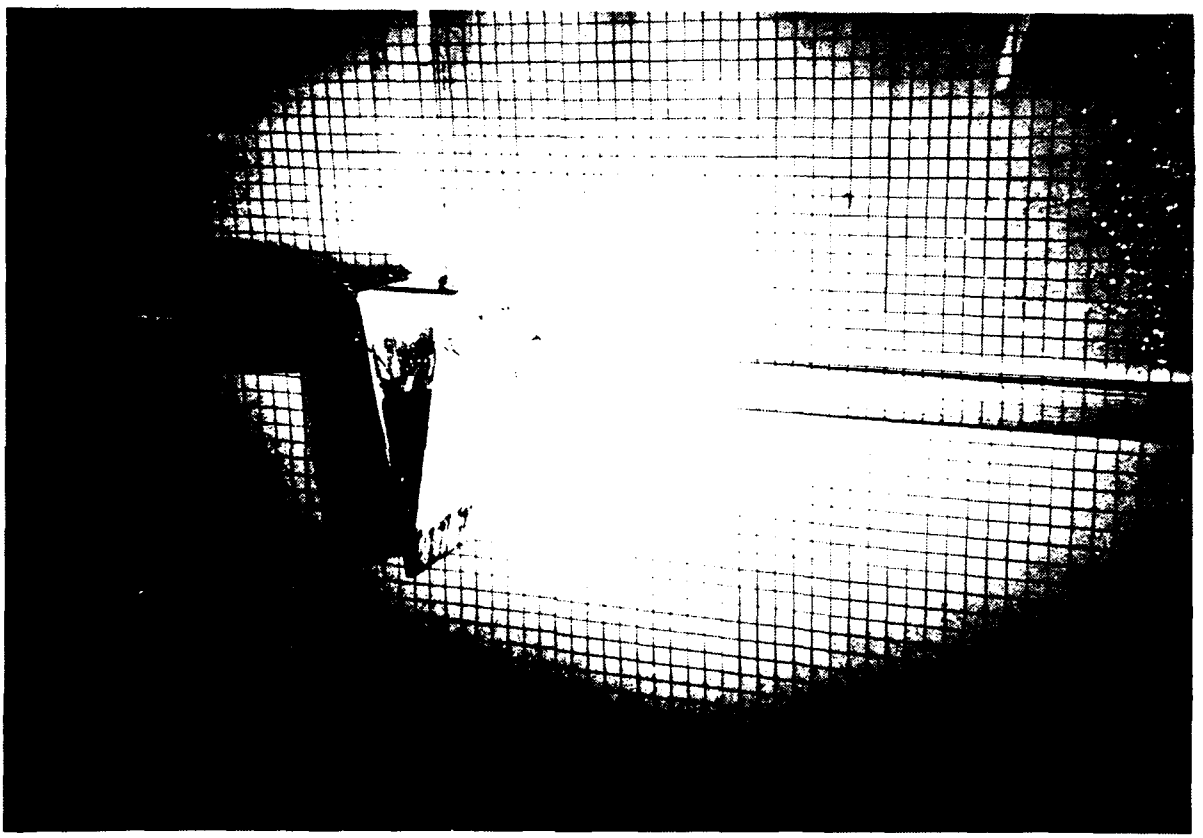

#17/21, t = 0.21s

Figure 3.3 Water entry of 9° wedge (oblique view).

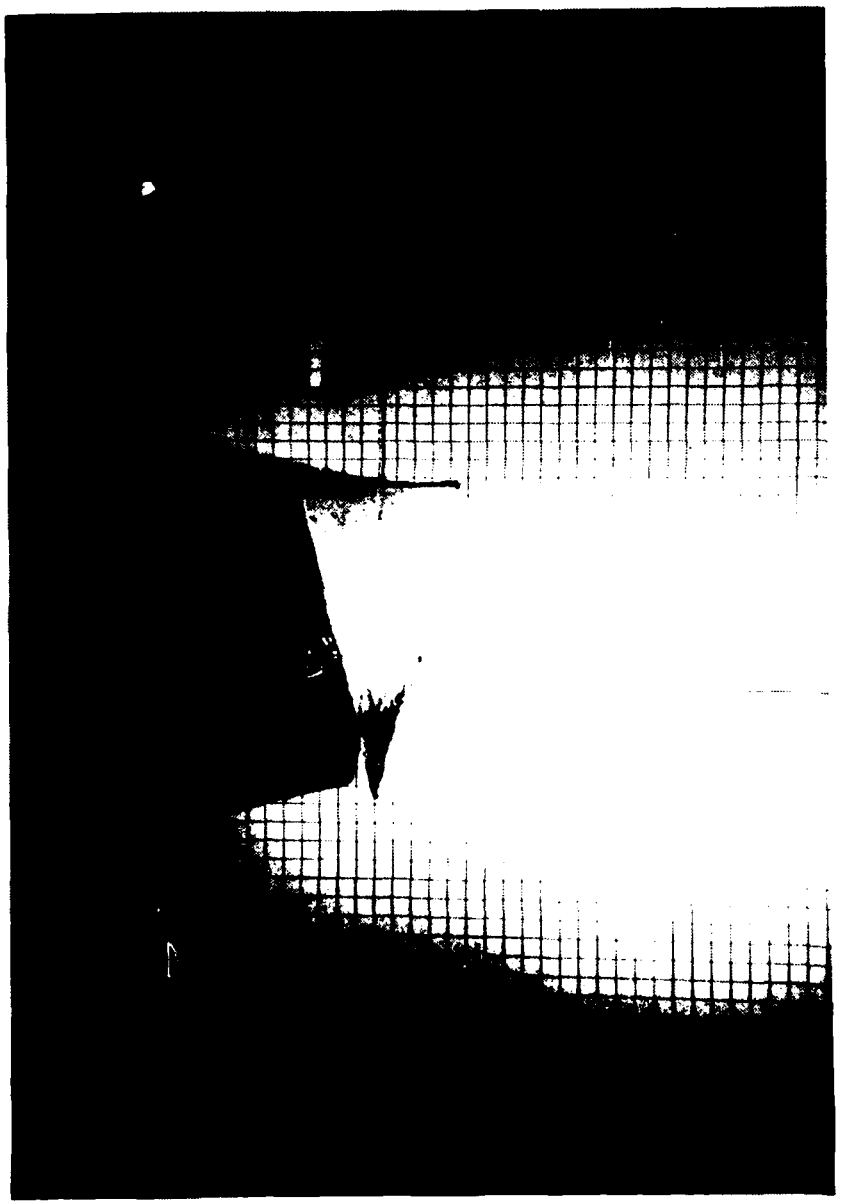

#17/15, t = 0.19s

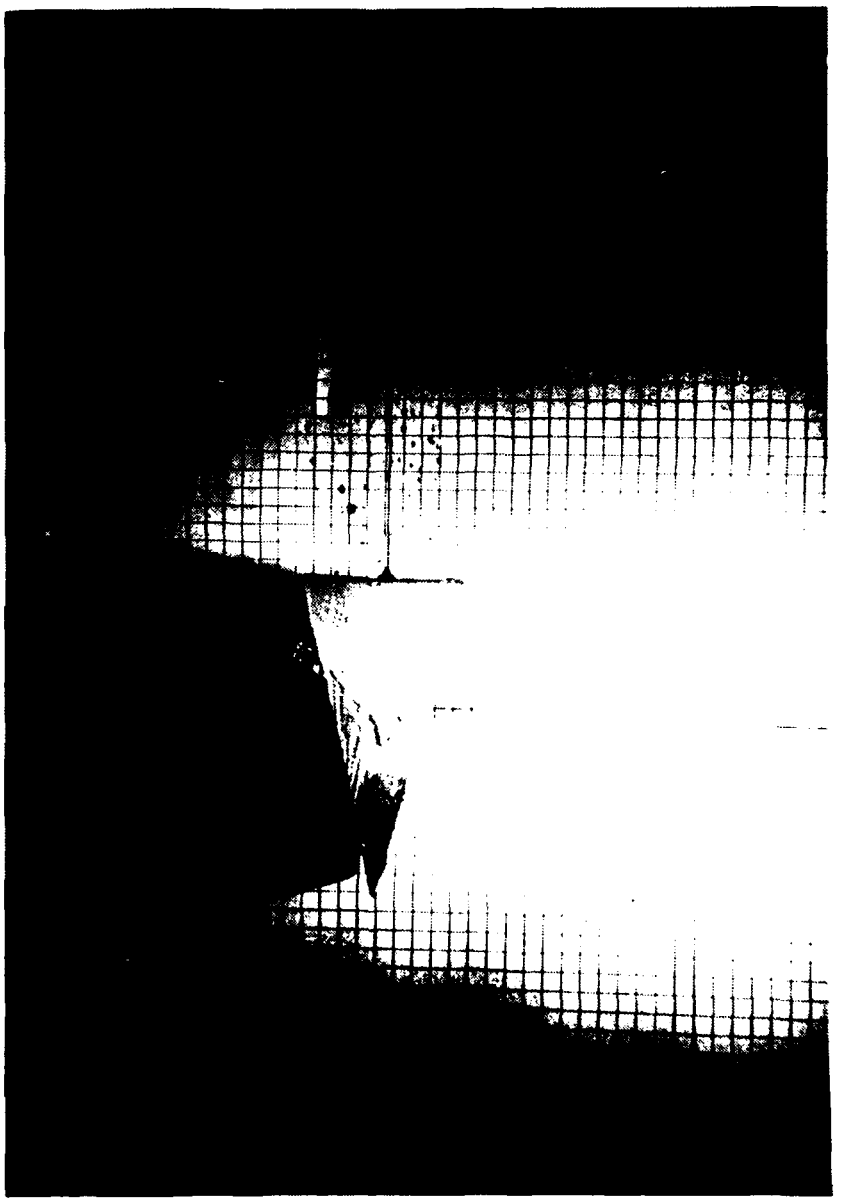

#17/17, t = 0.20s

Figure 3.4 Water entry of 15^{o} wedge.

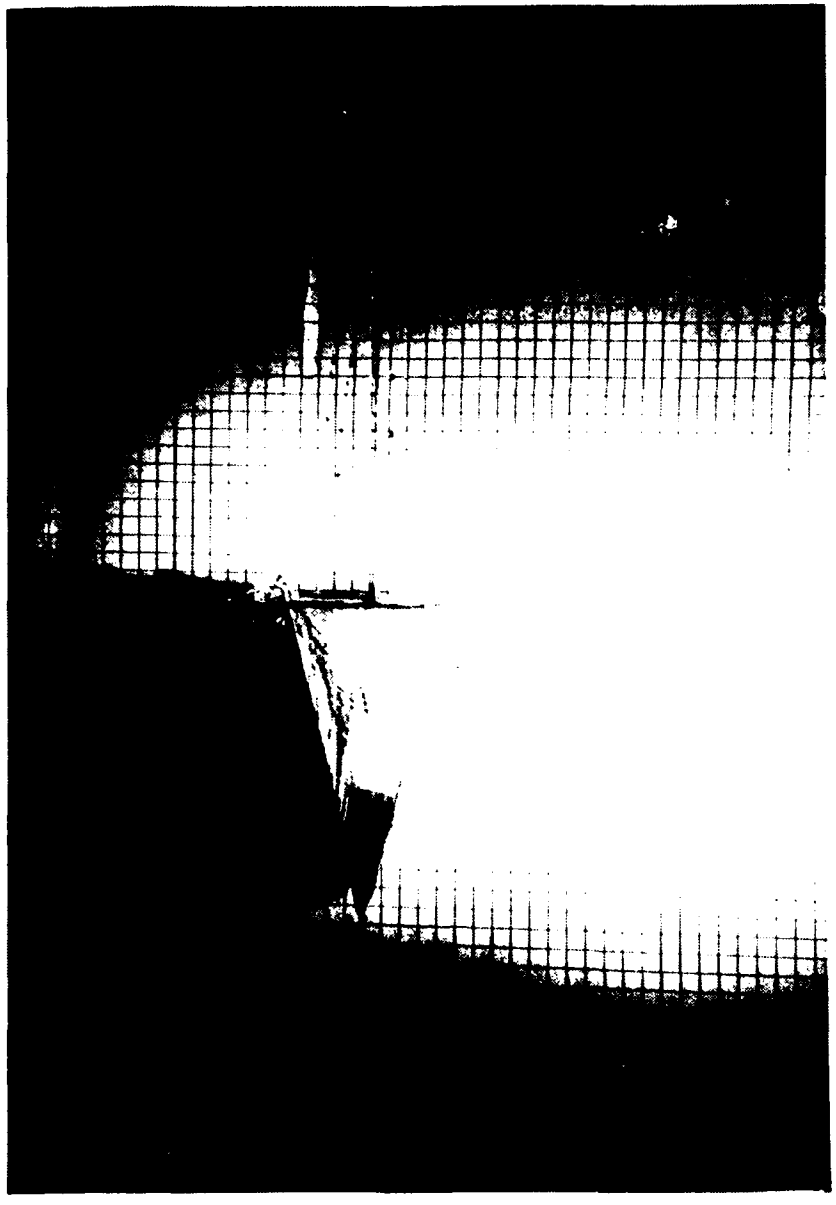

#17/20, t = 0.205s

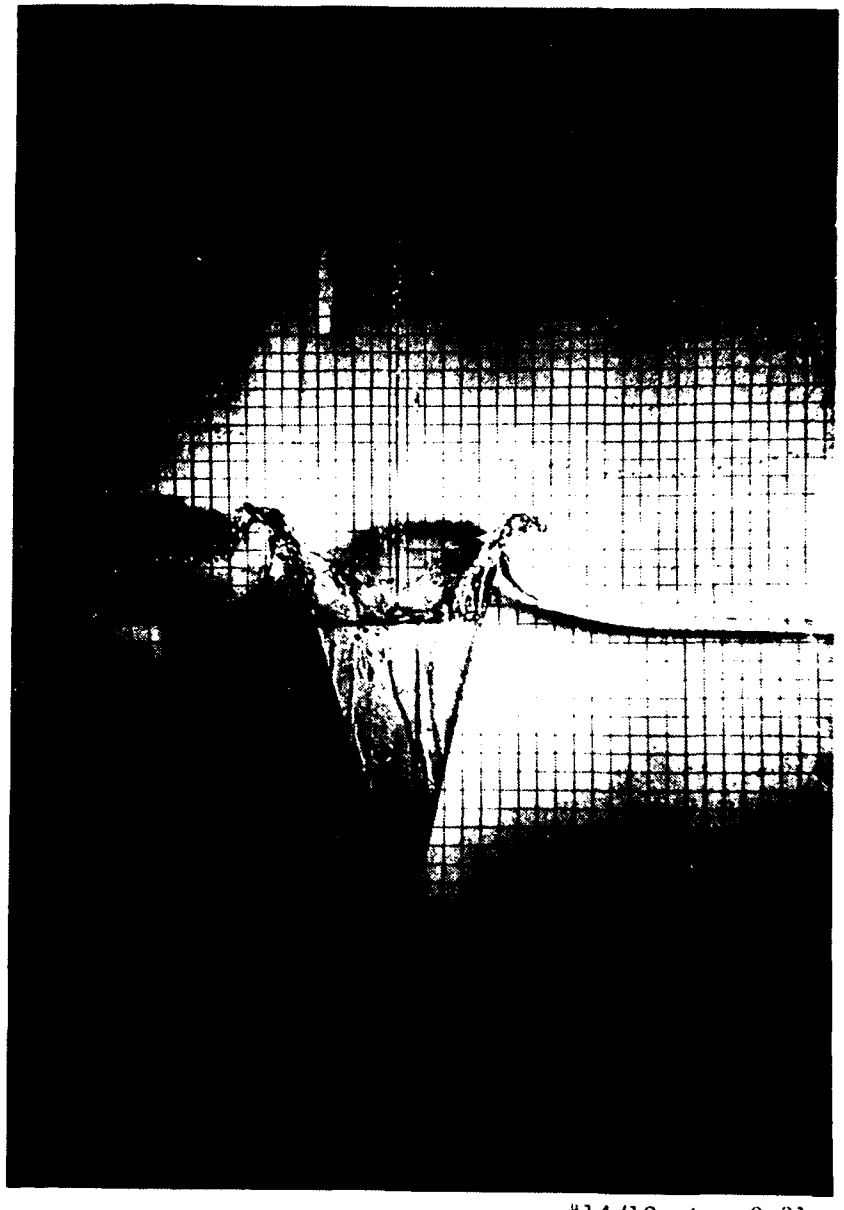

#14/10, t = 0.21s

Figure 3.4 (cont'd)

#14/11, t = 0.225s

Figure 3.4 (cont'd)

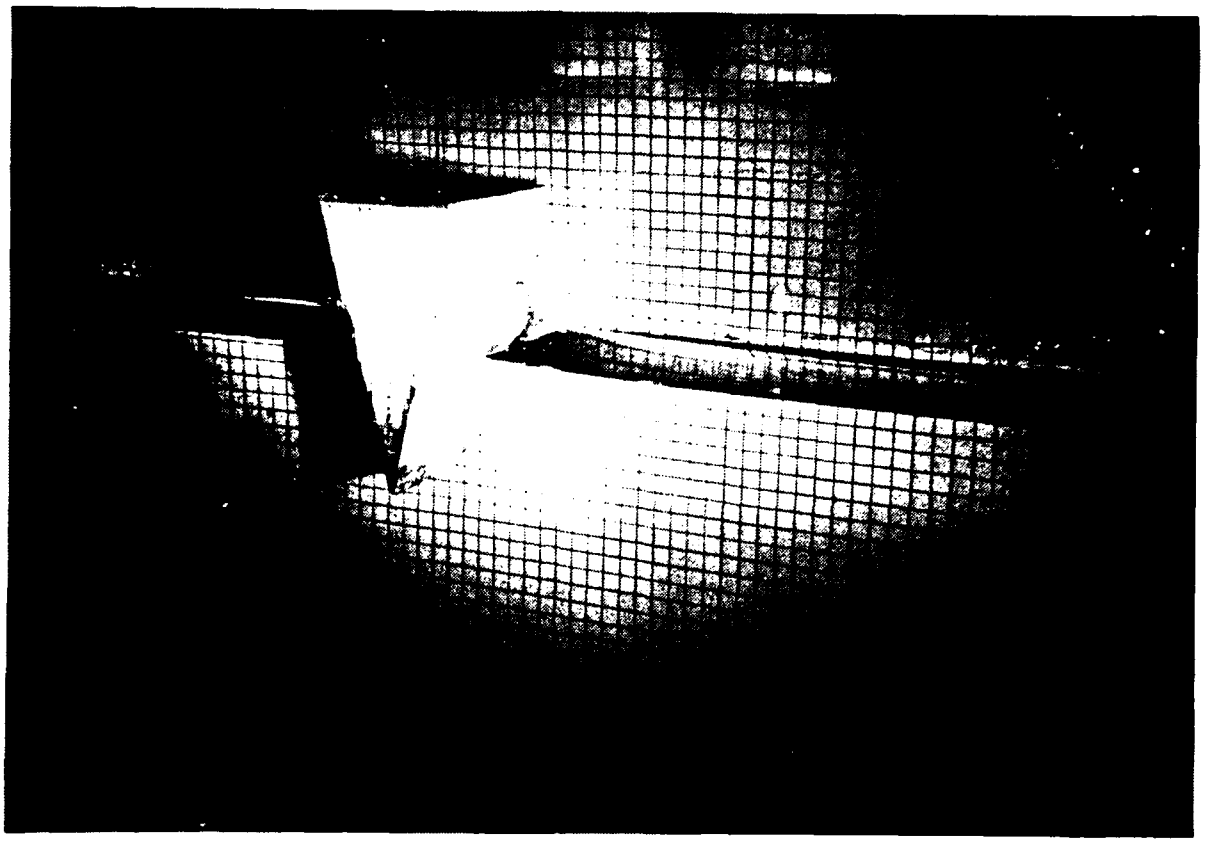

#17/1, t = 0.20s

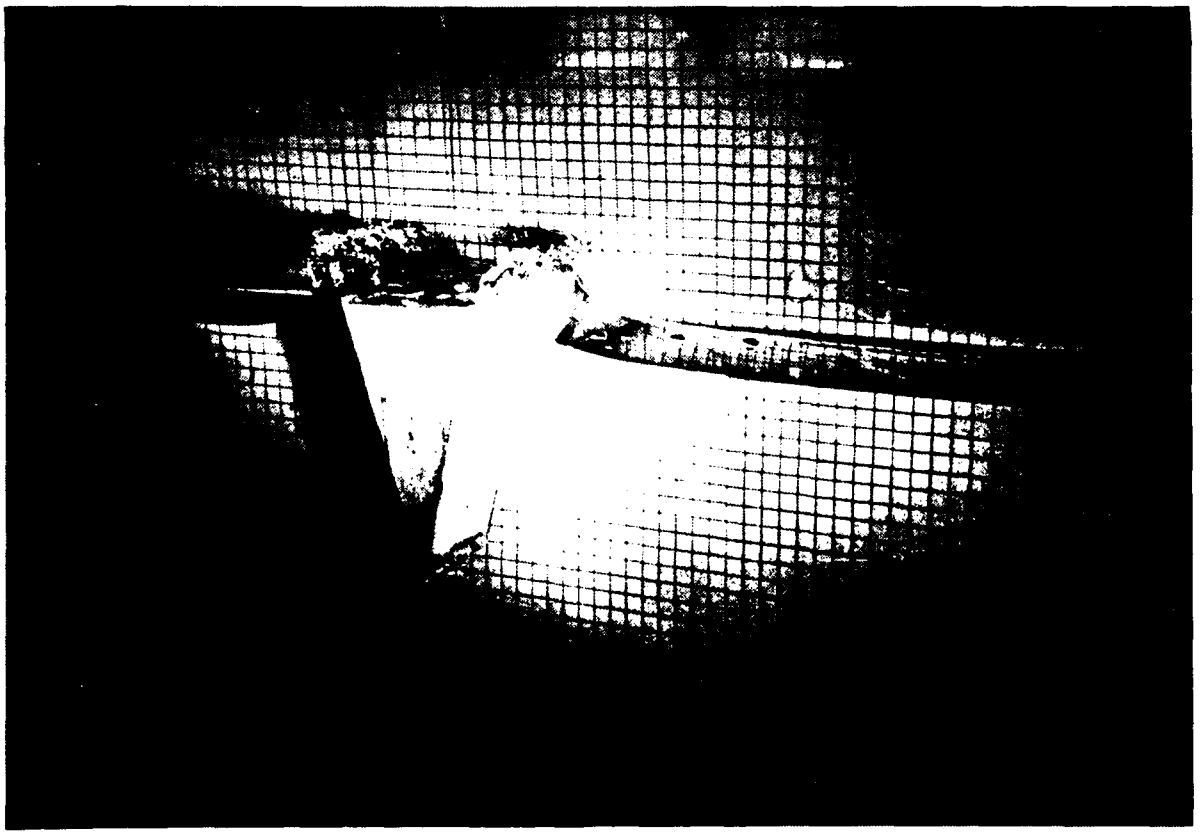

#17/2, t = 0.21s

Figure 3.5 Water entry of 15^{o} wedge (oblique view).

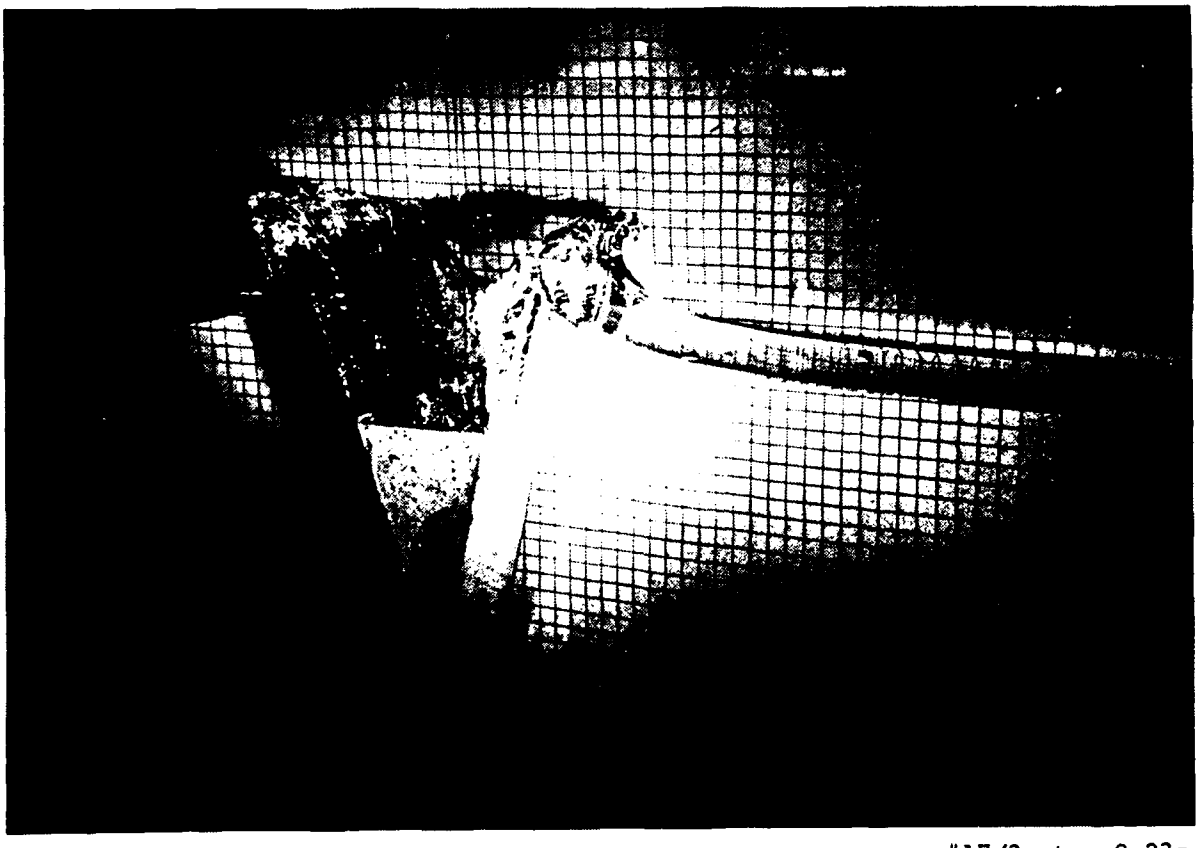

#17/3, t = 0.23s

Figure 3.5 (cont'd)

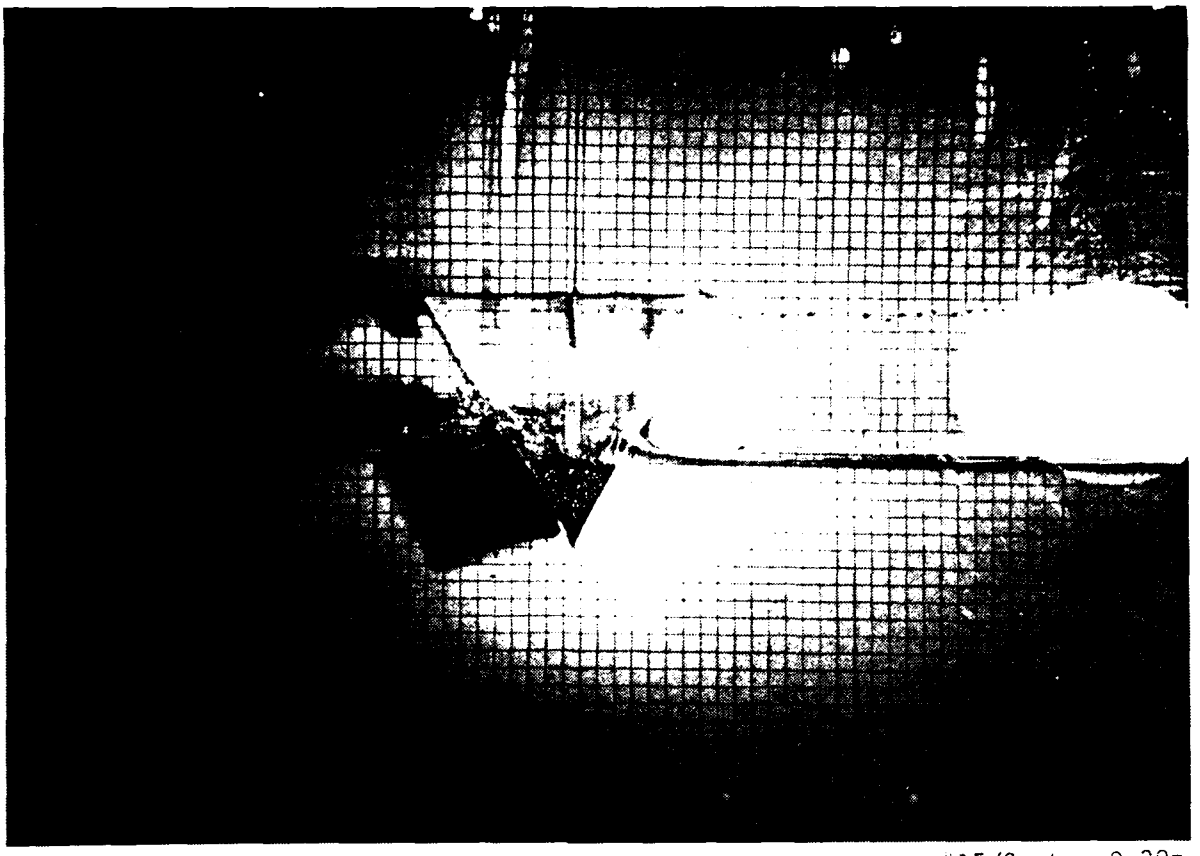

#15/2, t = 0.20s

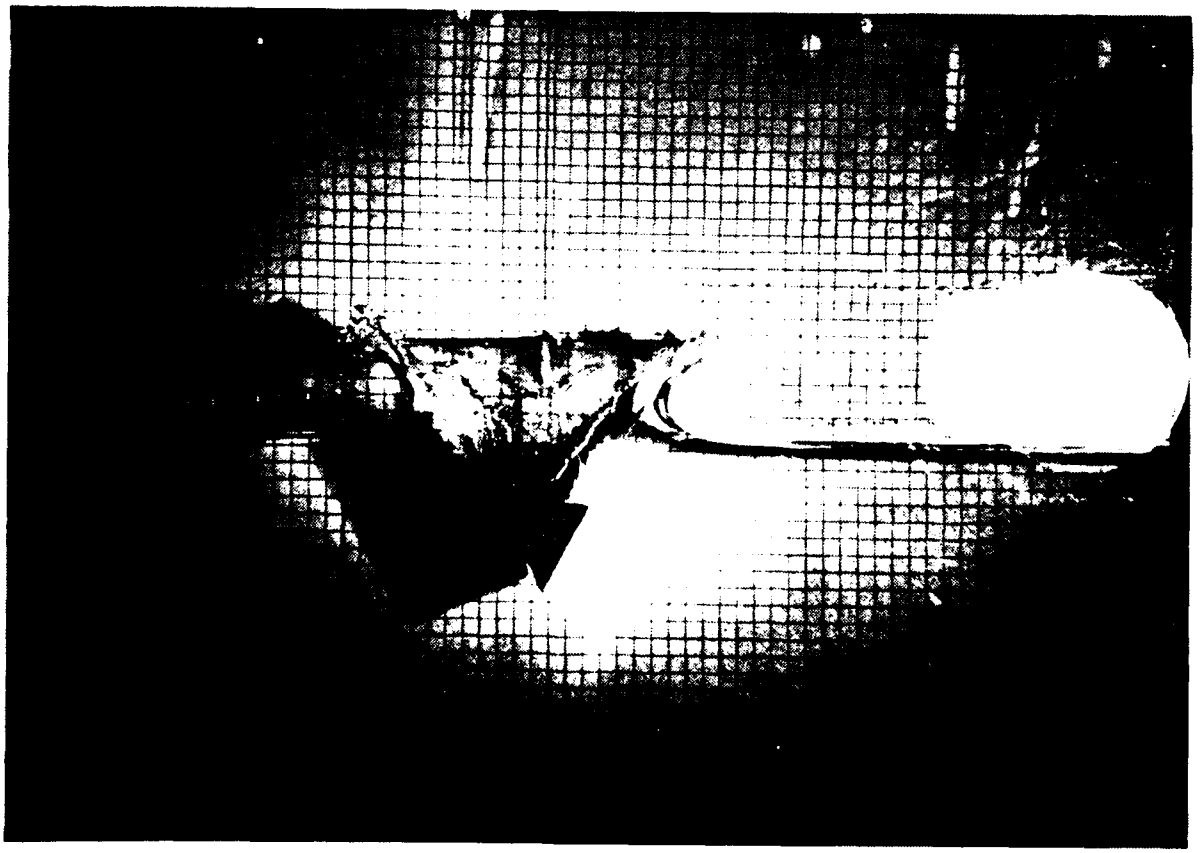

#15/3, t = 0.205s

Figure 3.6 Water entry of 30° wedge.

#15/8, t = 0.24s

#15/9, t = 0.25s

Figure 3.6 (cont'd)

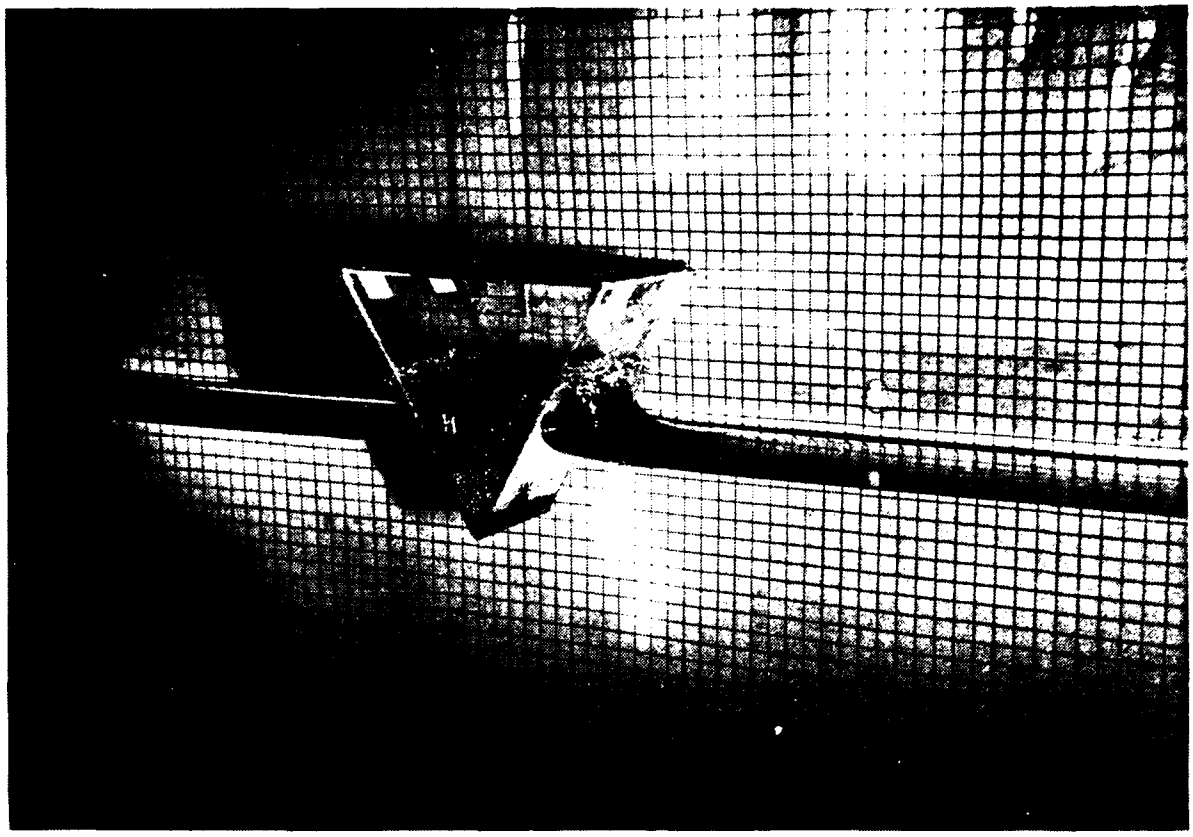

#16/18, t = 0.20s

#16/21, t = 0.21s

Figure 3.7 Water entry of 30° wedge (oblique view).

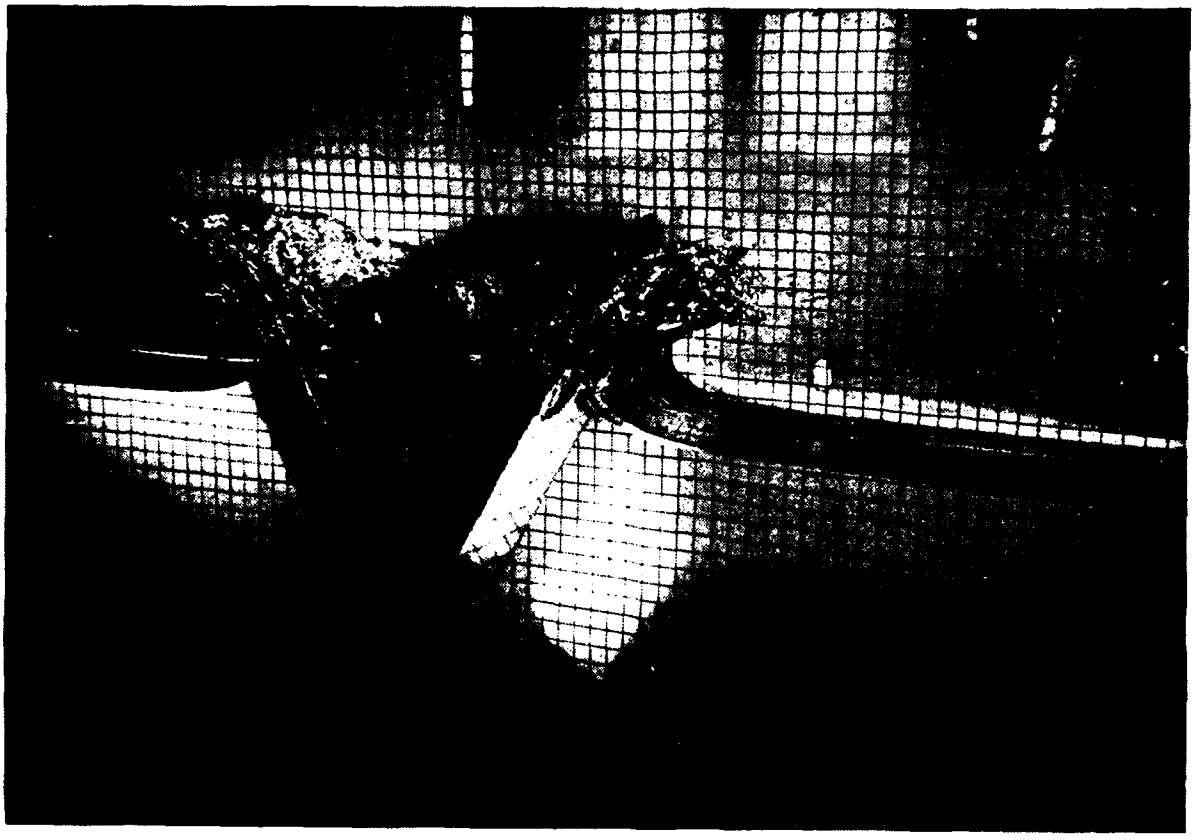

#16/22, t = 0.22s

Figure 3.7 (cont'd)

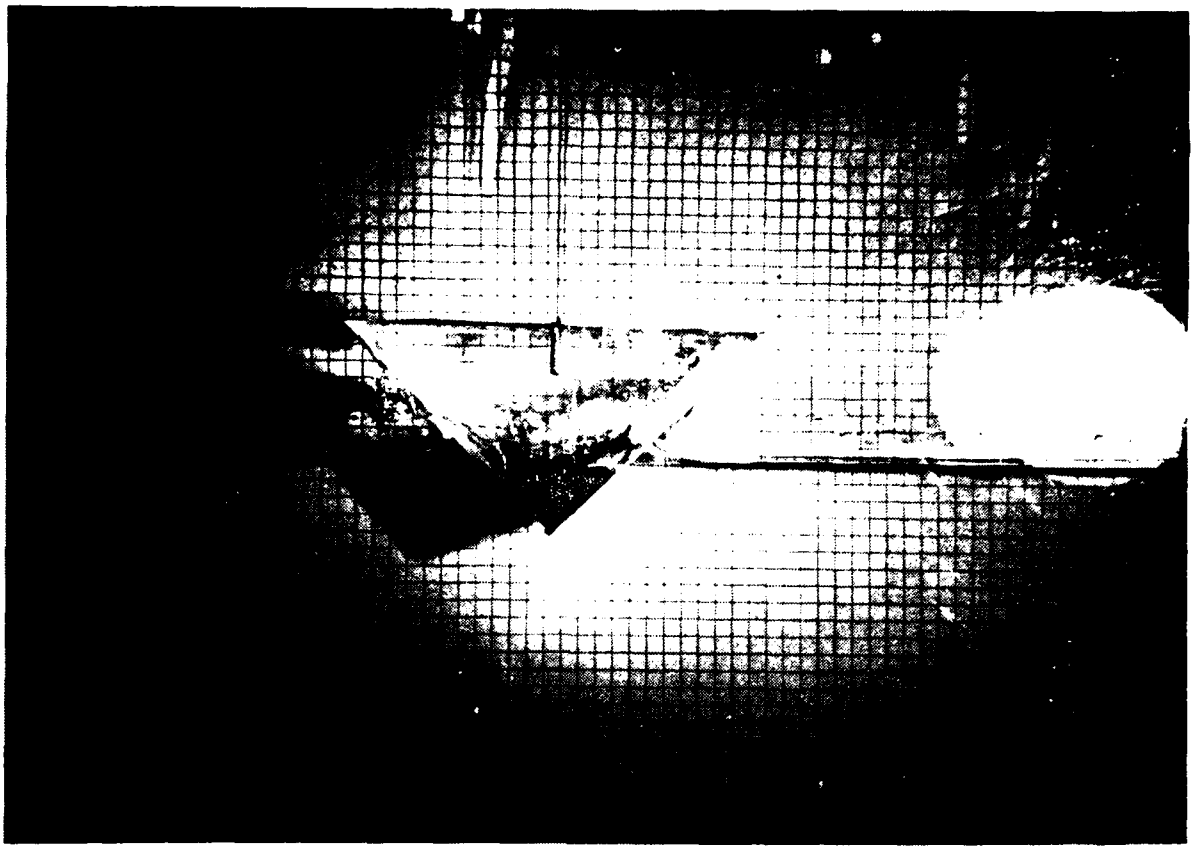

#15/13, t = 0.205s

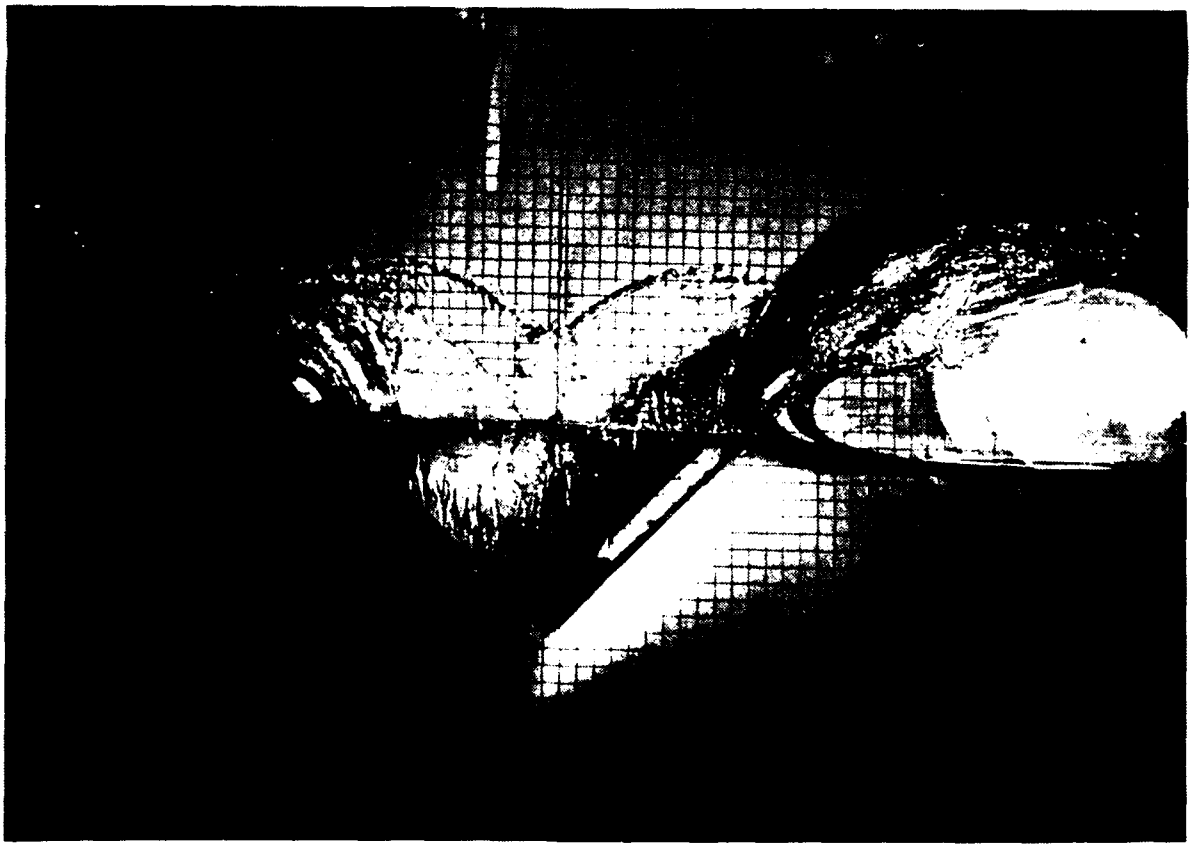

#15/14, t = 0.215s

Figure 3.8 Water entry of 45° wedge.

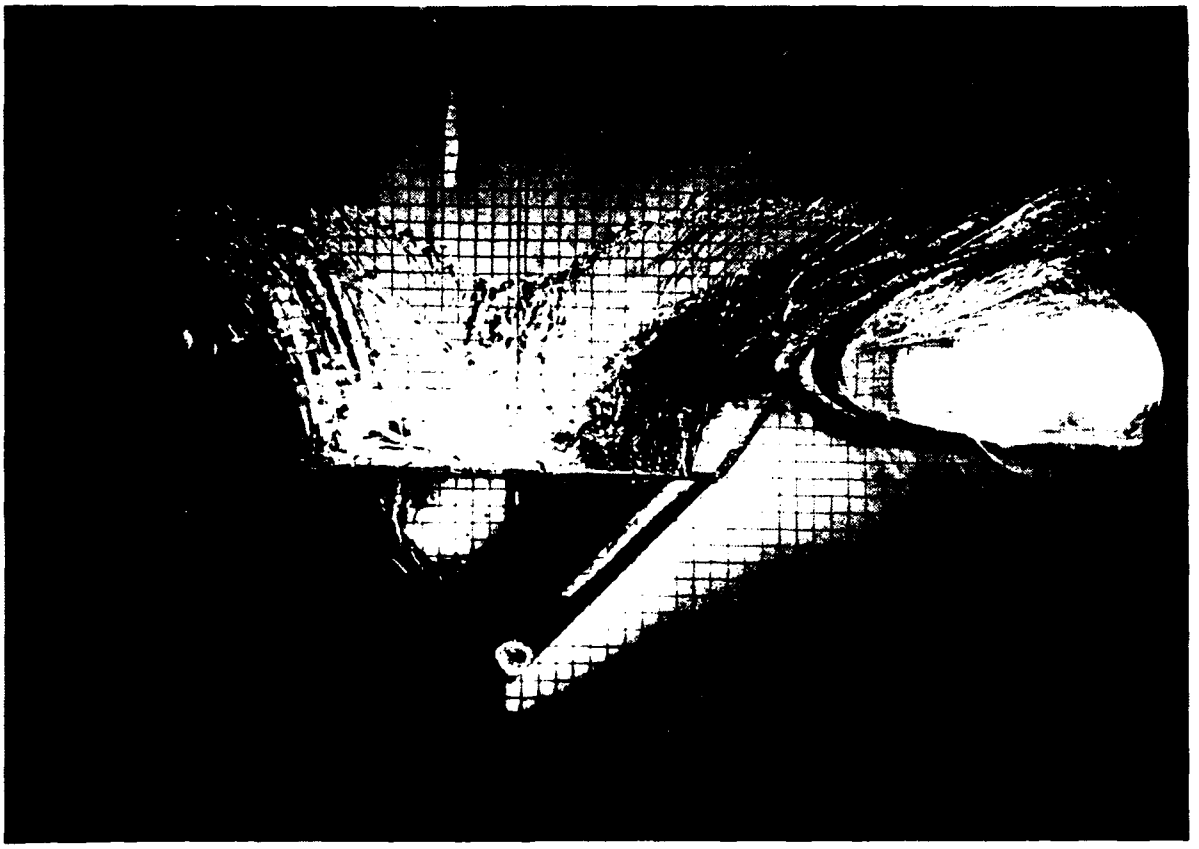

#15/15, t = 0.225s

Figure 3.8 (cont'd).

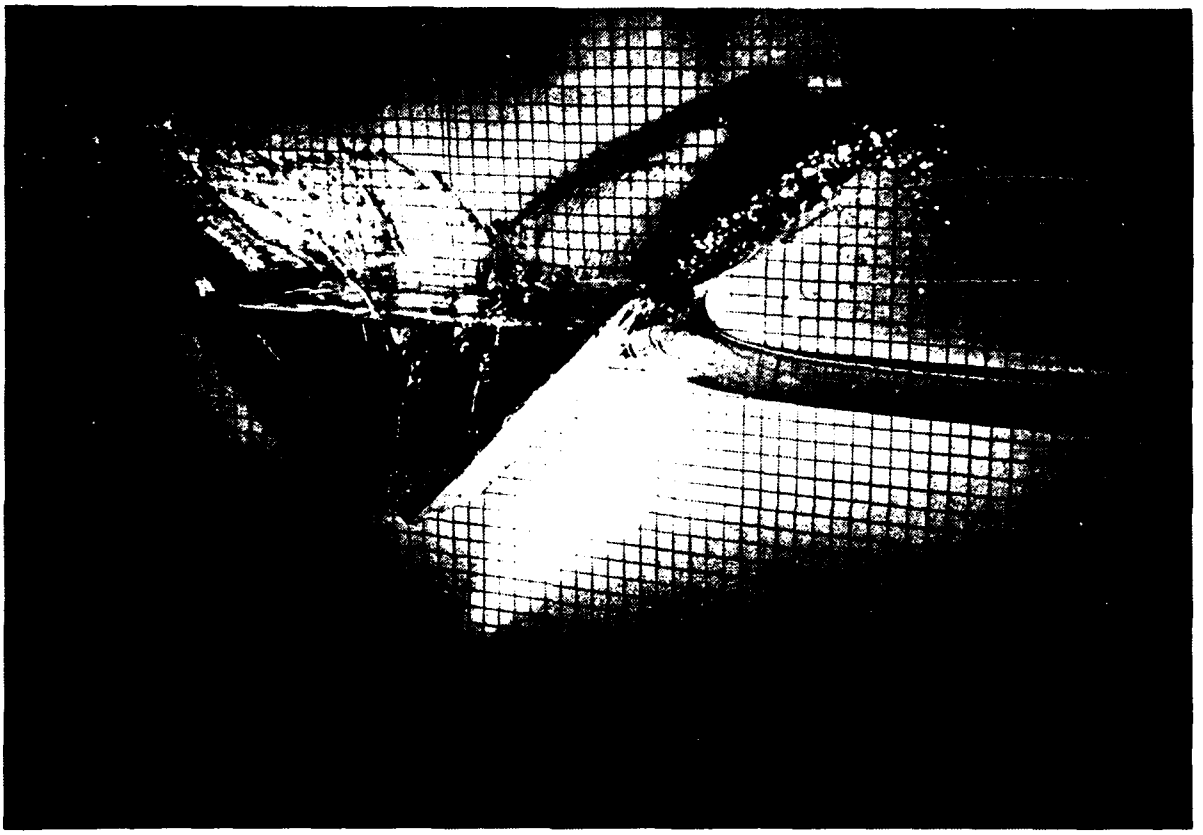

#17/5, t = 0.215s

Figure 3.9 Water entry of 45° wedge (oblique view).

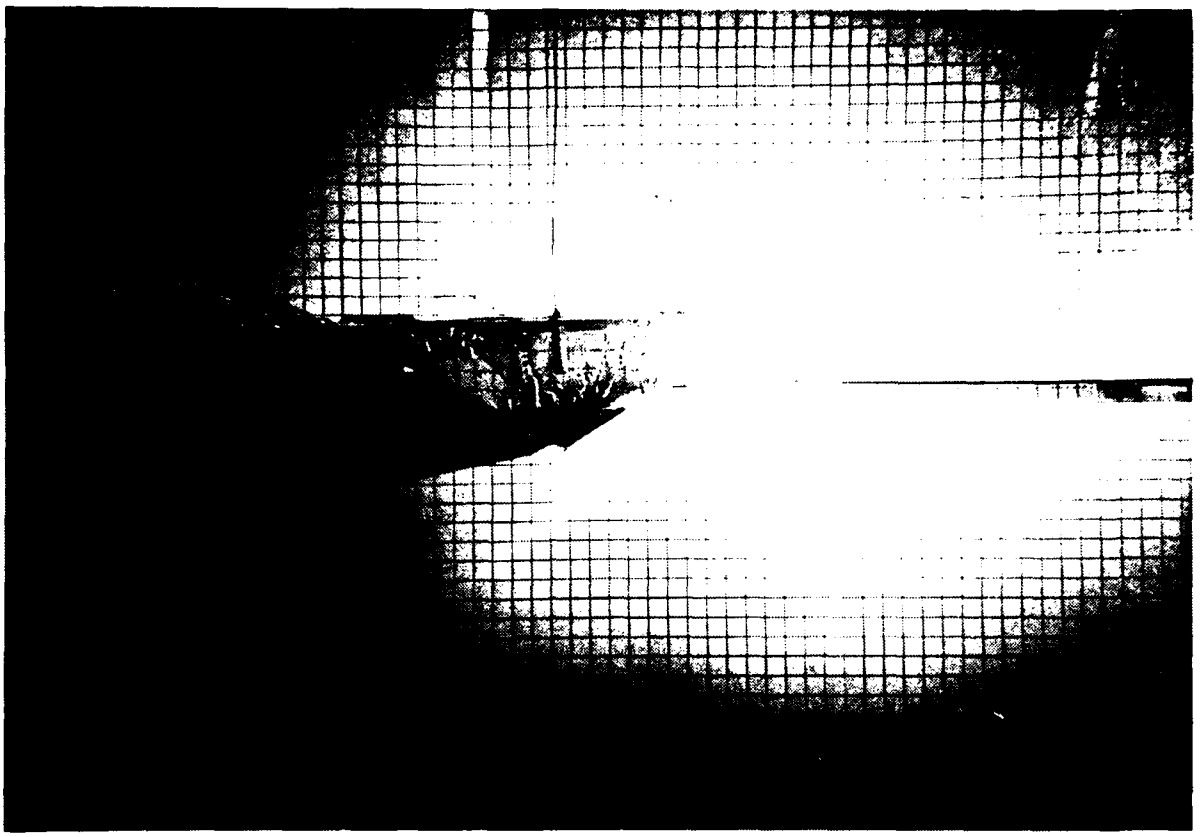

#17/14, t = 0.205s

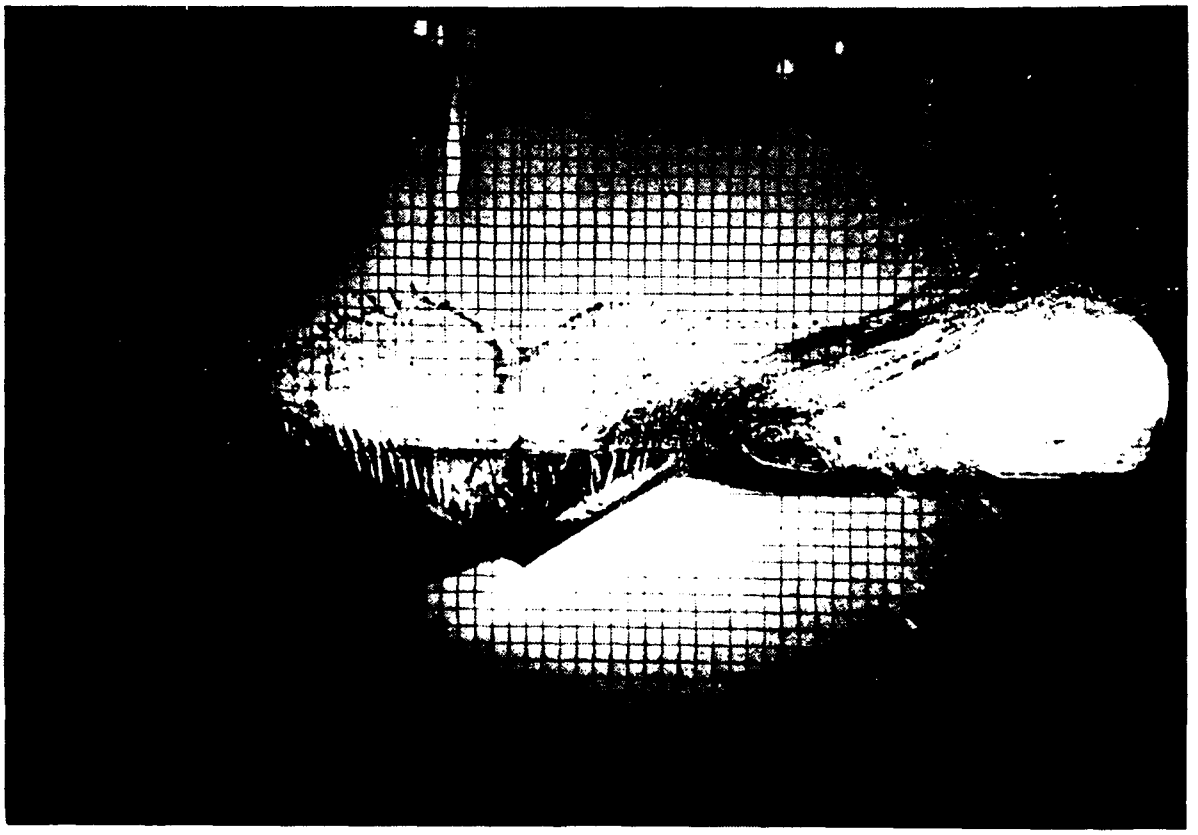

#16/2, t = 0.21s

Figure 3.10 Water entry of 60° wedge.

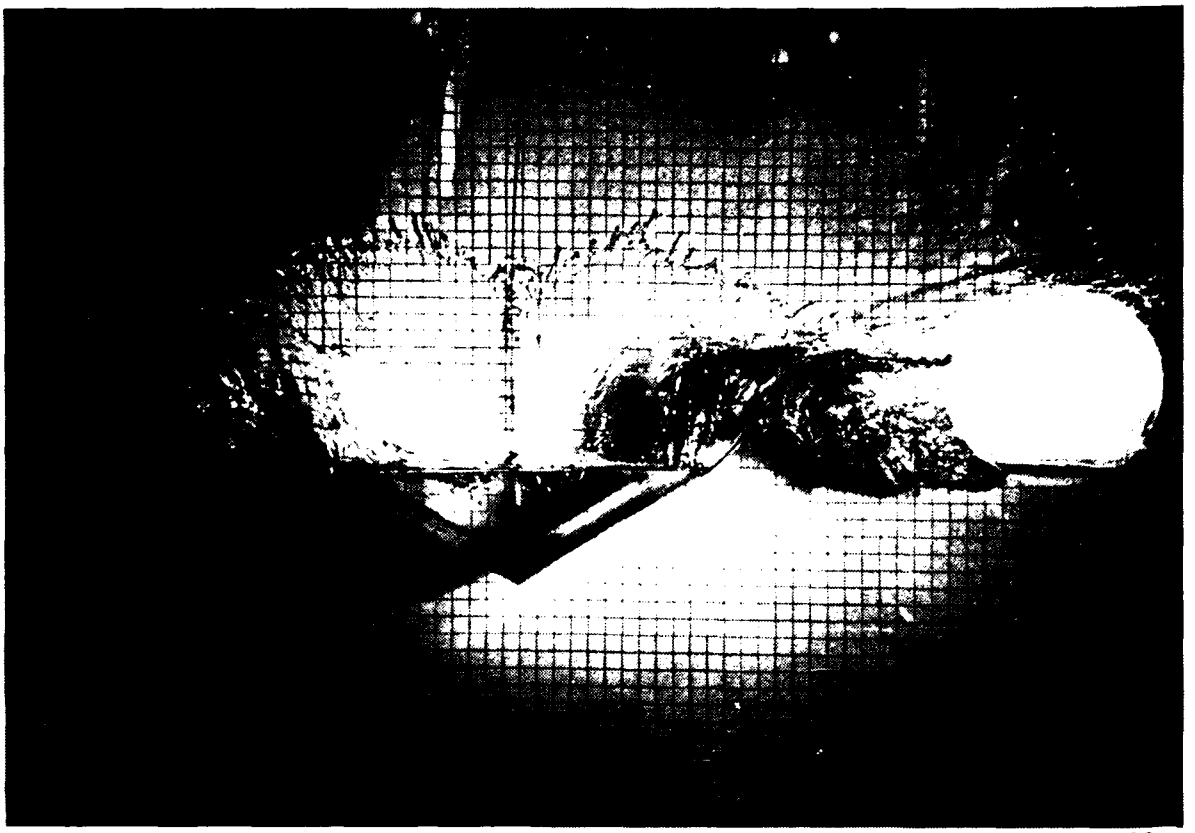

#16/4, t = 0.22s

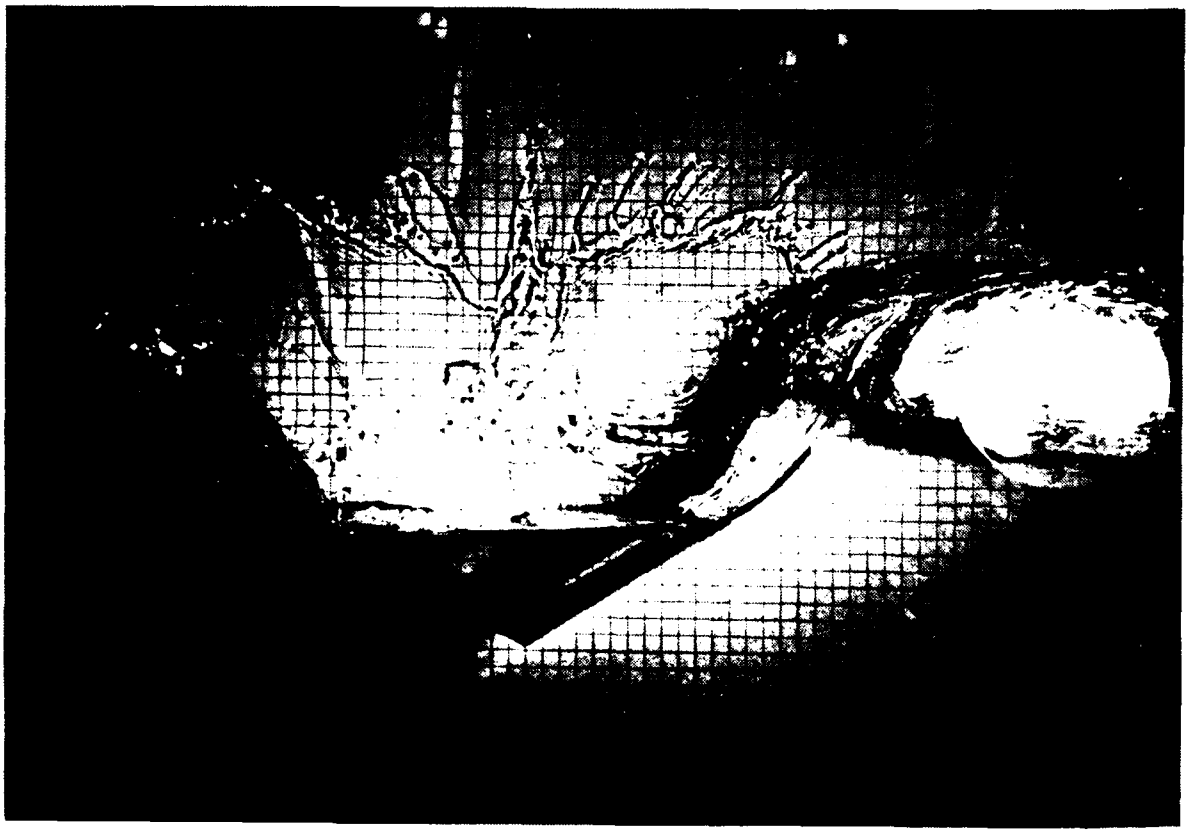

#16/11, t = 0.275s

Figure 3.10 (cont'd).

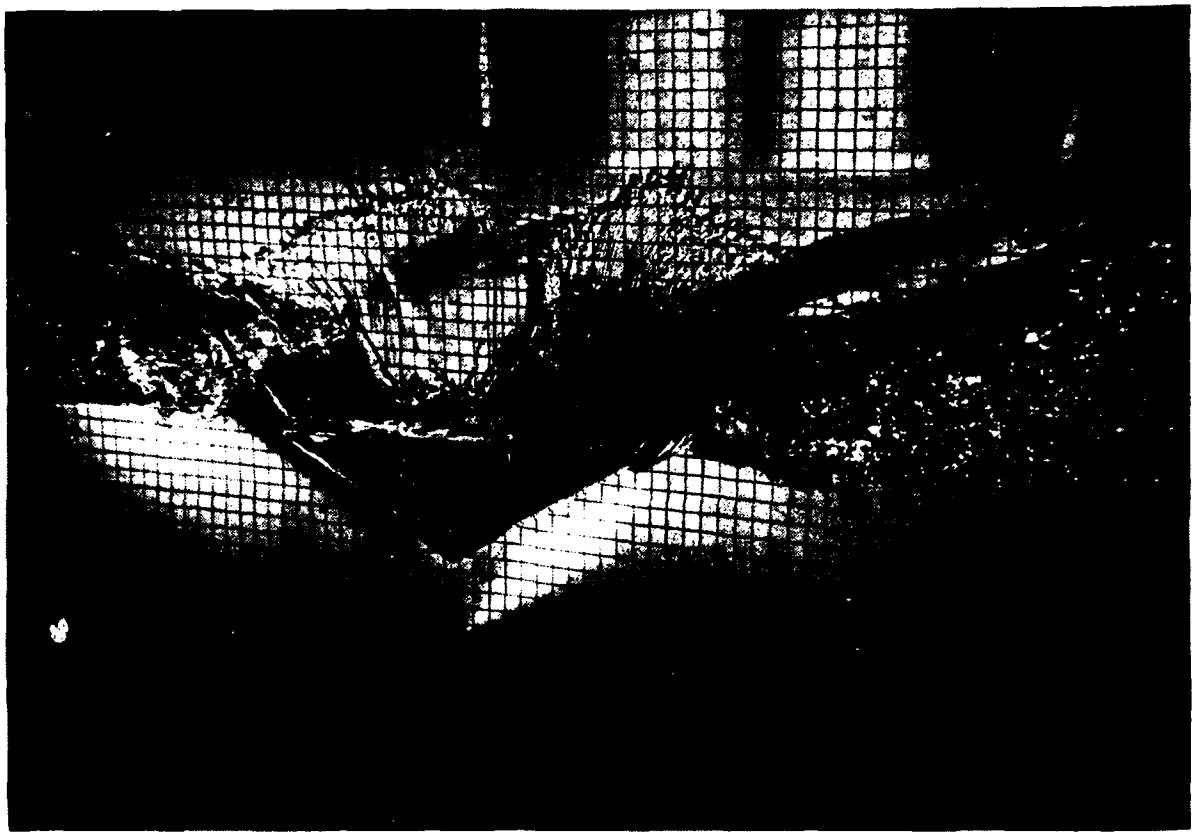

#16/12, t = 0.22s

Figure 3.11 60° wedge. (oblique view).

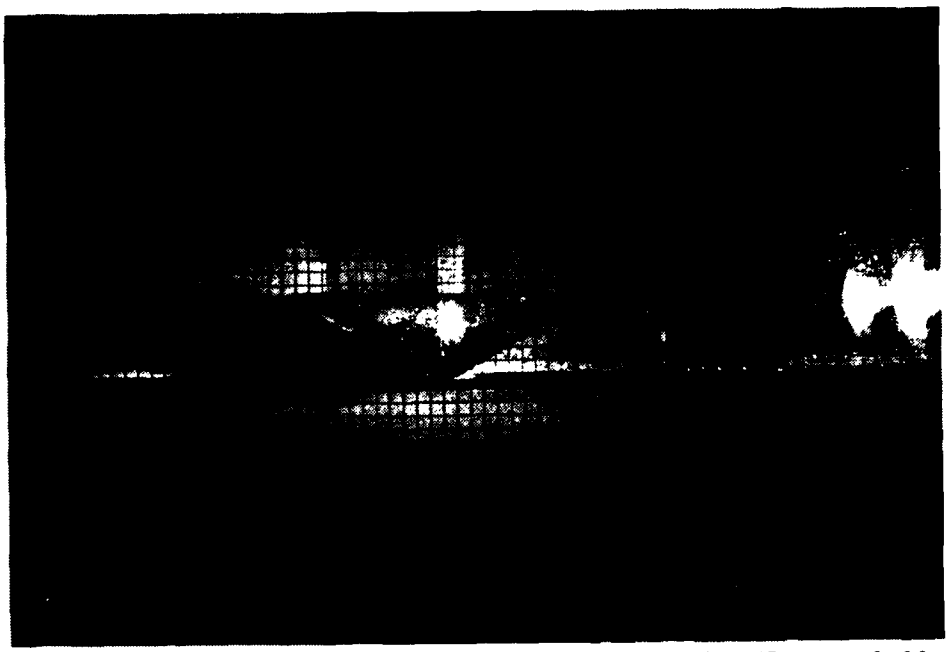

#20/7, t = 0.20s

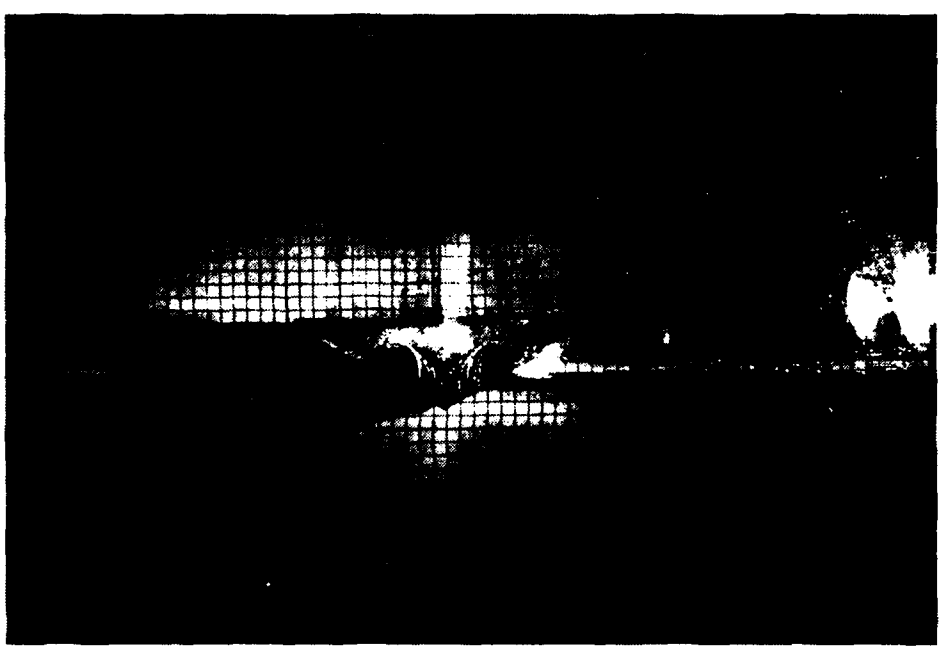

#20/8, t = 0.205s

Figure 3.12 Water entry of 60^{o} wedge, heavy wedge.

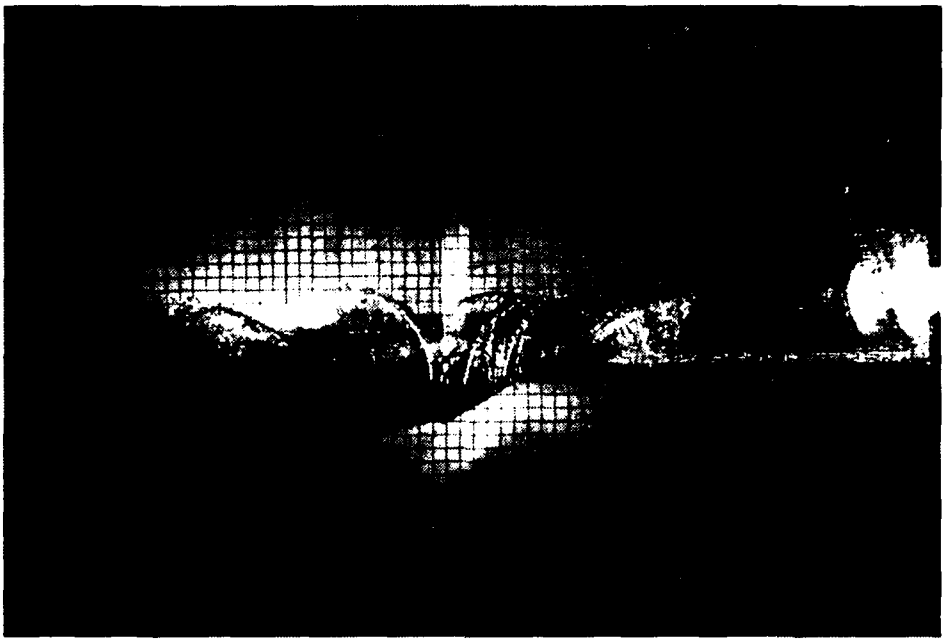

#20/9, t = 0.205s

#20/10, t = 0.205s

Figure 3.12 (cont'd)

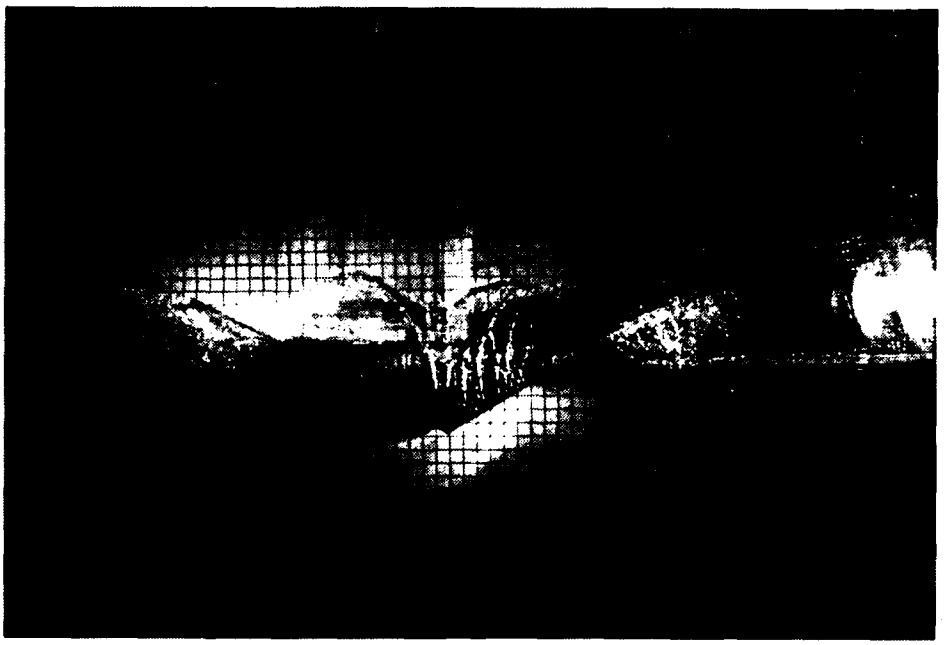

#20/11, t = 0.21s

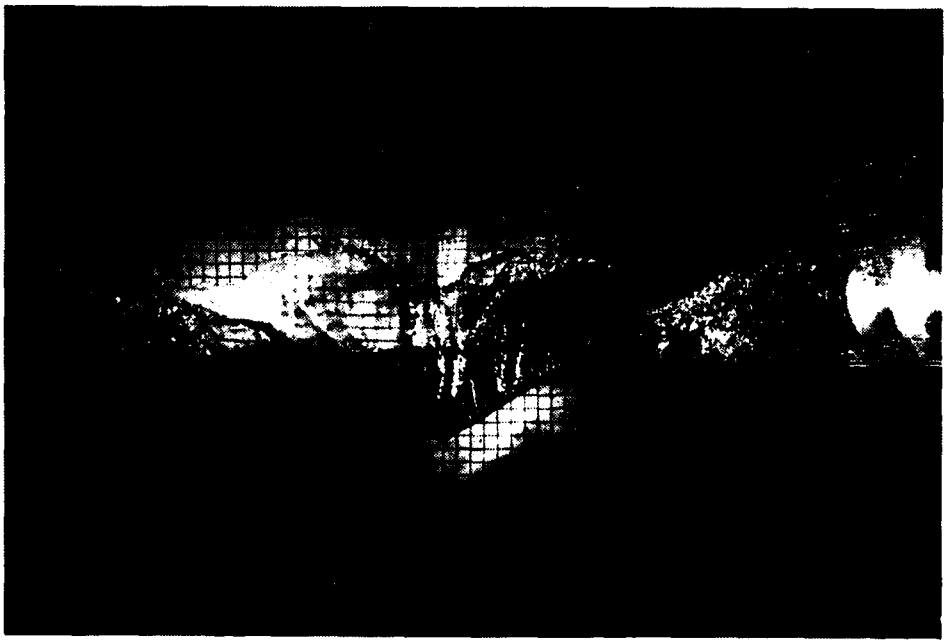

#20/12, t = 0.21s

Figure 3.12 (cont'd).

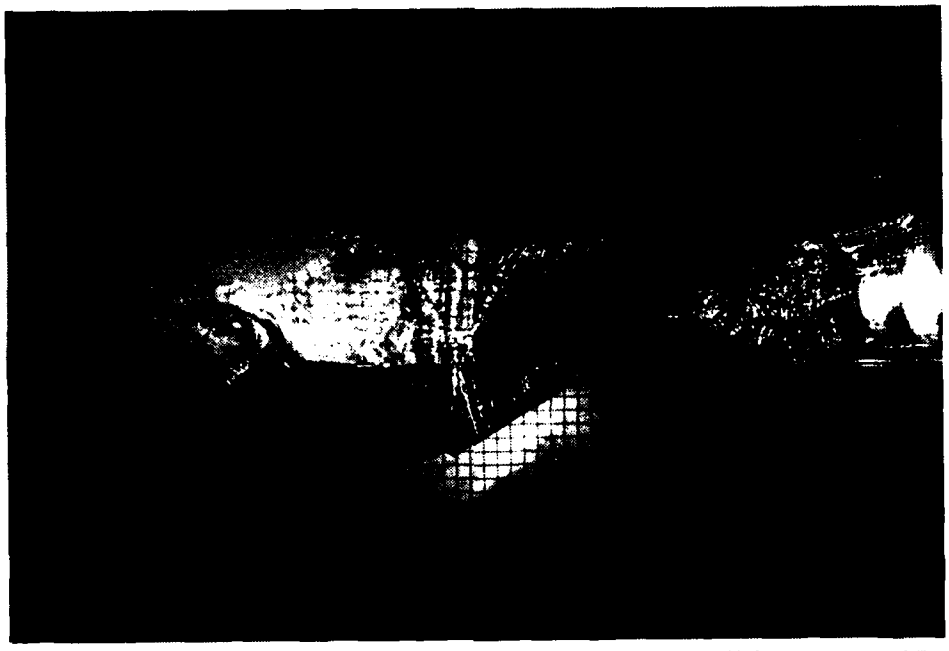

#20/15, t = 0.215s

#20/19, t = 0.23s

Figure 3.12 (cont'd).

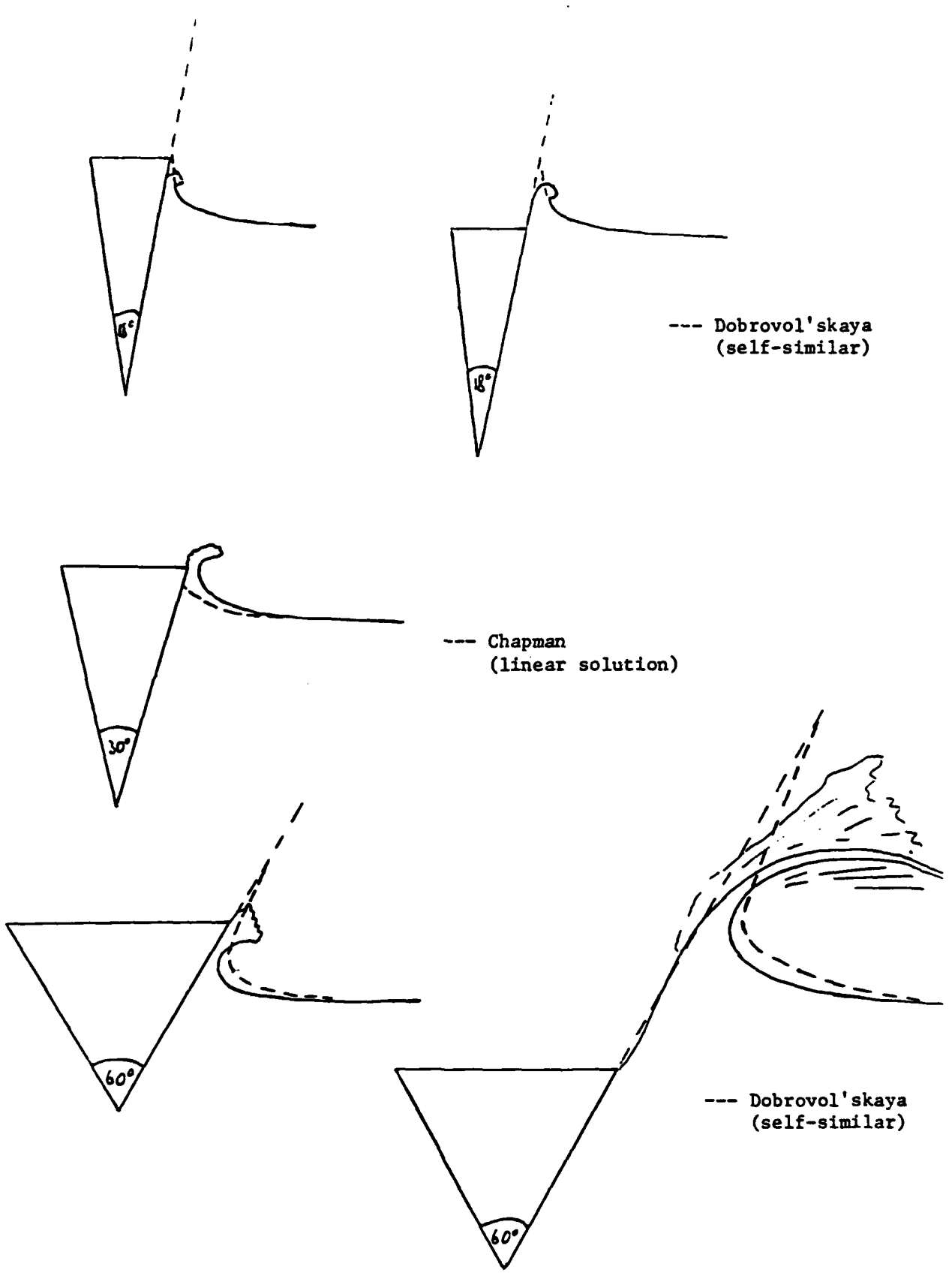

Figure 3.13 Comparison of experiments with existing theories

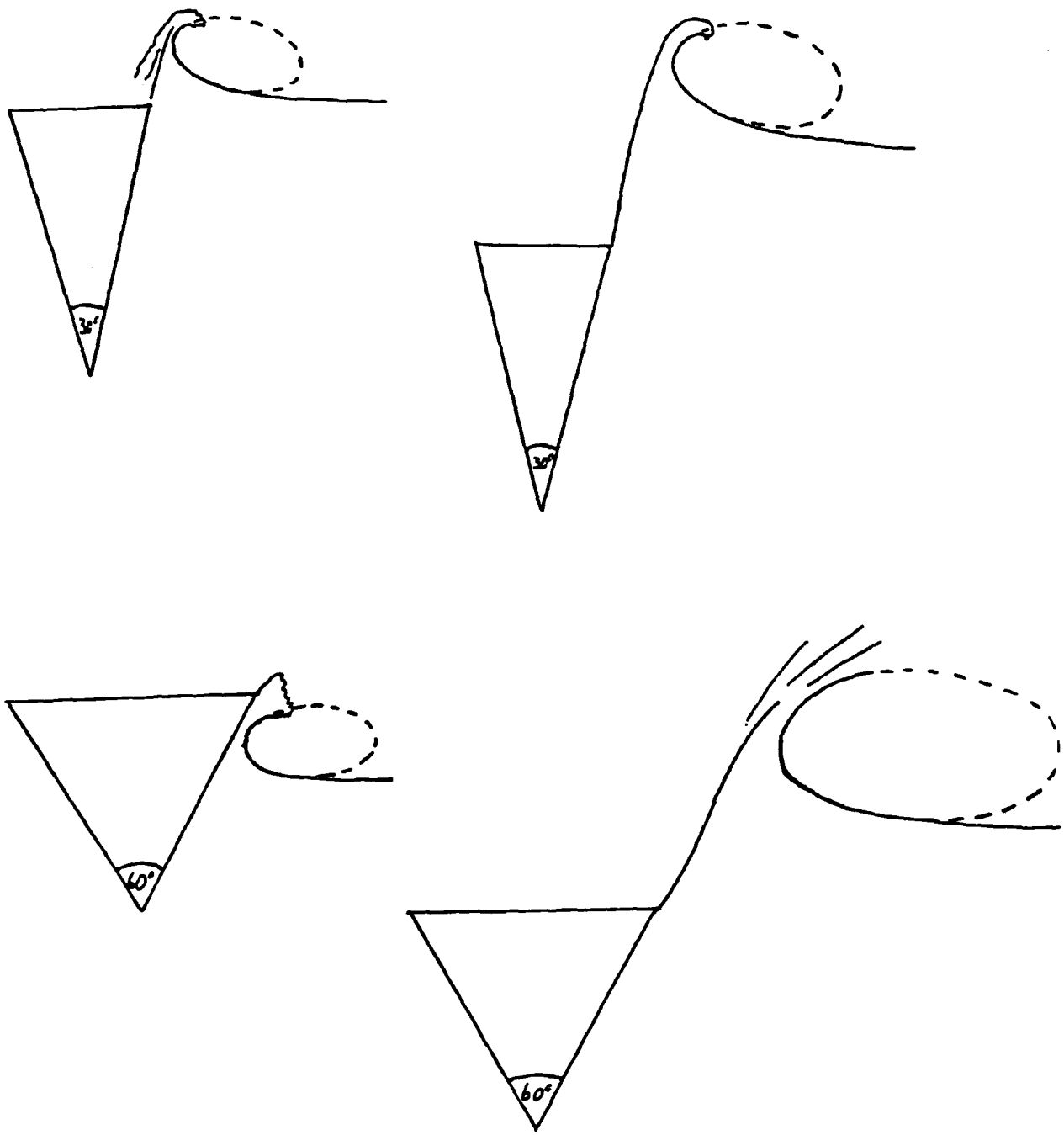

Figure 3.14 Selection of comparisons of experiments (——) with the $\sqrt{3}$ - ellipse of New (---)

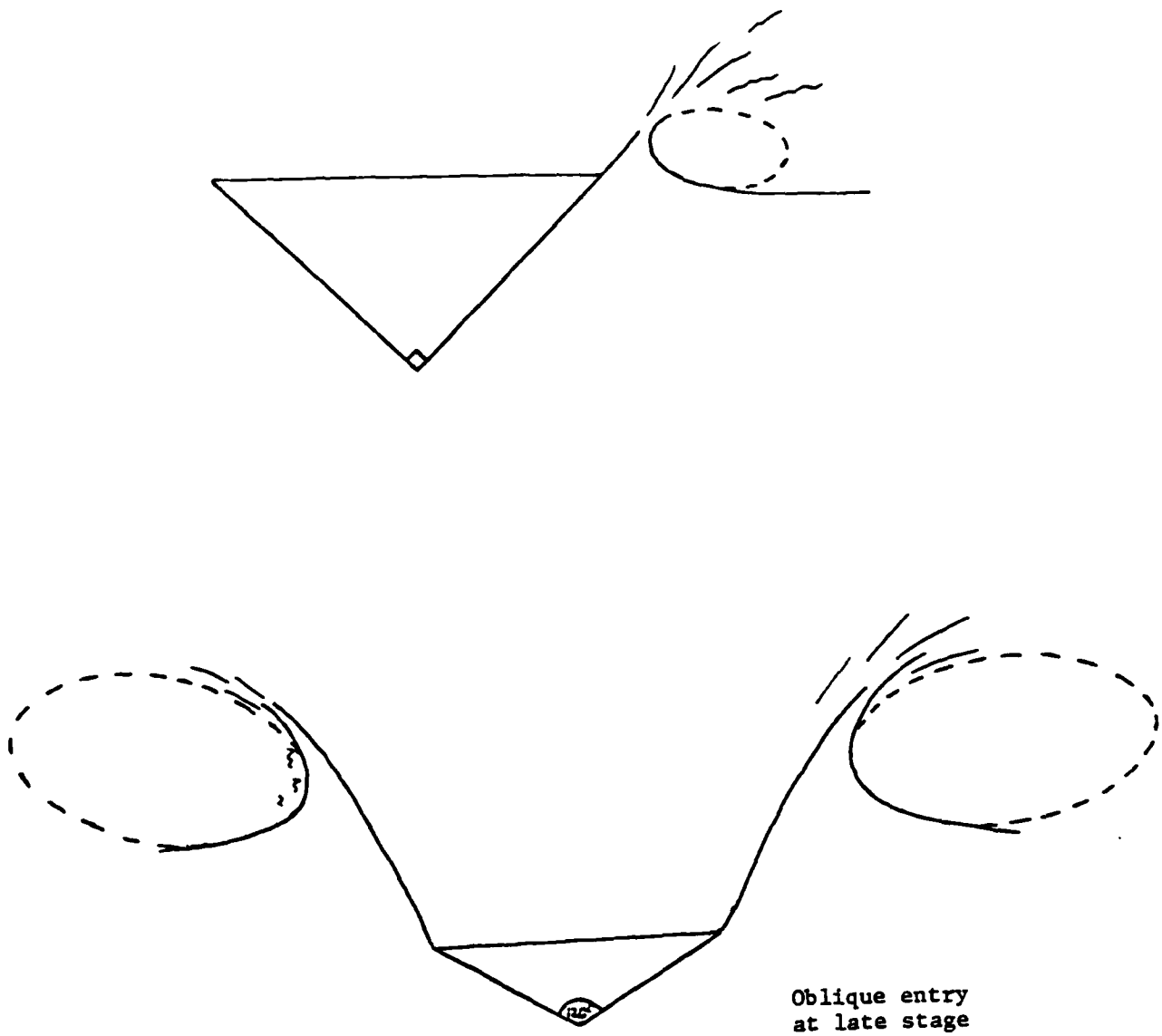

Figure 3.14 (cont'd)

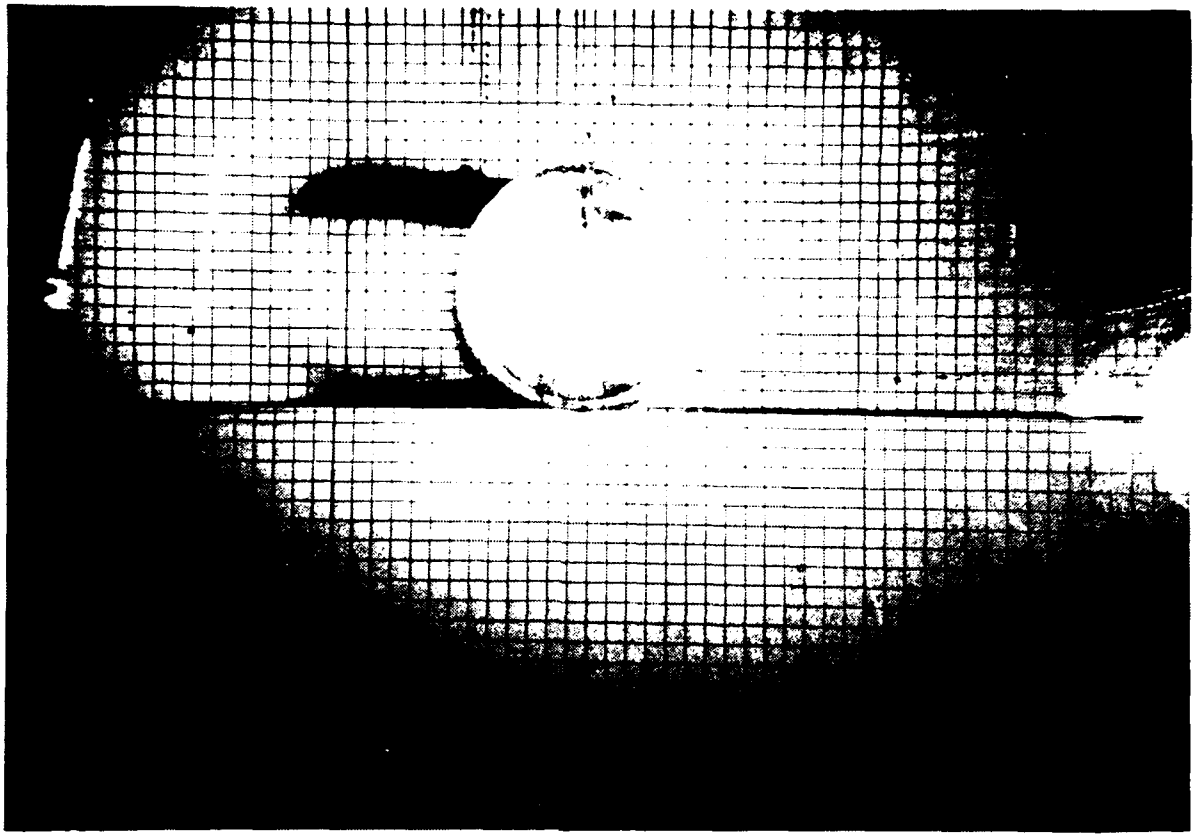

#8/3, t = 0.285s

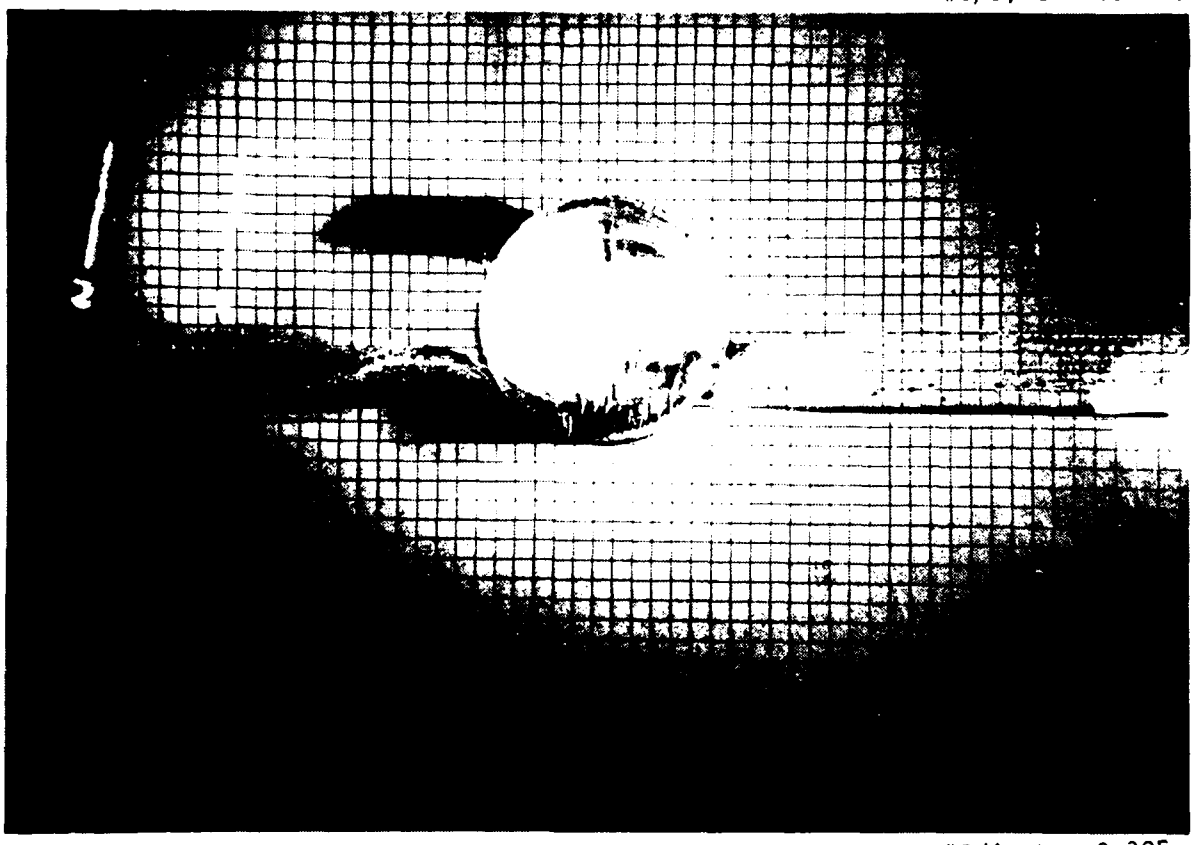

#8/4, t = 0.305s

Figure 4.1 Water entry of a half-buoyant circular cylinder outer dia = 11 cm.

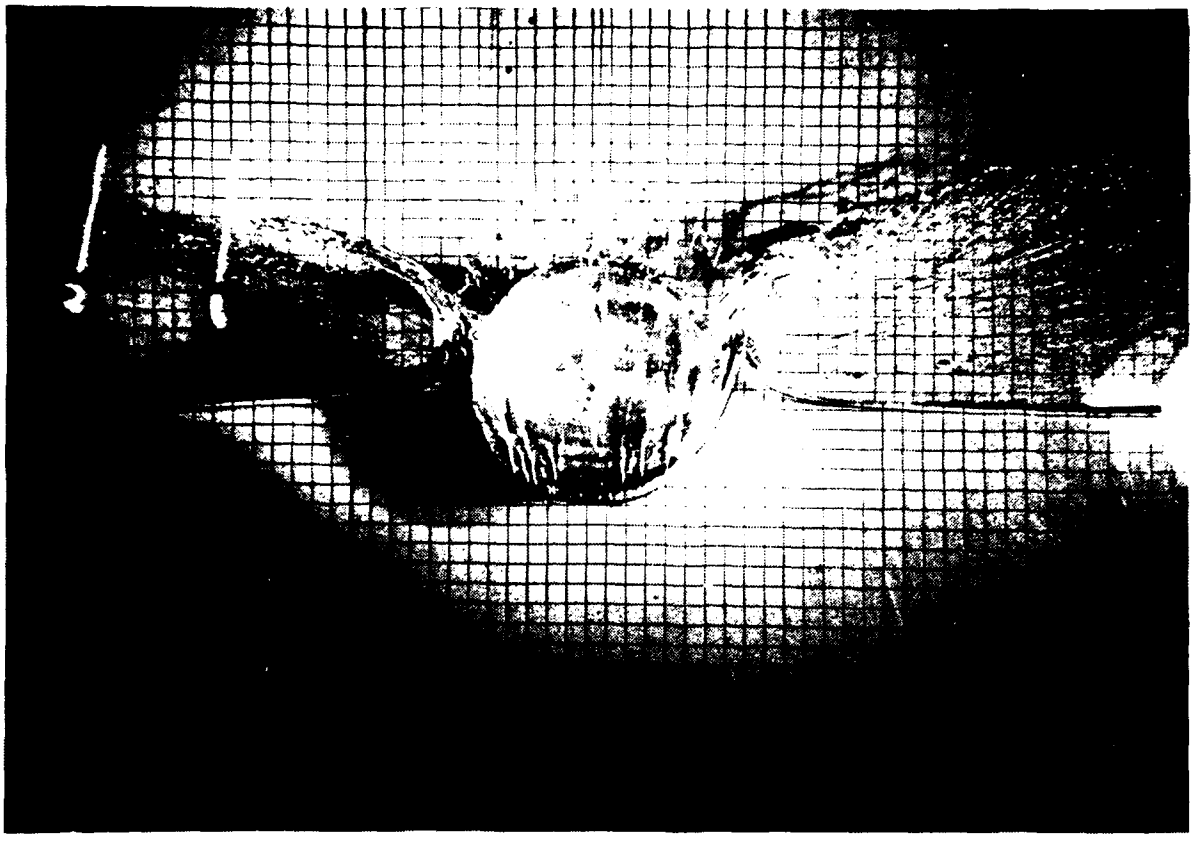

#8/7, t = 0.32s

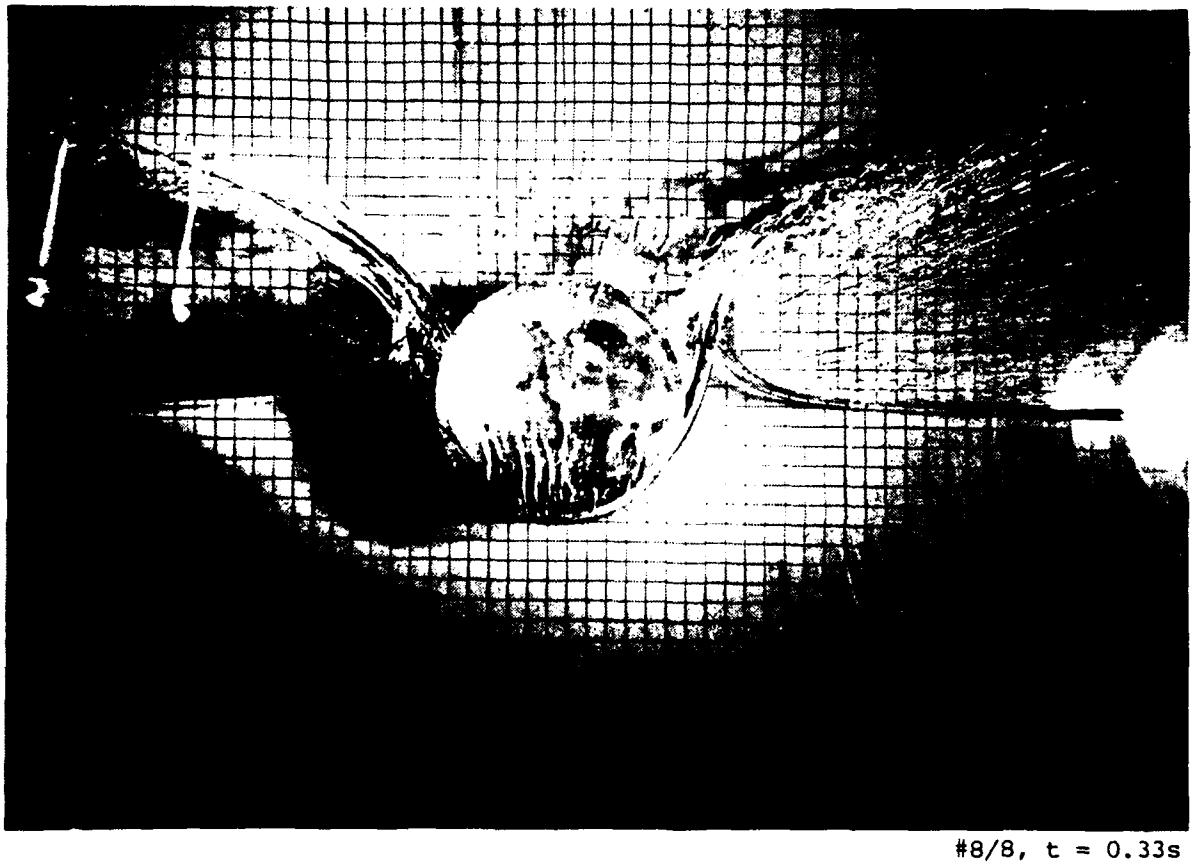

#8/8, t = 0.33s

Figure 4.1 (cont'd)

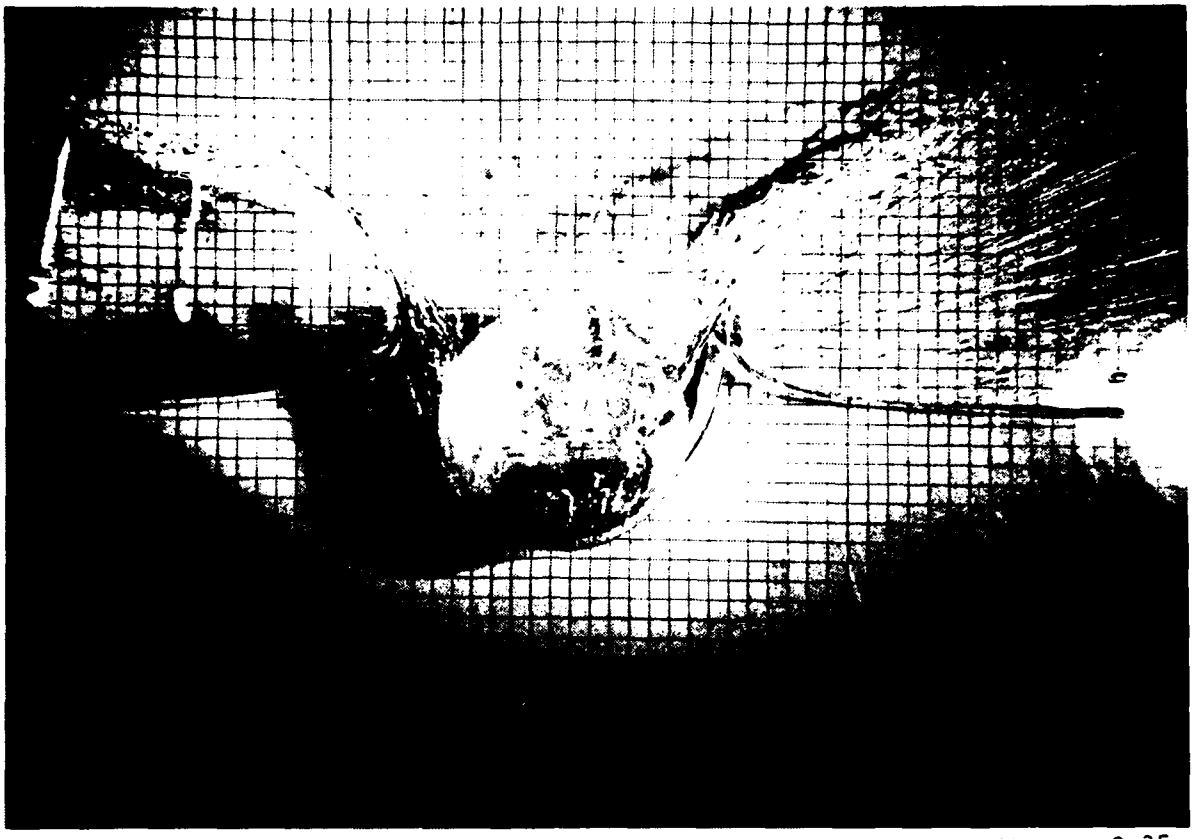

#8/9, t = 0.35s

#8/10, t = 0.385s

Figure 4.1 (cont'd)

#8/11, t = 0.42s

Figure 4.1 (cont'd)

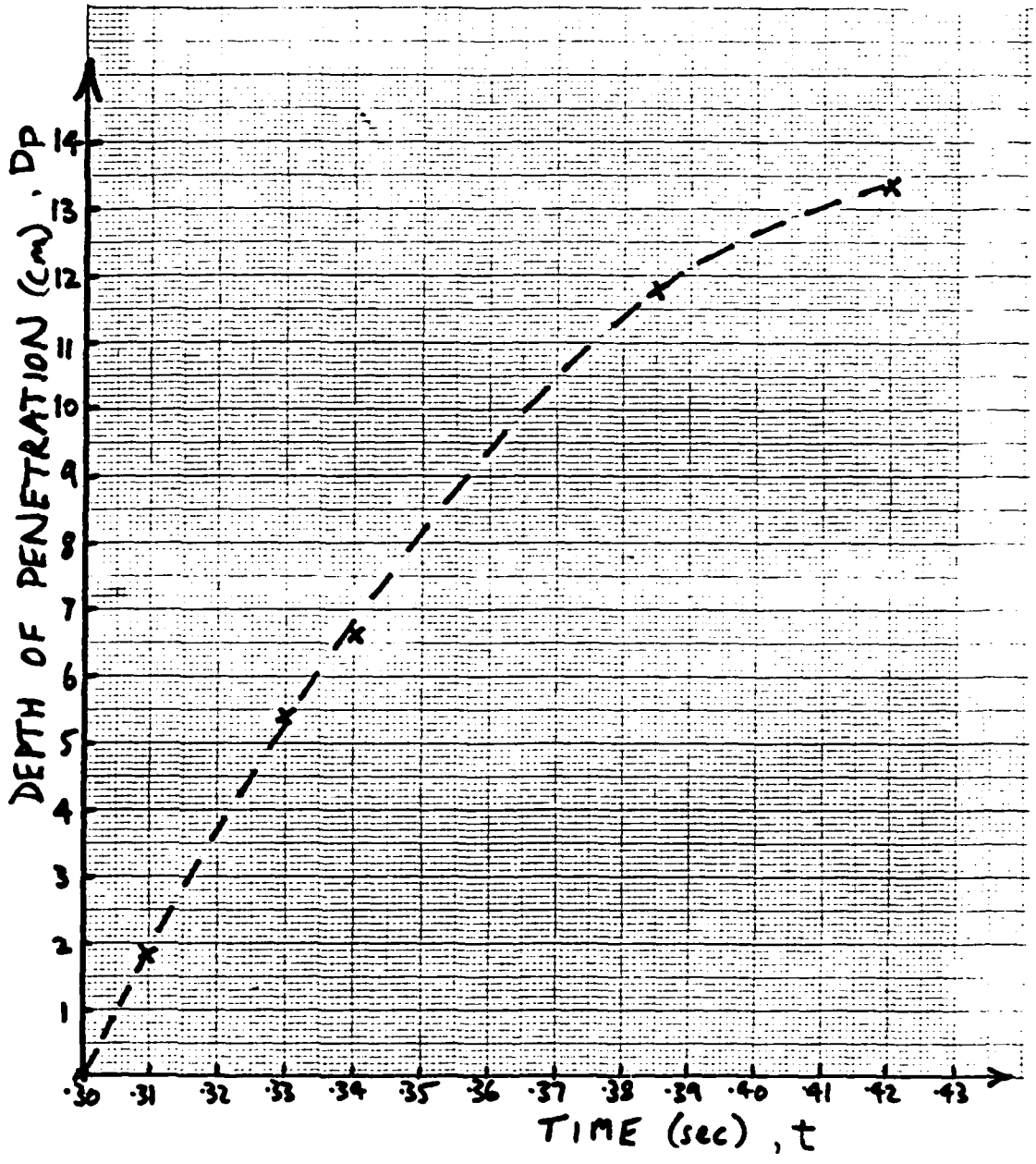

Figure 4.2 D_p - t relation for half-buoyant cylinder

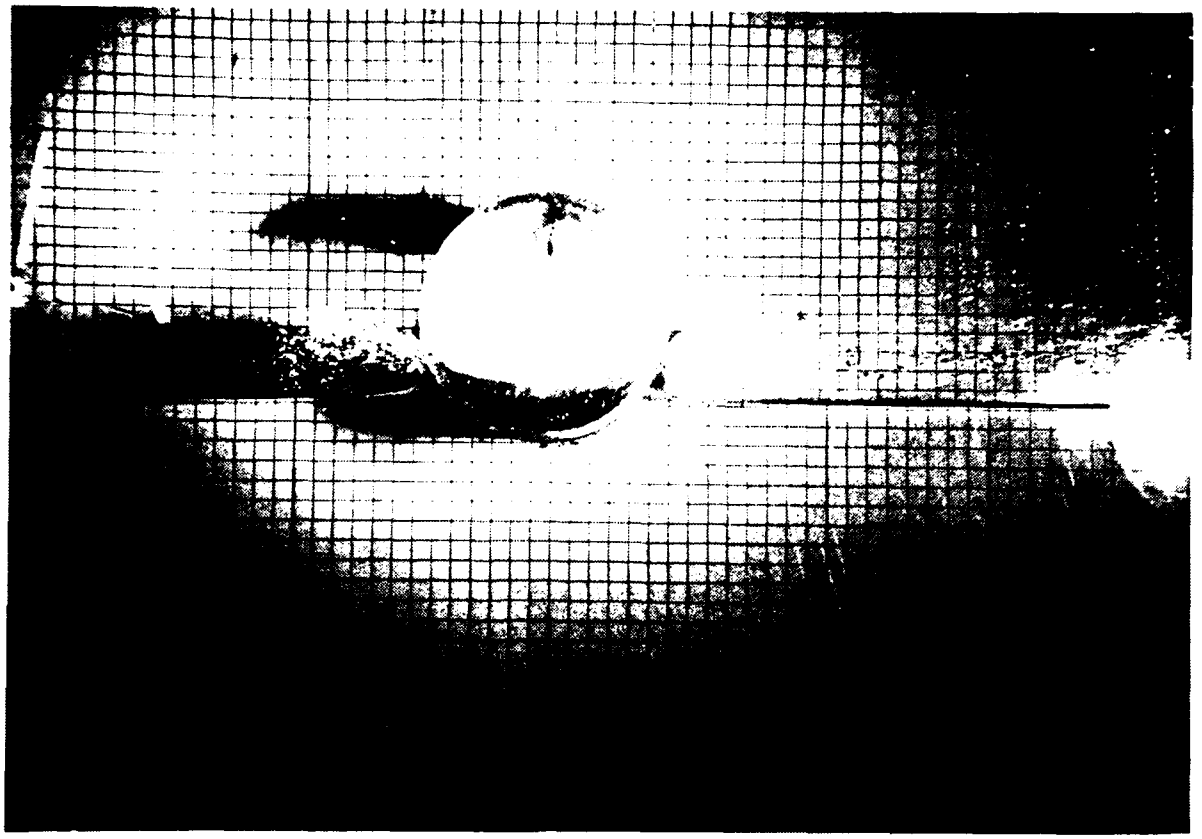

#8/15, t = 0.305s

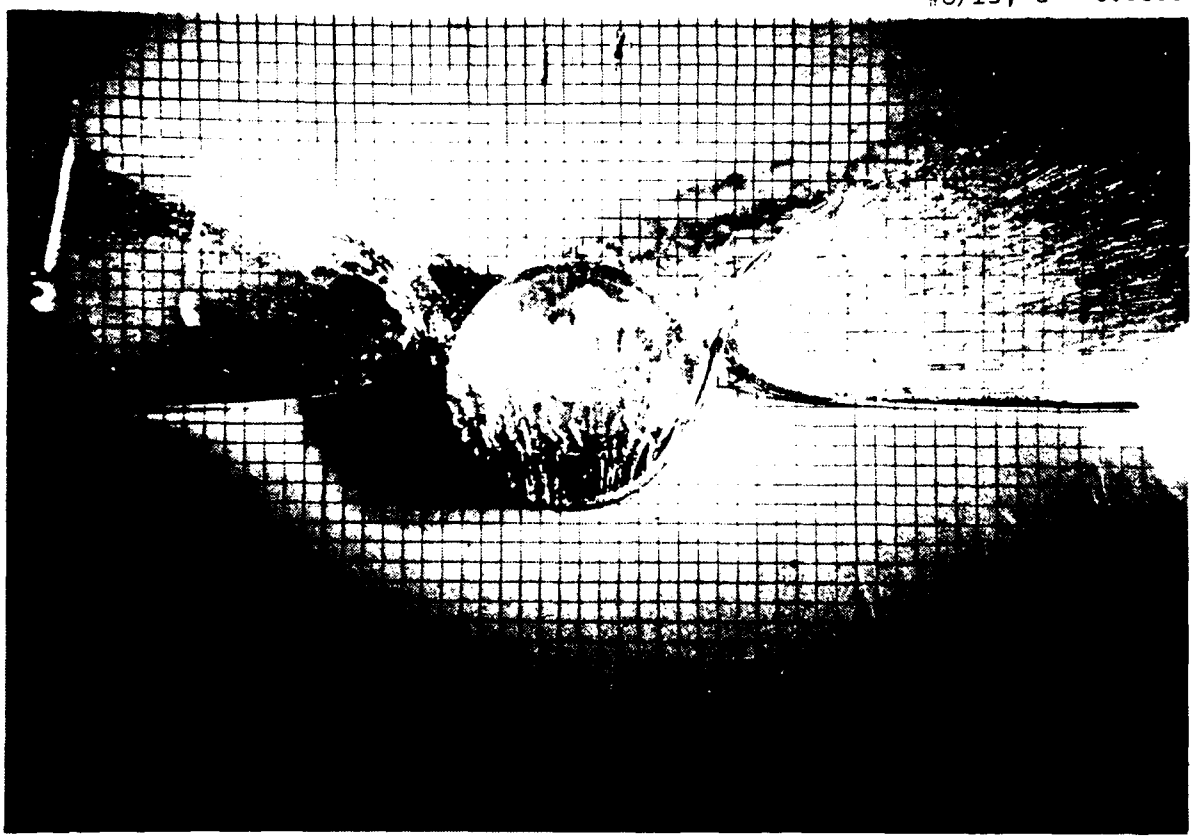

#8/16, t = 0.315s

Figure 4.3 Water entry of a neutrally-buoyant circular cylinder.

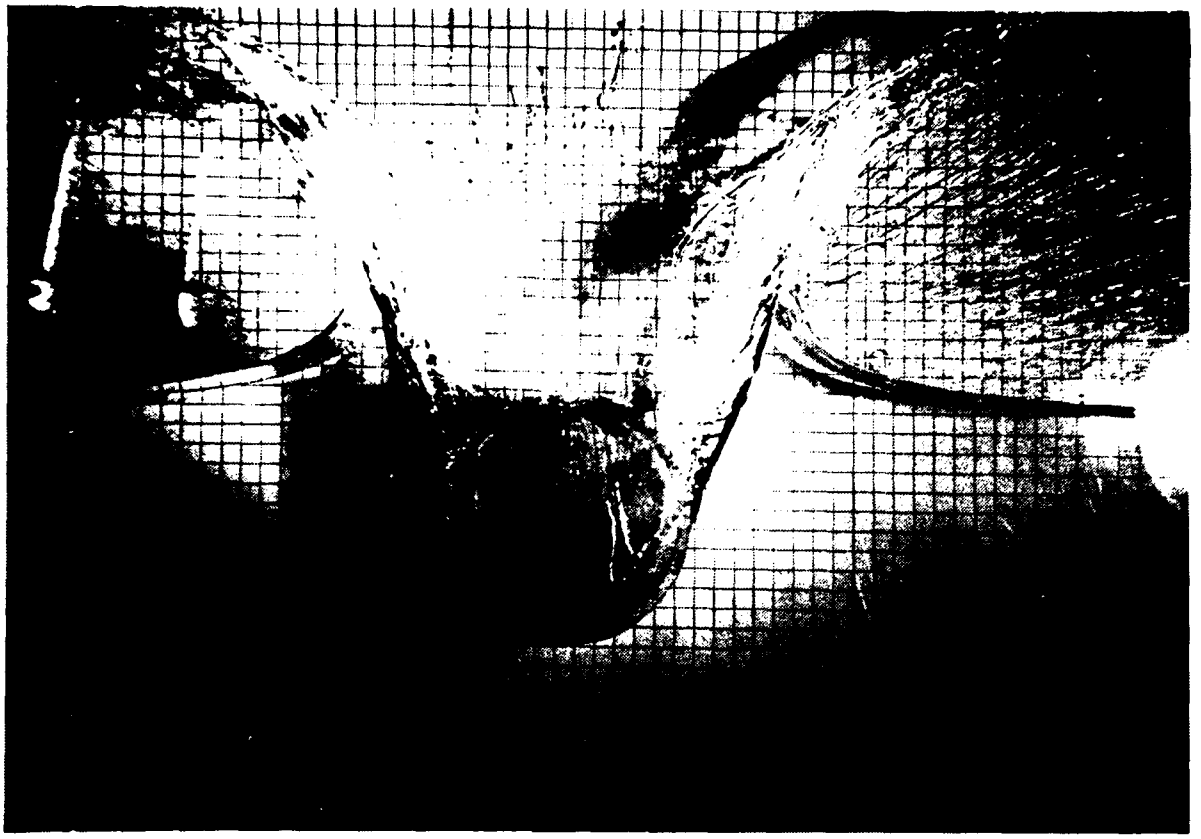

#8/17, t = 0.33s

#8/18, t = 0.34s

Figure 4.3 (cont'd)

#8/20, t = 0.39s

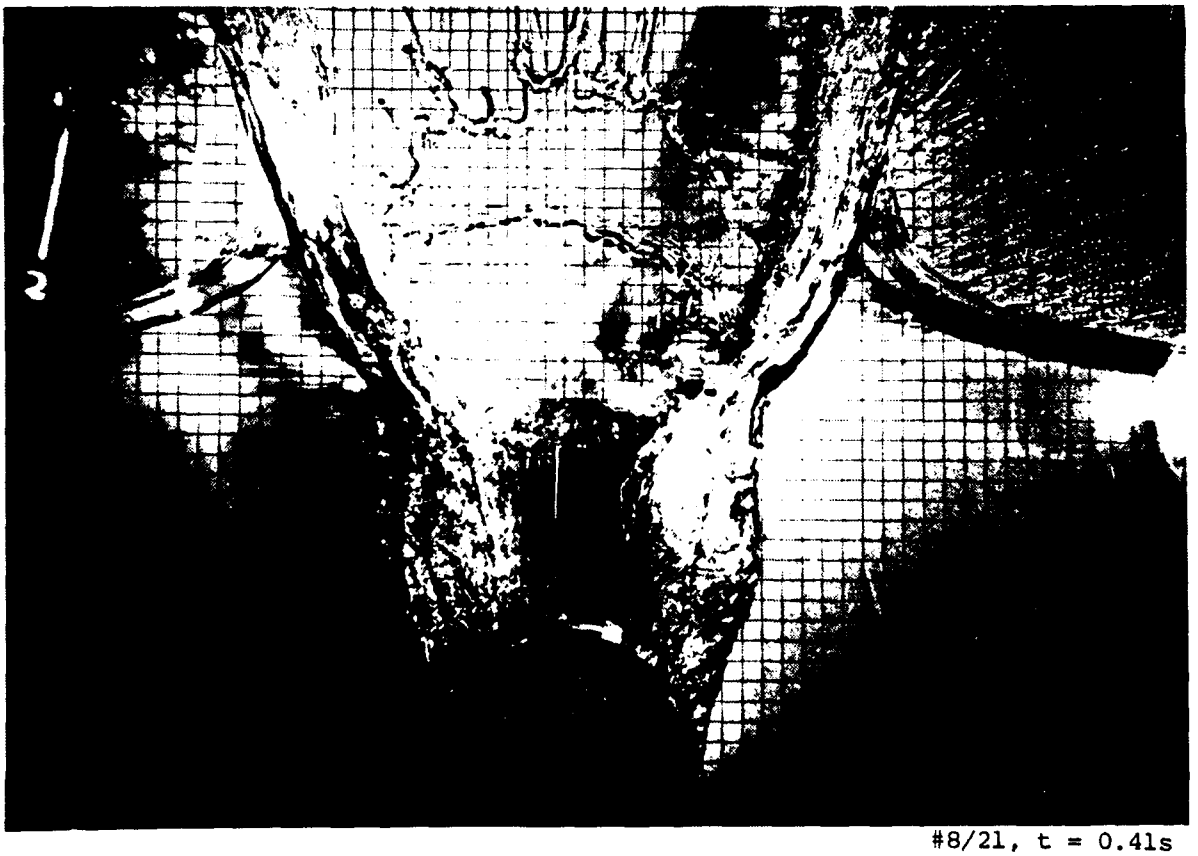

#8/21, t = 0.41s

Figure 4.3 (cont'd)

#10/i, t = 0.50s

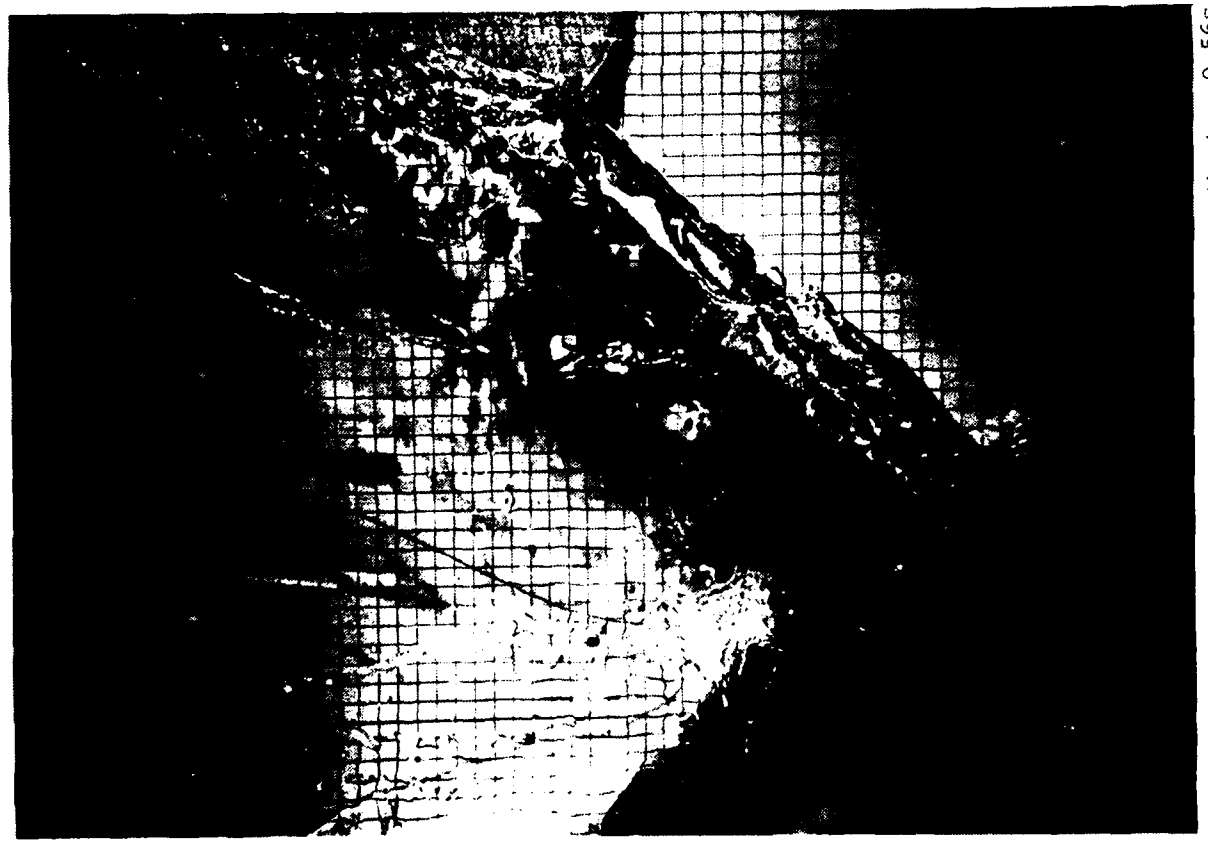

#10/4, t = 0.56s

Figure 4.3 (cont'd)

#10/6, t = 0.60s

#10/7, t = 0.69s

Figure 4.3 (cont'd)

#10/8, t = 0.75s

#10/9, t = 0.92s

Figure 4.3 (cont'd)

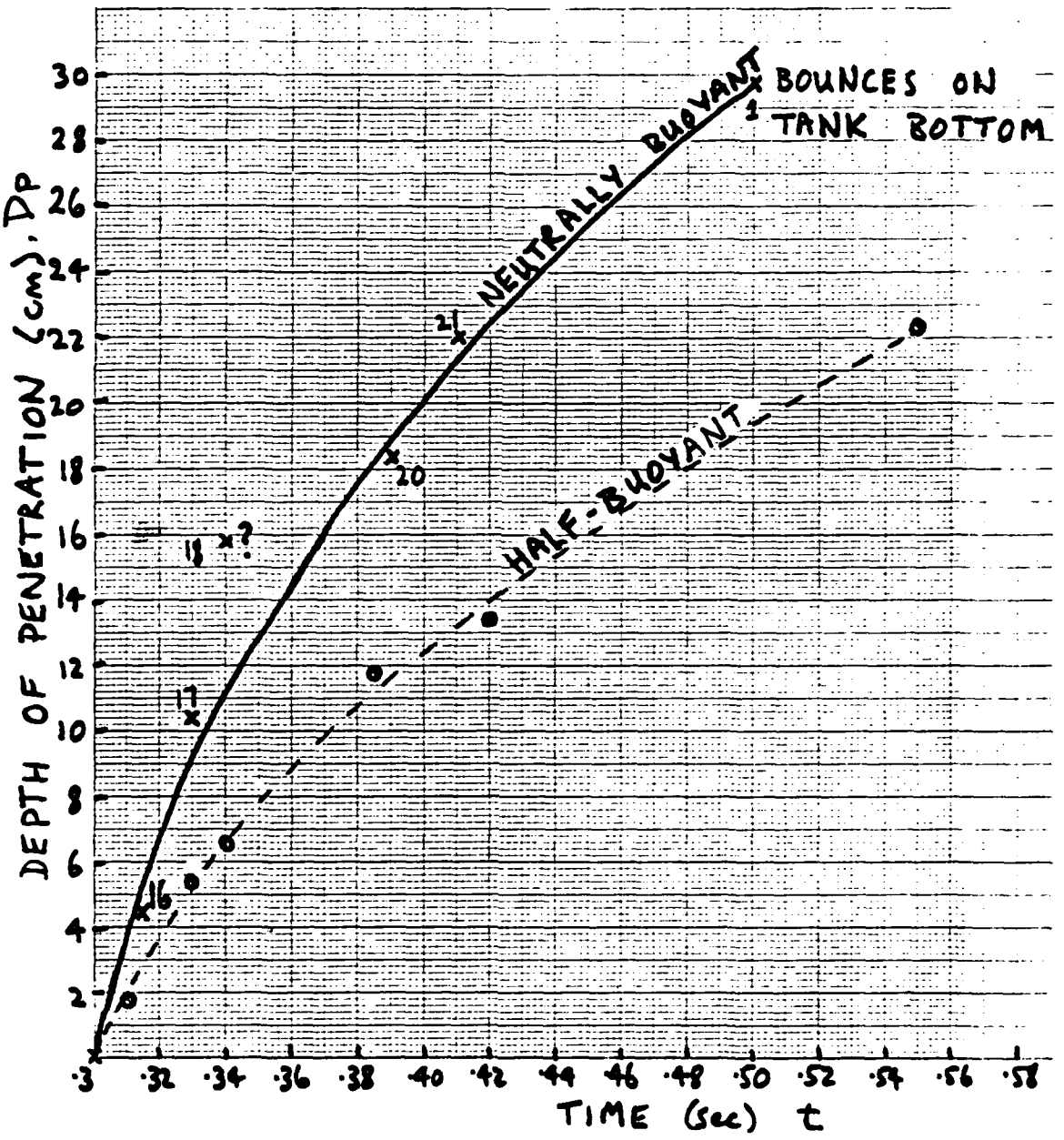

Figure 4.4 D_p - t relation for neutrally-buoyant cylinder

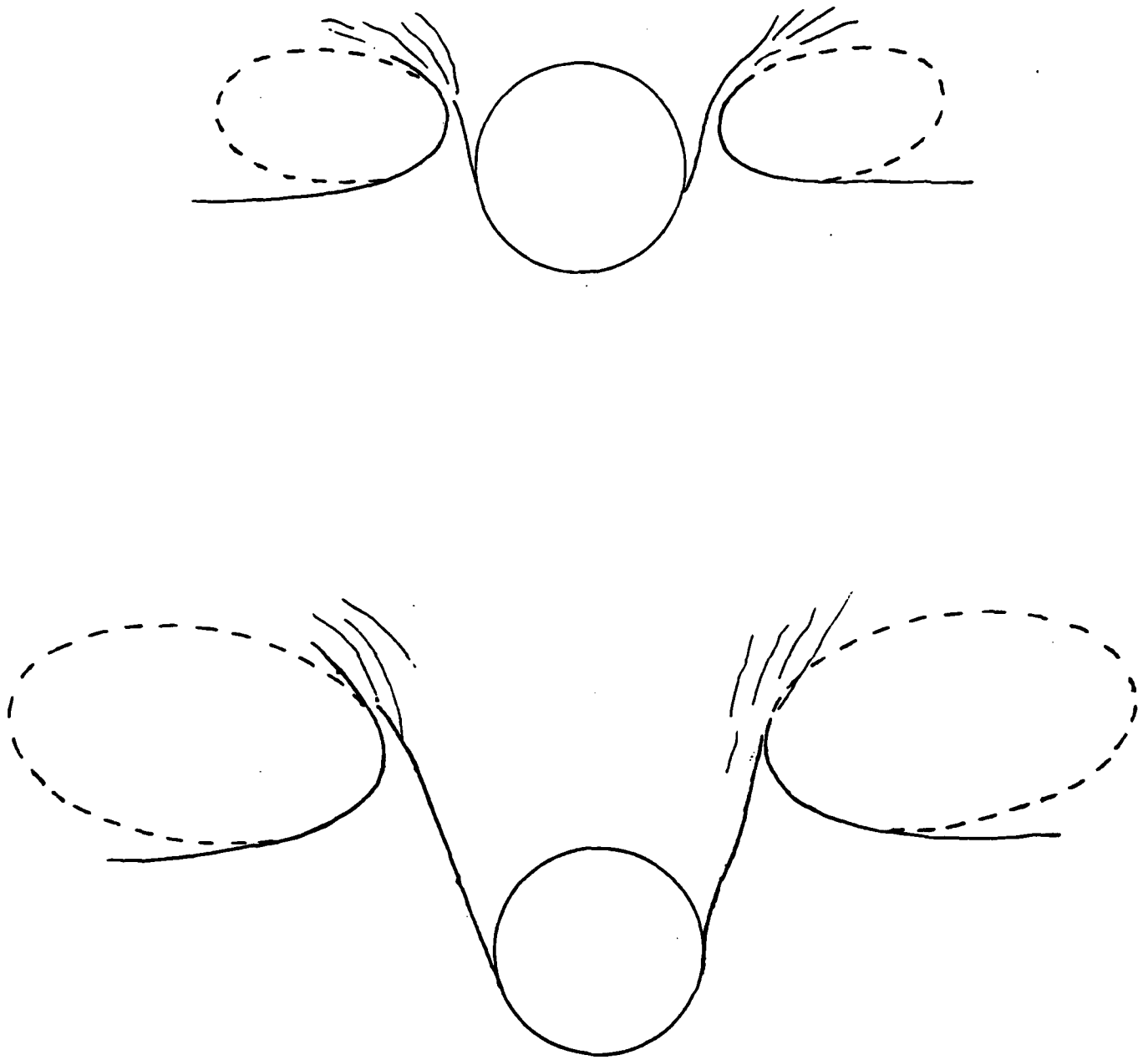

Figure 4.5 Comparison of experiments with the $\sqrt{3}$ - ellipse of New

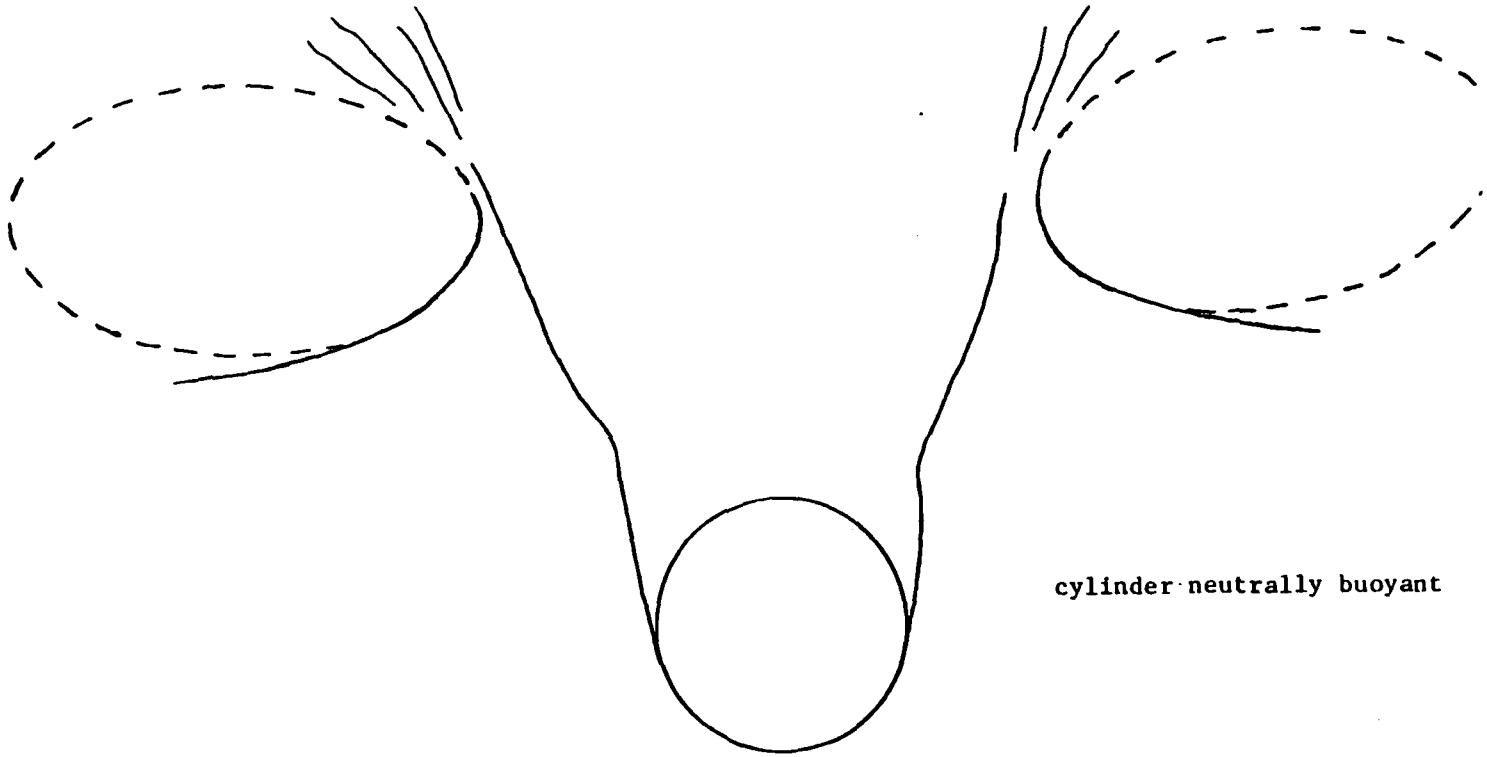

Figure 4.5 (cont'd)

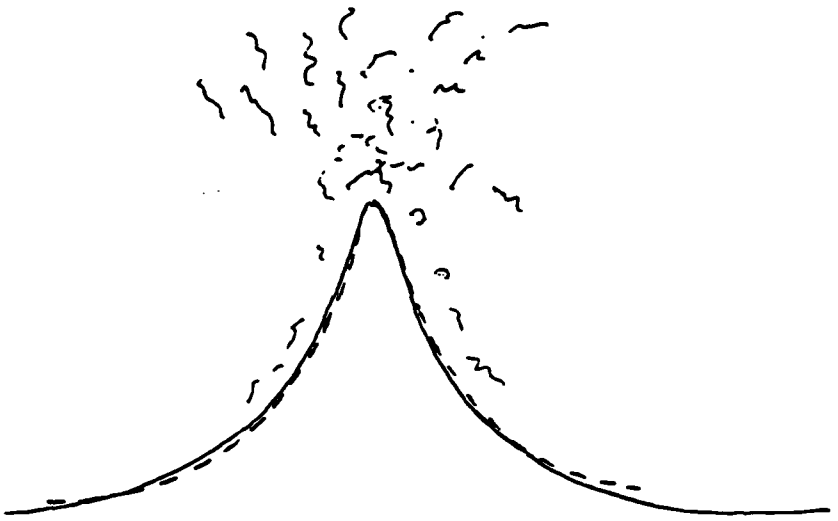

Figure 4.6 Comparison of the jet (——) with the overdriven standing wave of McIver and Peregrine (---)

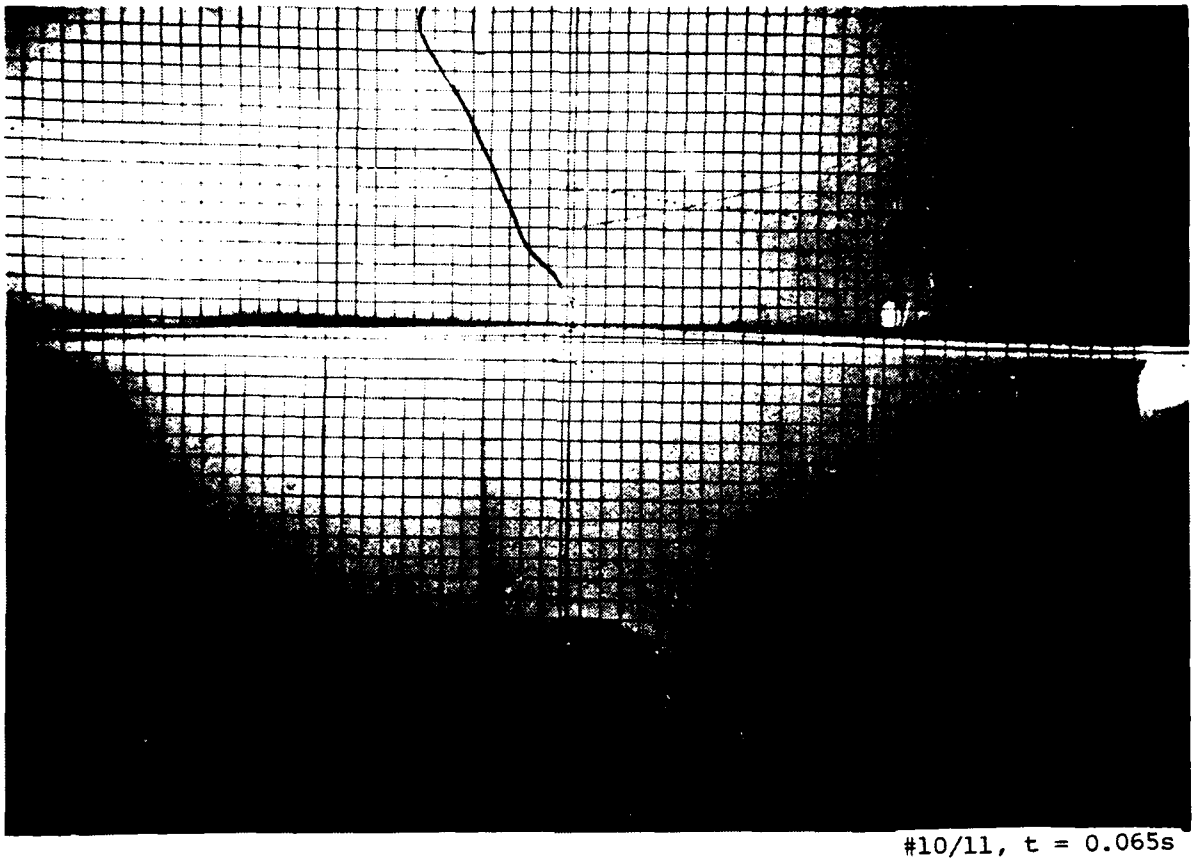

#10/11, t = 0.065s

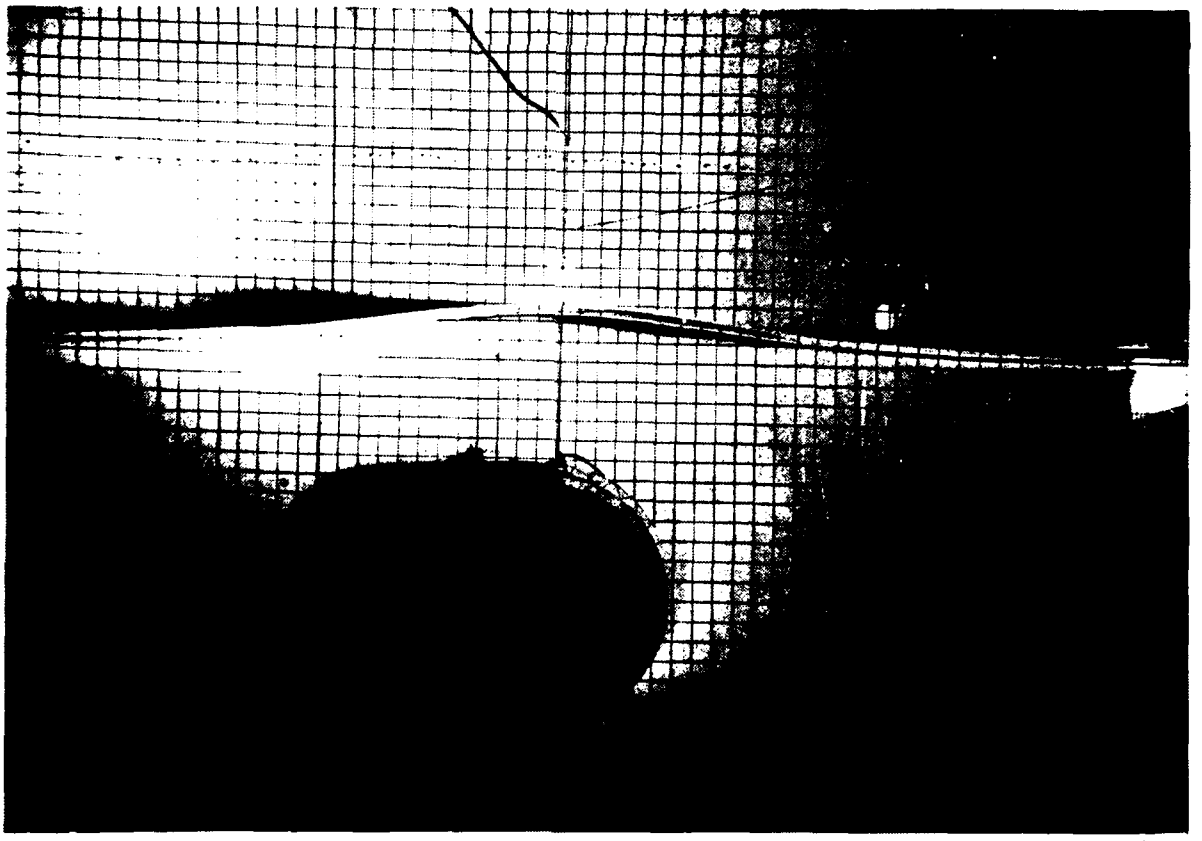

#10/12, t = 0.072s

Figure 5.1 Cylinder exit problem, out dia = 11 cm.

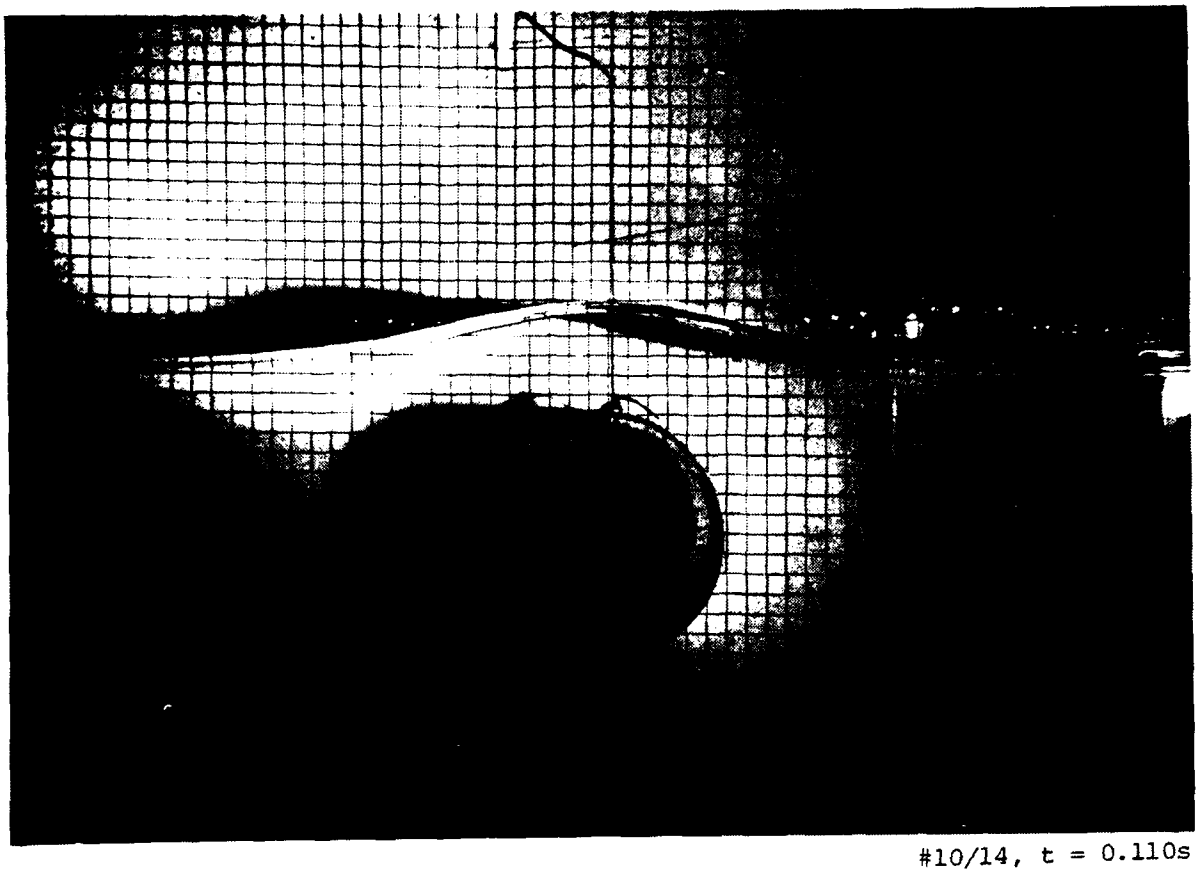

#10/14, t = 0.110s

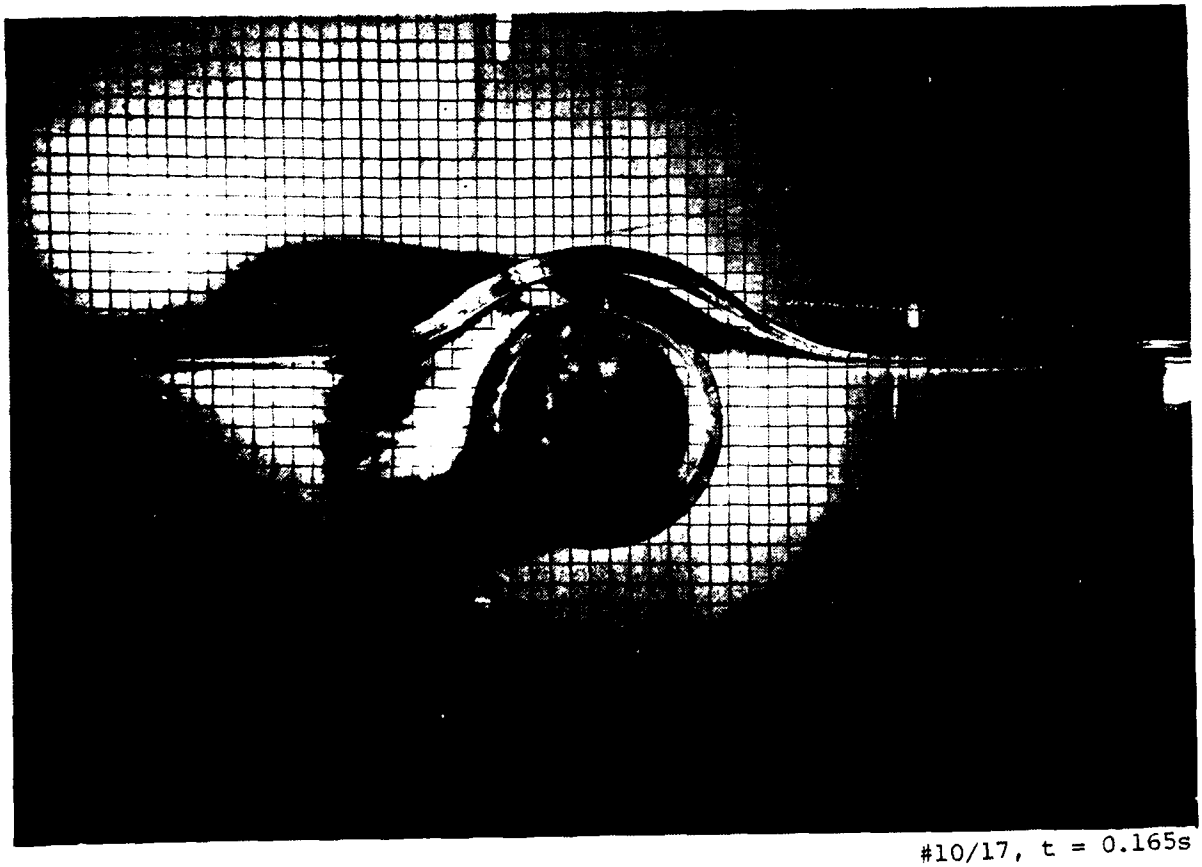

#10/17, t = 0.165s

Figure 5.1 (cont'd)

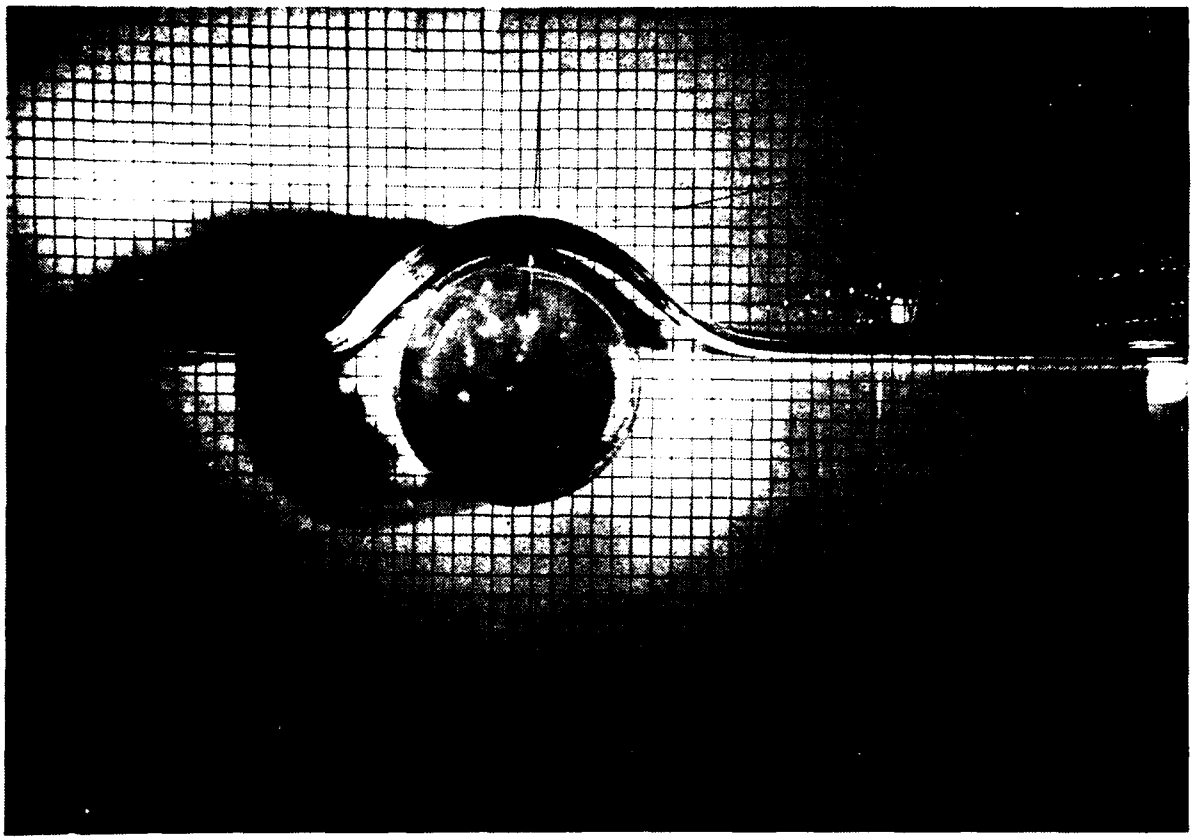

#10/19, t = 0.190s

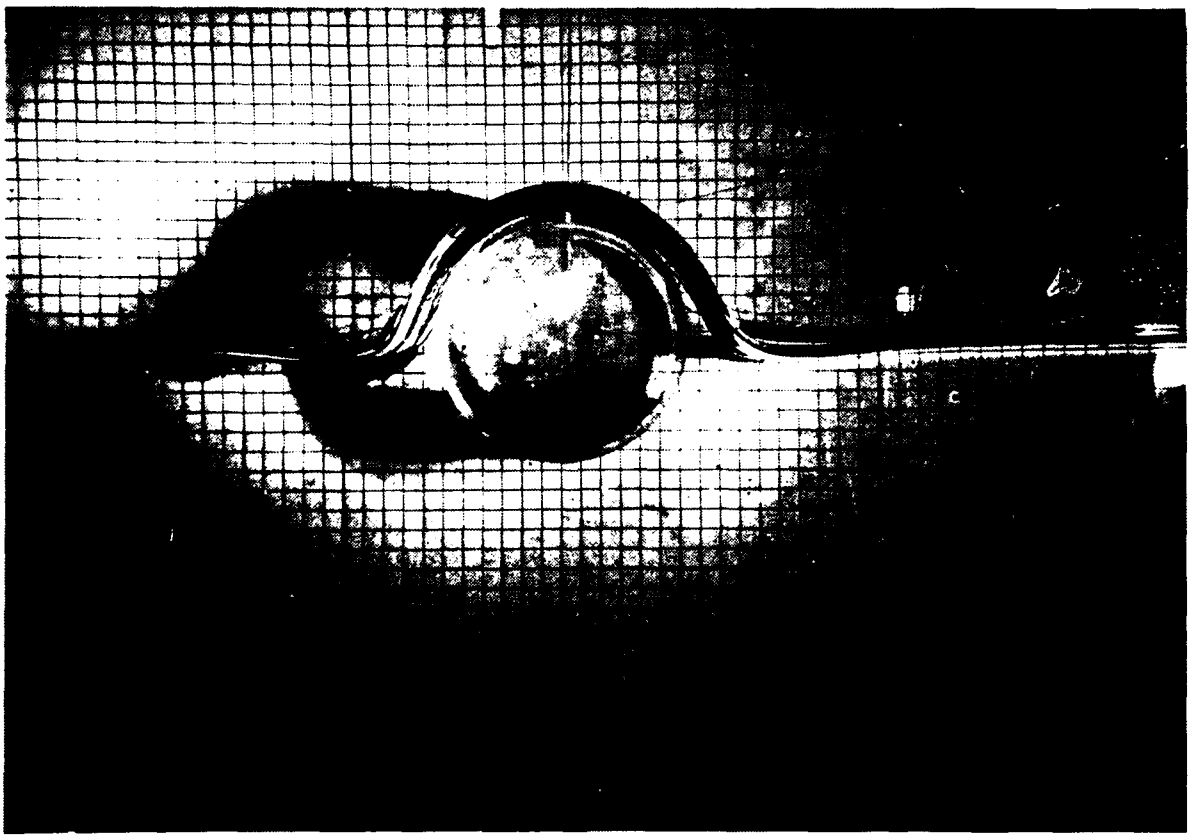

#10/21, t = 0.195s

Figure 5.1 (cont'd)

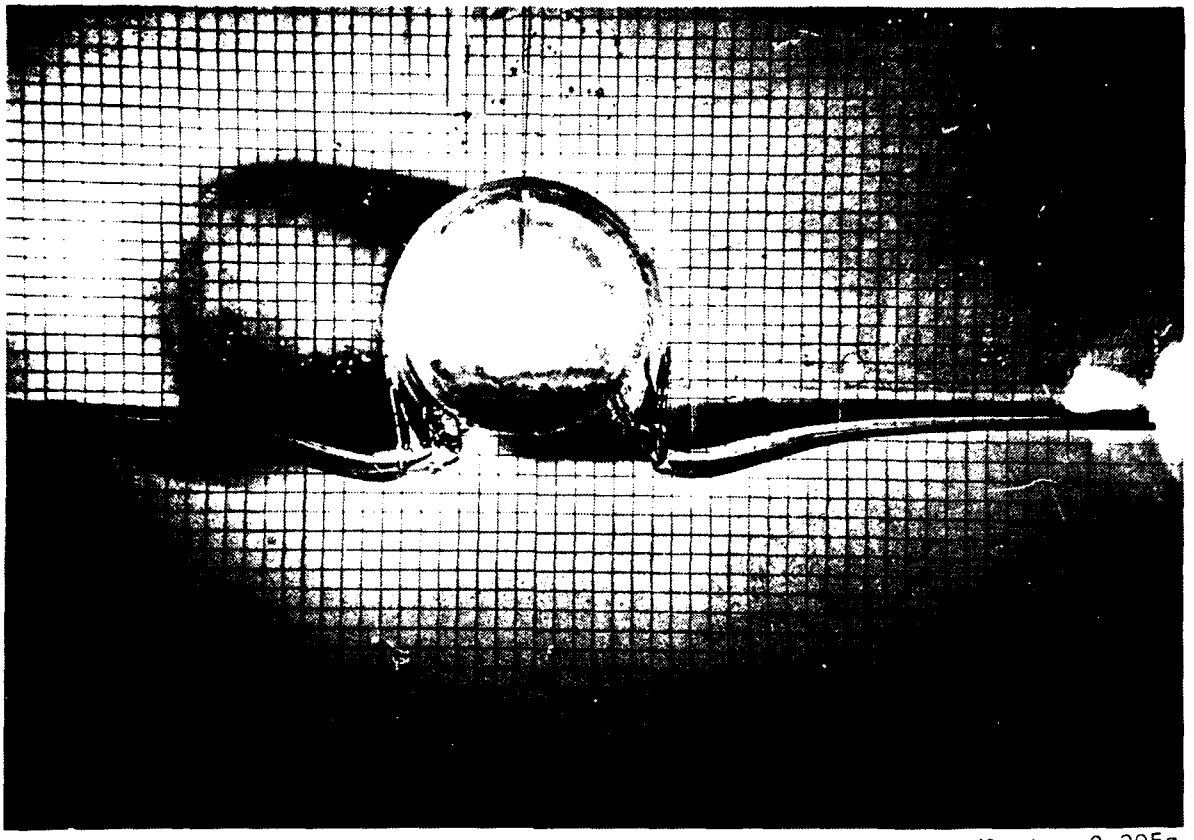

#11/2, t = 0.205s

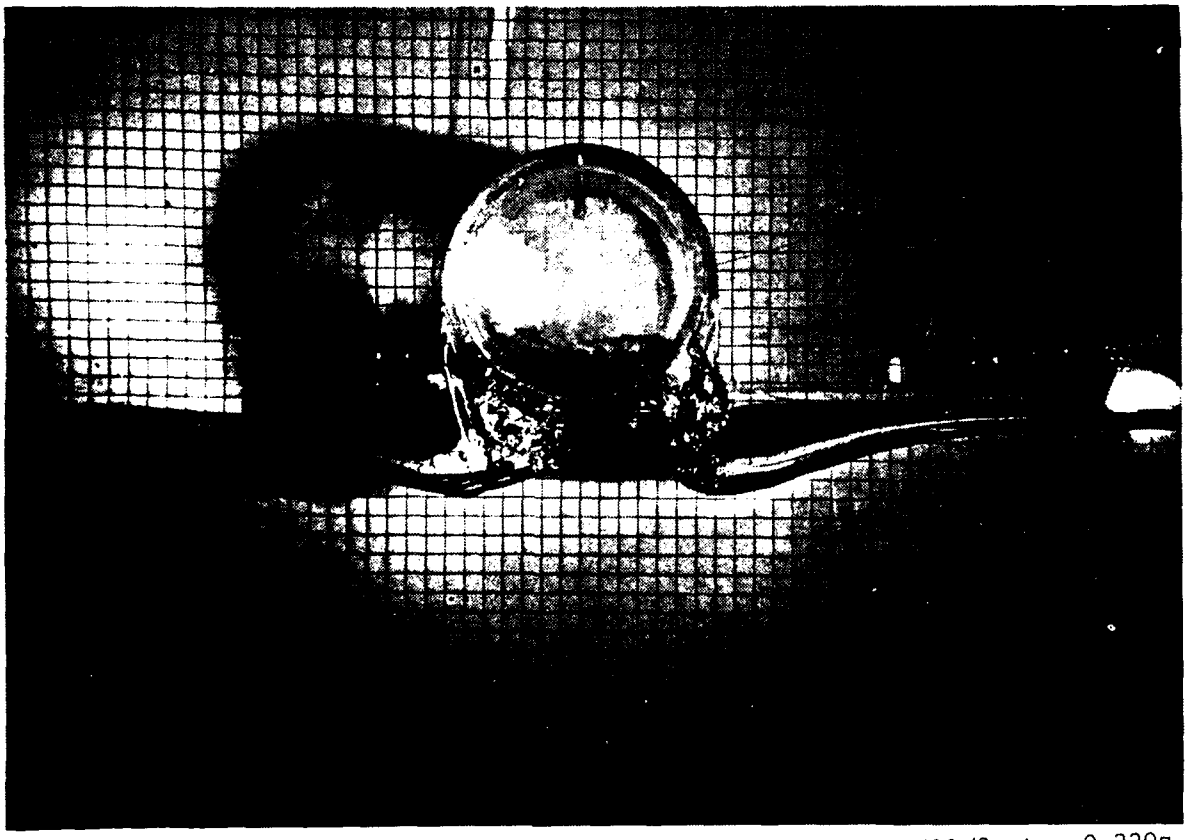

#11/3, t = 0.220s

Figure 5.1 (cont'd)

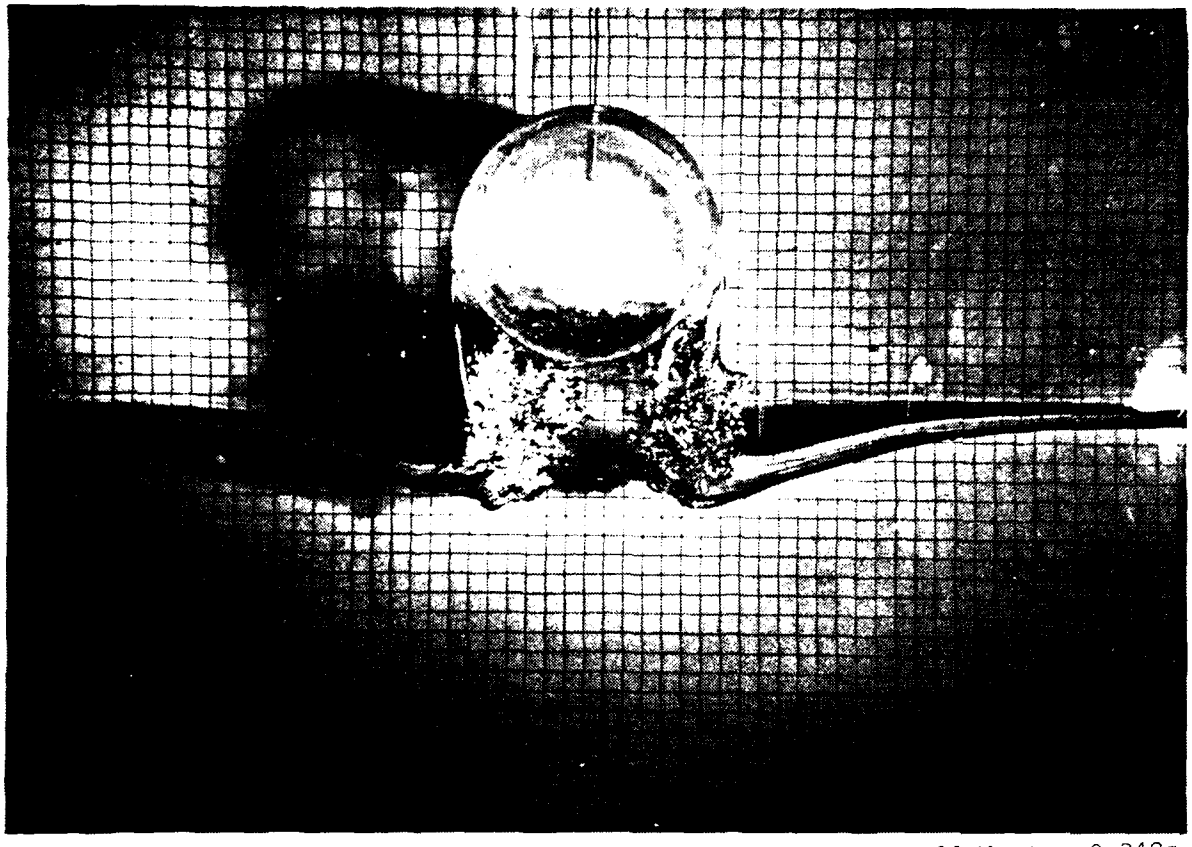

#11/4, t = 0.248s

#11/5, t = 0.280s

Figure 5.1 (cont'd)

#11/6, t = 0.290s

#11/8, t = 0.330s

Figure 5.1 (cont'd)

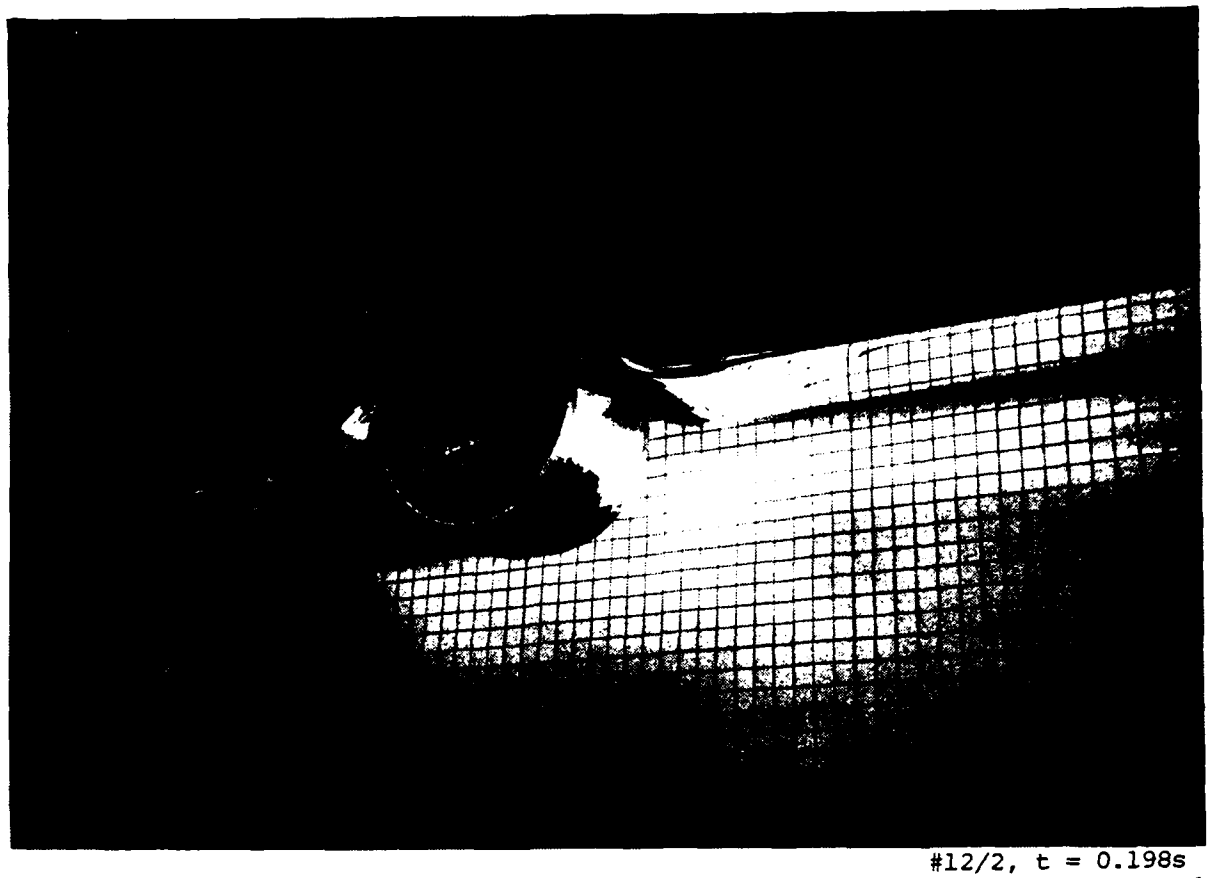

#12/2, t = 0.198s

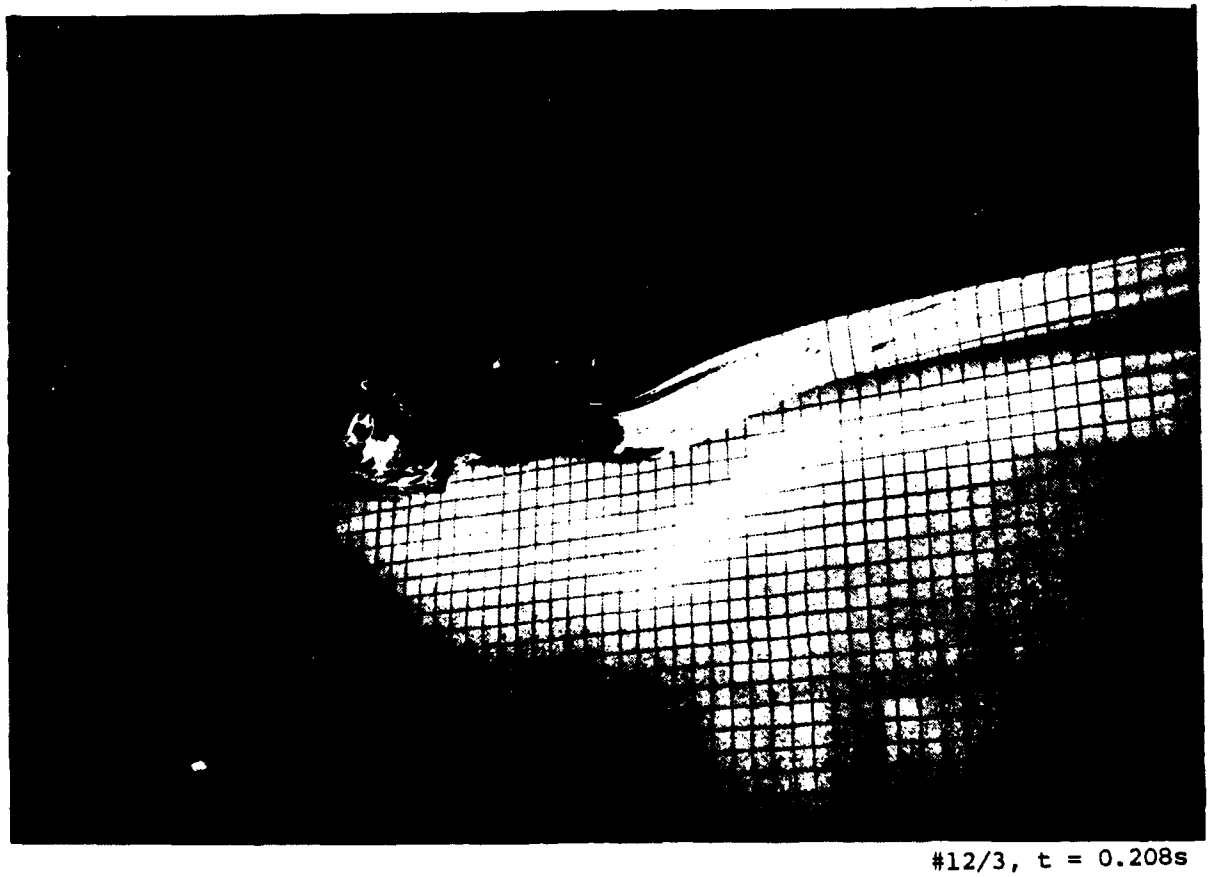

#12/3, t = 0.208s

Figure 5.2 Cylinder exit, oblique view.

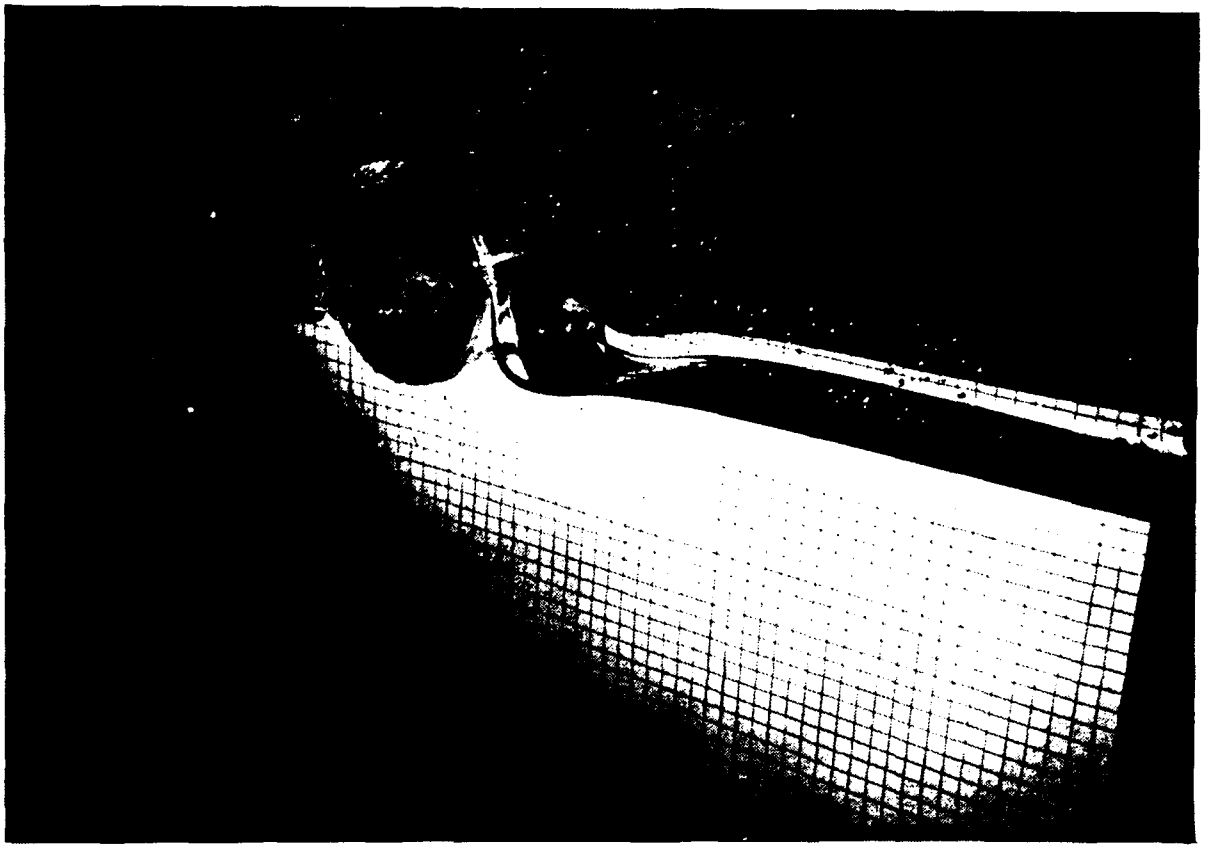

#12/12, t = 0.208s

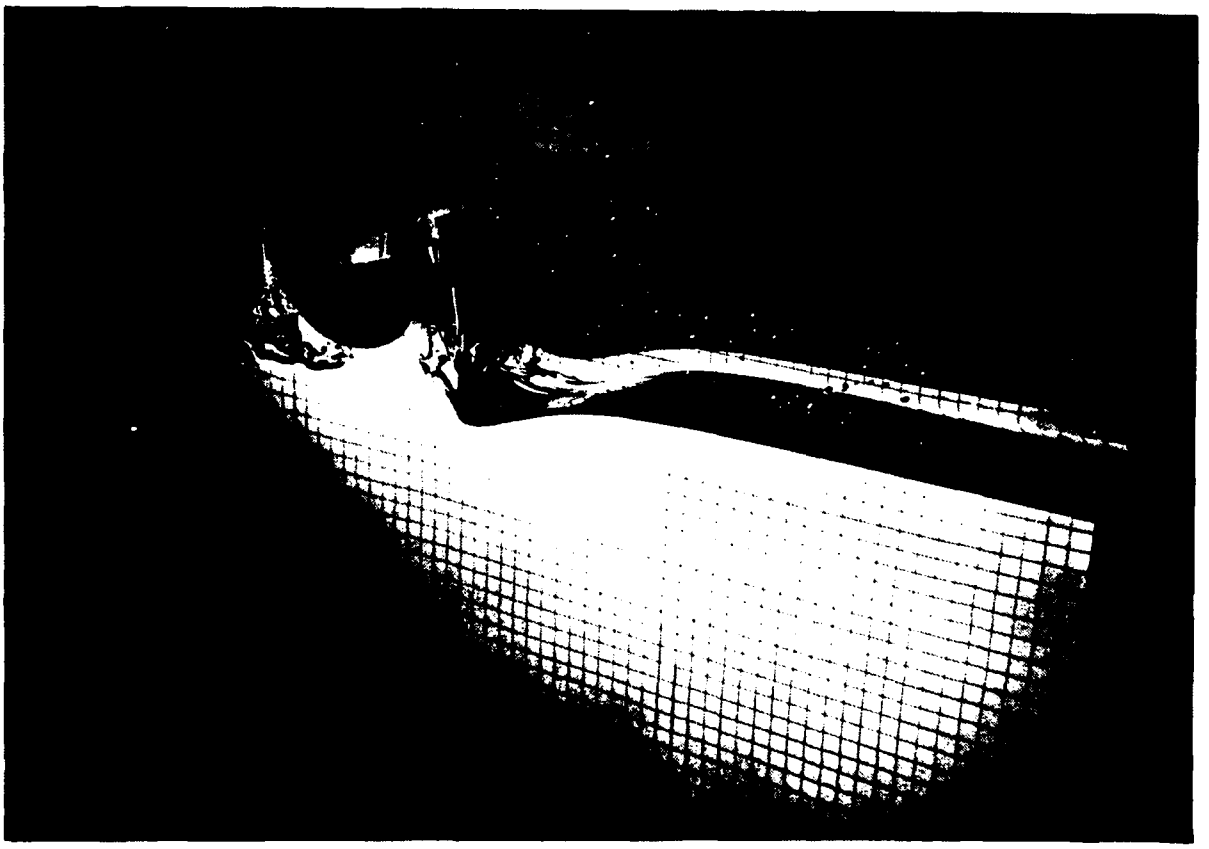

#12/13, t = 0.226s

Figure 5.2 (cont'd)

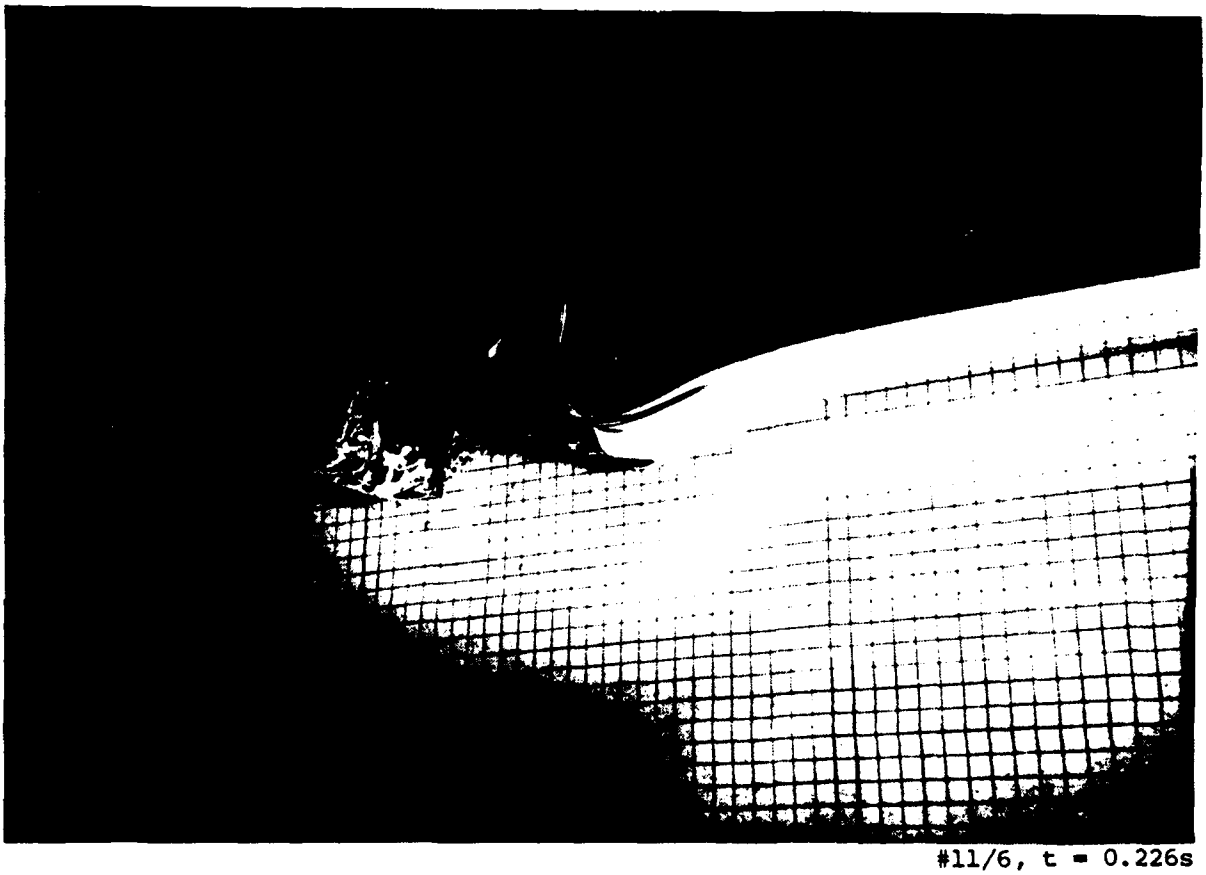

#11/6, t = 0.226s

Figure 5.2 (cont'd)

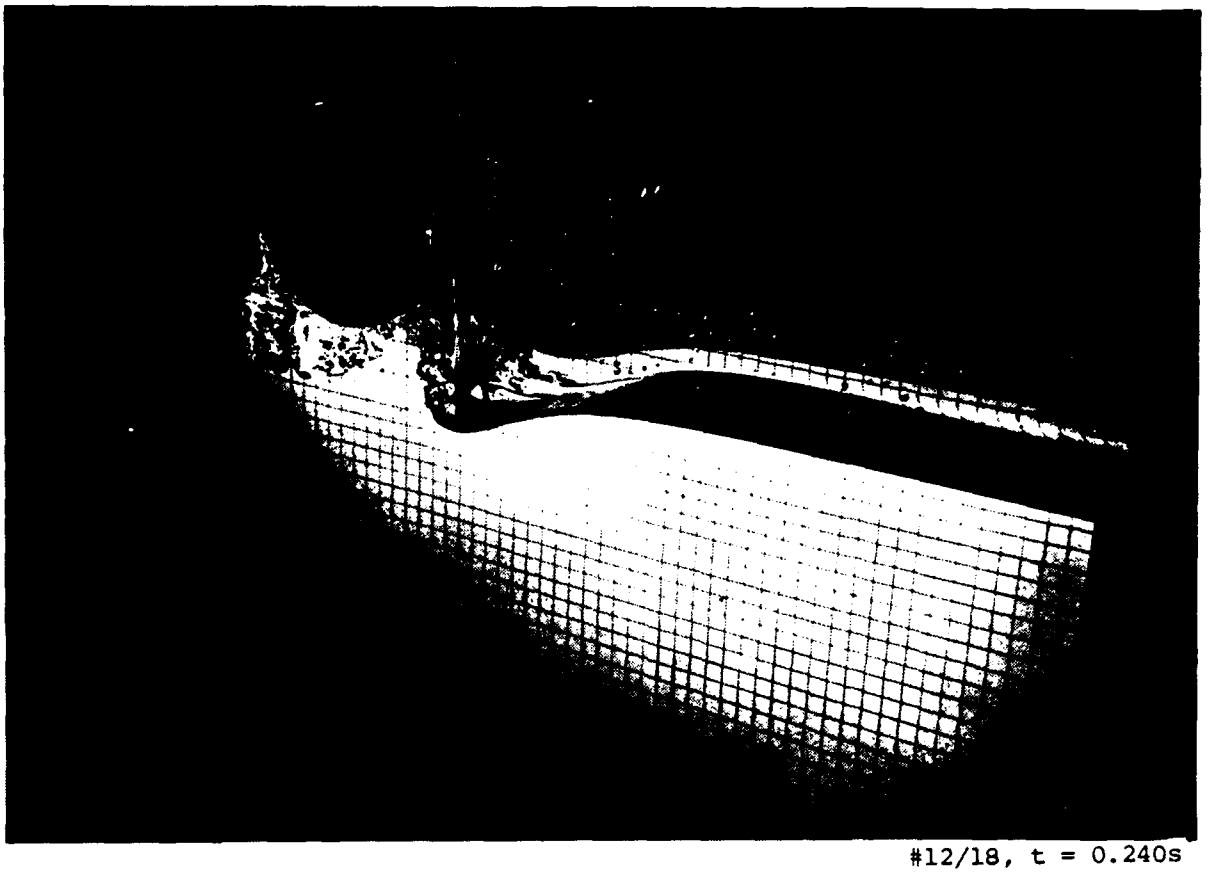

#12/18, t = 0.240s

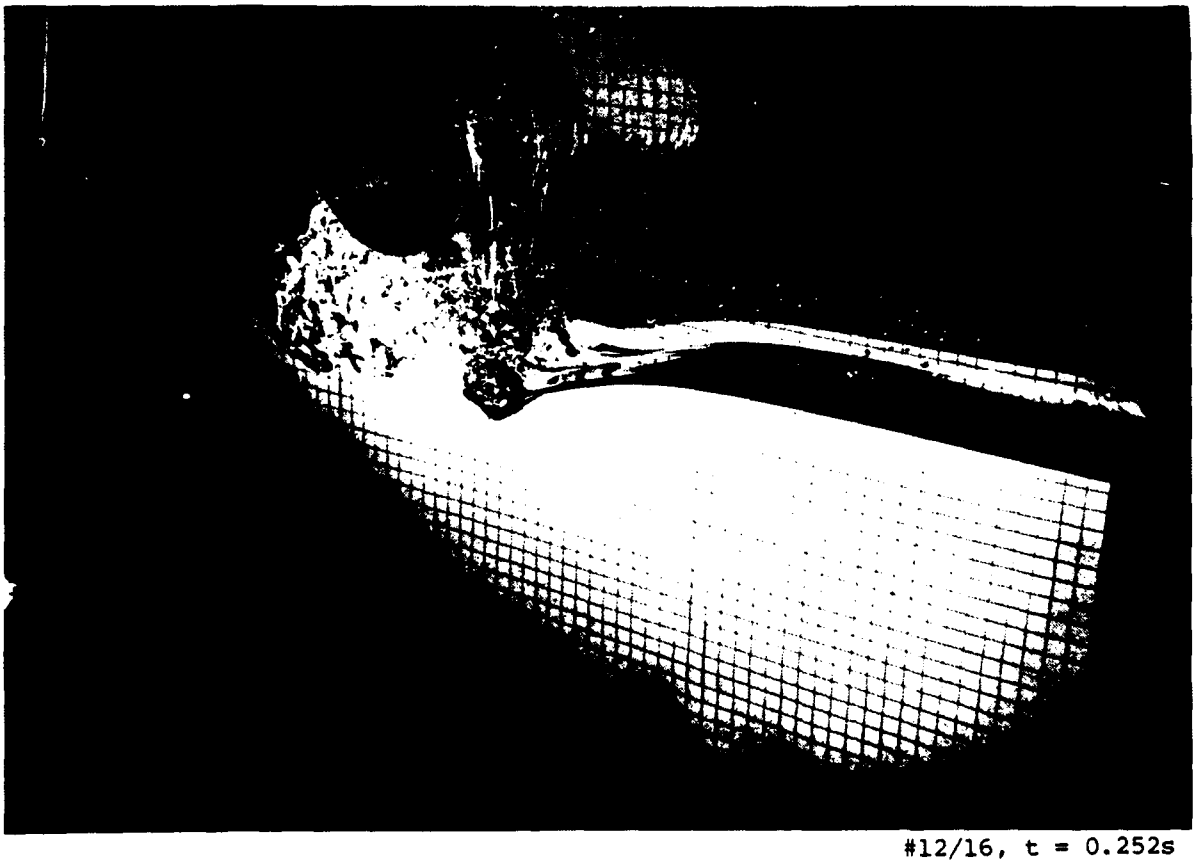

#12/16, t = 0.252s

Figure 5.2 (cont'd)

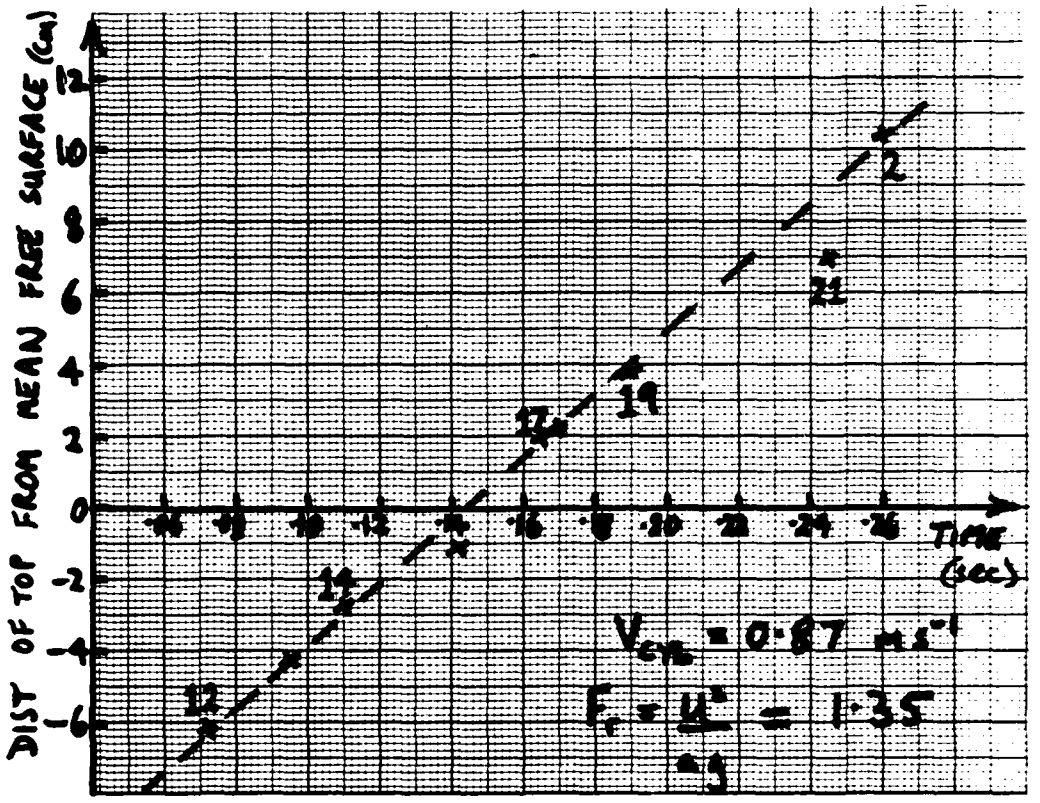

Figure 5.3 Measured velocities.

END

FILMED

12-85

DTIC